LRP 421/90 December 1990

THEORY OF PLASMA HEATING BY LOW-FREQUENCY WAVES: MAGNETIC PUMPING AND ALFVEN RESONANCE HEATING

J. Vaclavik and K. Appert

submitted for publication in Nuclear Fusion

THEORY OF PLASMA HEATING BY LOW-FREQUENCY WAVES:

MAGNETIC PUMPING AND ALFVEN RESONANCE HEATING

J. Vaclavik and K. Appert

Centre de Recherches en Physique des Plasmas

Association Euratom - Confédération Suisse

Ecole Polytechnique Fédérale de Lausanne

21, Av. des Bains, CH-1007 Lausanne, Switzerland

Abstract

The present status of the theory of plasma heating by low-frequency waves is reviewed from a unified point of view.

CONTENTS

1. INTRODUCTION

The heating of magnetically confined plasmas to high temperatures is one of the main problems of controlled thermonuclear fusion research. A general method for doing this is by means of radio-frequency electromagnetic fields. The principle of the method consists of converting energy of the oscillating field into thermal energy of the plasma particles. The energy conversion can occur via various mechanisms depending on the range of frequencies of the applied field.

One of the particular methods which have been pursued since the advent of fusion research is that using the frequency range below the ion cyclotron frequency. In the radio-frequency community it is usually termed low-frequency wave heating. Its principle characteristics can be summarized as follows. The mechanisms of energy conversion involve collisional dissipation due to resistivity, viscosity, etc. as well as collisionless dissipation due to Cerenkov resonance: transit time magnetic pumping and Landau damping. The electromagnetic field in the plasma is excited by external oscillating currents flowing in a suitable antenna. The wave field may then undergo two main types of interaction:

1) Its energy is directly dissipated by some of the mechanisms mentioned above. It results in a global heating of the plasma. The schemes based on this type of interaction will be referred to as magnetic pumping schemes.

2) The wave field is mode converted into a quasi-electrostatic wave

at the spatial Alfvén resonance. This wave is then damped either in the neighbourhood of the resonance or as it propagates away. As a result, the plasma heating is fairly localized. The schemes involving mode conversion will be referred to as Alfvén resonance heating schemes.

This paper aims at reviewing the present status of the theoretical work related to magnetic pumping and Alfvén resonance heating. Although it will attempt to include all the material relevant to heating of laboratory plasmas the main emphasis will be placed on Alfvén resonance heating of tokamak plasmas, which is currently being investigated both theoretically and experimentally. The body of the paper will be dominated by linear theory since the development of nonlinear theory has not been as dramatic nor have the experiments shown evidence of significant nonlinear activity. It should be noted that some of the topics touched on here have been reviewed by Hasegawa and Uberoi [217] and by Appert and co-workers [137,159].

This review is organized as follows. Section 2 contains a brief history of the origin and development of the theory of low-frequency wave heating. Since we cannot here discuss or even mention all the papers which have contributed to this development, we limit ourselves to references to those studies which have, in our opinion, made decisive contributions. We apologize if, through oversight or ignorance, we have incorrectly assessed or neglected any other studies.

A general formulation of the central problem of linear theory is presented in Section 3. The keystone of this formulation is the di-

electric tensor operator which contains essentially all the information about the electromagnetic properties of a plasma system. It can assume various forms depending on complexities of the physics and geometry involved. In the literature to be reviewed here there have been a number of different plasma models considered. The basic equations of the most important and frequently used plasma models are discussed in Section 4.

Section 5 deals with the modelling of antennae in particular geometries and summarizes the expressions for the electromagnetic fields excited in the vacuum region surrounding the antennae. The explicit expressions for the dielectric tensor operator corresponding to the plasma models and geometries considered are obtained in Section 6.

The properties of the electromagnetic waves in the relevant frequency range are discussed in Section 7. Included in the discussion are general characteristics of the waves in unbounded plasmas and spectral characteristics of the oscillations in bounded systems. Specific schemes of magnetic pumping and Alfvén resonance heating are reviewed in Sections 8 and 9.

Section 10 is concerned with a relation between heating in the low-frequency range and that in the ion cyclotron range of frequencies. The article concludes with Section 11 which contains general comments and discusses some unresolved theoretical problems.

Finally, the Appendix outlines the derivation of the dielectric tensor operator of a hot, inhomogeneous, current-carrying plasma column.

Concluding this section we wish to make the following comment. In trying to present a coherent account of the subject under review, we frequently use arguments quite different from those of the original contributors. Yet we have attempted proper assignment of credit to all of the authors cited.

2. BRIEF HISTORY OF THE SUBJECT

In less than twenty years, the theory of low-frequency wave heating has acquired a vast literature. We survey the major contributions here, assuming (conveniently, but only temporarily) that the reader is familiar with the pertinent terminology.

2.1 Magnetic Pumping

The theory of plasma heating by low-frequency fields was independently initiated by Budker [1] in 1951, Spitzer and Witten [2] in 1953, and Schlüter [3] in 1957. They have shown that an oscillating electric field perpendicular to a confining magnetostatic field can be used to heat a plasma via the gyro-relaxation effect: exchange of energy between perpendicular and parallel degrees of freedom of the plasma particles due to collisions. Since the oscillating electric field was to be produced by changing the confining magnetic field in

time, this method of heating has received the name "magnetic pumping". The theory of gyro-relaxation heating was further developed in Refs. [5,11,13] which included the effects of ion viscosity, electron and ion heat conductivities and the generation of sound waves.

When particle collision frequencies are much smaller than the frequency of the oscillating field the gyro-relaxation heating is not efficient. Another mechanism of energy transfer for this case was considered by Berger et al. [4] in 1958. They have shown that significant heating can be obtained when the transit time for the particles across a pumping section of the plasma is comparable to the period of the oscillating field. The energy transfer is caused by a force parallel to the magnetostatic field which arises from interaction between the pumping field and the magnetic moment of the particle. The scheme based on this collisionless mechanism was denoted by the term "transit time heating".

The pumping magnetic field in general excites compressional motion in the plasma. This motion, in particular variation of the electron pressure, in turn produces an electric field parallel to the magnetostatic field. Thus an additional force acts on the plasma particles. As a result, the particles may gain kinetic energy via the Landau damping associated with this force. The importance of this mechanism was pointed out by Stepanov [8] in 1963. On considering electromagnetic waves travelling along the magnetostatic field he has shown that the Landau damping considerably enhances the heating rate. Moreover, he concluded that in the case of a strongly non-isothermal

plasma the heating becomes especially effective if the phase velocity of the pumping waves is close to the velocity of the ion acoustic waves. Further improvement on the modelling of transit time heating by compressional magnetic perturbations were made in Refs. [9,11,37,98].

All these studies have concentrated on the heating of ions by magnetic perturbations with frequencies much smaller than the frequency of the fast magnetoacoustic wave. The possibility of electron heating by making use of the fast magnetoacoustic wave was for the first time discussed by Dolgopolov and Stepanov [51] in 1965 and later on by Canobbio [25] and by Lashmore-Davies and May [27].

In 1971, Koechlin and Samain [19,20] suggested to use a torsional rather than a compressional magnetic perturbation for the transit time heating of ions. They have argued that for large-aspect-ratio tokamaks this scheme is more efficient than the compressional magnetic pumping while using a lower working frequency. The theory of torsional magnetic pumping was further developed in Refs. [21,26].

The collisionless heating schemes mentioned so far are all based on the Cerenkov resonance that involves only the particle velocity component parallel to the magnetostatic field. A scheme based on the Cerenkov resonance that involves also perpendicular velocity components was proposed by Canobbio [38,39] in 1976. This scheme, called toroidal drift magnetic pumping, requires the pumping field that excites torsional perturbations in a toroidal geometry. It was shown that the heating efficiency of this scheme is higher than that of torsional magnetic pumping.

In all the papers referred to, the amplitude of the electromagnetic field was assumed to be sufficiently small so that the linear theory was applicable. The use of stronger fields, however, may lead to a nonlinear distortion of the particle distribution function. It is then necessary to develop a theory that takes this effect into account. There are in fact two such theories. The first one, which is based on the quasilinear approximation, was put forward by Dolgopolov and Sizonenko [12] in 1967 (see also Ref. [55]). The other, which uses a single-wave approximation, was advanced by Canobbio [15,21,25] in the early 1970s. It follows from both theories that for the same field amplitude the nonlinear energy absorption is smaller than that calculated from the linear theory.

The efficiency of plasma heating by electromagnetic waves strongly depends on the way in which the energy is transferred from an antenna to the plasma. As early as 1960 Frank-Kamenetskii [6,7] pointed out that the energy transfer can be facilitated if an eigenmode of electromagnetic oscillations in a bounded plasma system is excited. Specifically, he suggested to use an eigenmode of the fast magnetoacoustic wave. Hence this method of plasma heating was denoted by the term "magnetoacoustic resonance". It should be borne in mind that this method is rather generic, since it can be used in conjunction with any dissipative mechanism. The magnetoacoustic resonance that involves collisional dissipation was studied in a number of papers by the Fribourg group [10,14,16-18,23] in the late 1960s and early 1970s and by the Australian group [41-44] in the late 1970s (see also Ref. [45]). On using a two-fluid plasma model that includes collisional as well as collisionless damping mechanisms in a pheno-

menological manner, the magnetoacoustic resonance was investigated in a series of papers by the Brussels group [22,28-31,34-36,47] in the 1970s. Finally, a kinetic theory of magnetoacoustic resonance was put forward in Refs. [49,50] in 1980.

2.2 Alfvén Resonance Heating

The development of theoretical work related to Alfvén resonance heating had begun as early as 1965-66 in pioneering papers by Dolgopolov and Stepanov [51,53]. On considering a simple model they have shown that the collisional or Landau damping of the fast magnetoacoustic wave in an inhomogeneous plasma can be strongly enhanced if the condition for the spatial Alfvén resonance is satisfied. The resulting absorbed power was estimated to be of the same order of magnitude as the circulating power. They have thus predicted one of the most typical characteristics of Alfvén resonance heating.

Alfvén resonance heating as a scheme for heating tokamak plasmas was first proposed in 1973-74 independently by Tataronis and Grossmann [60], and Hasegawa and Chen [61,62]. An important result of the latter authors, obtained using an ideal MHD model in a slab geometry, was the finding that the absorbed power is strongly enhanced if the surface mode (the first radial eigenmode of the fast magnetoacoustic wave) is excited in the plasma (see also Ref. [65]). Later on it was shown by the same authors [72,73], using a simple kinetic model in a slab geometry, that in a hot plasma the fast magnetoacoustic wave is mode-converted into the kinetic Alfvén wave in the neighbourhood of the spatial Alfvén resonance (see also Ref. [66]). The amount of absorbed

power was found to be the same as that obtained from the MHD calculations. Moreover, these authors have considered nonlinear heating processes due to parametric decay instabilities excited by the converted kinetic Alfvén wave (see also Ref. [74]). The effects of resistive dissipation on energy absorption at the spatial Alfvén resonance were investigated by Kapraff and co-workers [68,76] in 1975. They have demonstrated that the results found in ideal MHD are unaltered for plasma resistivities of the order typical of tokamaks.

The first numerical calculations based on the MHD equations in a cylindrical geometry were carried out in 1976 [75]. The authors confirmed the importance of the excitation of the surface mode. A simple analytical model for resonance absorption of the surface mode in cylindrical geometry was given in Ref. [77] (1978). More detailed numerical computations [84,111] (1980) using an MHD cylindrical code revealed that the presence of an equilibrium plasma current can dramatically improve the coupling to the innermost resonance surfaces. The phenomenon was later identified [103] (1982) as being due to the effects of magnetic field curvature.

The first extensive cylindrical kinetic calculations which took into account the effects of finite ion Larmor radius and parallel electron dynamics (Landau damping) were carried out in 1982 [107]. The authors confirmed the importance of an equilibrium plasma current. Moreover, their results indicated the excitation of the quasi-electrostatic surface wave modes near the plasma periphery.

The possibility of using mangetoacoustic cavity modes (higher radial eigenmodes of the fast magnetoacoustic wave) for plasma heating

in large tokamaks was discussed for the first time in 1978 [81] within the context of an MHD model in a slab geometry. On including in the analysis also the transit time pumping mechanism, the authors have concluded that this mechanism can compete with Alfvén resonance absorption for high radial mode numbers. Furthermore, it was shown that these modes have typically much higher cavity Q than the surface mode. The theory of plasma heating by cavity modes was further advanced in Refs. [82,86,114,119,157] (1979-1985) within the context of cold plasma models in slab and cylindrical geometries, while Refs. [94,161,183] (1980-1987) treated this problem using cylindrical kinetic models.

The first calculations based on the MHD equations in a real toroidal tokamak geometry were performed in 1980 [87,109]. It was found that for a circular cross-section the overall coupling is much the same as that obtained from the cylindrical version except for some additional resonance surfaces which may be excited due to the interaction of different poloidal modes. Some additional deviations appear for non-circular cross-sections due to elipticity, triangularity, etc.

The existence of global eigenmodes of the Alfvén wave in the cylindrical models was noticed for the first time in 1982 [104,106, 107]. It was shown that their frequencies lie just below the lower edge of the Alfvén continuum (the lowest frequency for which there is an Alfvén resonance layer in the plasma) and that they are "generated" by the curvature of the equilibrium magnetic field lines [106,113] or by the gyrotropy effects [119].

Although the finite ω/ω_{ci} effects, which stem from the inclusion of the Hall term in Ohm's law, had been considered in some previous treatments (see e.g. Refs. [96,107]), their importance for the excitation of the surface mode was pointed out for the first time in 1983 [119]. It was shown that these effects strongly modify the coupling of the modes with $m<0$, m being the poloidal wavenumber (see also Ref. [123]). A more detailed picture of the influence of finite frequency effects on the spectrum of a cylindrical cold plasma was obtained in Refs. [120,126,128,129,141,164] (1983-1986). Some subsequent studies, which had taken into account the finite frequency effects on the resonance absorption of the surface mode, were presented in Refs. [135,136,138,147,153,160,172,181,182] (1984-1987). In 1985-86 these effects have been included in the toroidal numerical code LION [145,159,166,180].

Finally, rather general expressions for the dielectric tensor operator of a hot plasma in slab and cylindrical geometries have been derived in Refs. [174,178] (1987) and an appropriate local power absorption formulated in Ref. [173] (1987). They have been incorporated into different versions of the numerical code ISMENE [165].

The present state of affairs can be summarized as follows. The most advanced tools for the theoretical modelling of Alfvén resonance heating are cylindrical kinetic codes: Australian [139,161,168], Lausanne [165,177-179], Sukhumi [123,154,175,184] and Texas [107,162,183]. The most developed is the Lausanne code ISMENE: it takes into account finite frequency effects, Larmor radius terms up to the second order, the gradients of equilibrium quantities, an equili-

brium current, Landau damping, transit time magnetic pumping and resistivity. It allows one to compute all variable field components, the perturbed electron density, the total power delivered by an antenna and the local power deposition profile. On the other hand, the codes which treat a real toroidal tokamak geometry are less advanced. The most developed is LION [166]: it is based on a cold plasma model which takes into account finite frequency effects and an equilibrium current. It can, however, be used only to calculate the total power delivered by an antenna.

3. FORMULATION OF THE LINEAR PROBLEM; ENERGY CONSERVATION LAW

A magnetized plasma is considered in the presence of small-amplitude electromagnetic oscillations. The plasma is assumed to occupy a region V_p which is surrounded by a pure vacuum region V_v. The electromagnetic oscillations are excited by currents flowing in an antenna which is placed in the vacuum region, and the entire system is surrounded by a perfectly conducting wall. The time variation of the antenna currents and the electromagnetic fields is assumed to be of the form $\exp(-i\omega t)$, where ω is an imposed frequency. Maxwell's equations for the electric field component, $\vec{E}$, of the electromagnetic oscillations in the plasma can then be written as

$$\nabla \times \nabla \times \vec{E} = \left(\frac{\omega}{c}\right)^2 \overleftrightarrow{\varepsilon} \cdot \vec{E} , \tag{3.1}$$

where $\overleftrightarrow{\varepsilon}$ is the dielectric tensor operator defined by the relation

$$\vec{j} = \frac{\omega}{4\pi i} \left(\overleftrightarrow{\varepsilon} - \overleftrightarrow{I}\right) \vec{E} , \tag{3.2}$$

$\vec{j}$ being the linear current density induced by the electromagnetic field and $\overleftrightarrow{I}$ is the unit tensor.

In the vacuum region the electric field component, $\vec{E}_v$, obeys the equation

$$\nabla \times \nabla \times \vec{E}_v = \left(\frac{\omega}{c}\right)^2 \vec{E}_v + \frac{4\pi i\omega}{c^2} \vec{j}_a , \tag{3.3}$$

where $\vec{j}_a$ is an imposed antenna current density satisfying the constraint

$$\nabla \cdot \vec{j}_a = 0 . \tag{3.4}$$

The magnetic field components, $\vec{B}$ and $\vec{B}_v$, of the oscillations in both the regions can be obtained from Faraday's law

$$\left\{\vec{B}, \vec{B}_v\right\} = \frac{c}{i\omega} \nabla \times \left\{\vec{E}, \vec{E}_v\right\} . \tag{3.5}$$

Equations (3.1) and (3.3) must be supplemented by appropriate boundary conditions. Assuming that $\vec{j} \to 0$ at the plasma boundary, the matching conditions at the plasma-vacuum interface are

$$\vec{n}_p \times \left(\vec{E} - \vec{E}_v\right) = 0 , \tag{3.6}$$

$$\vec{n}_p \times \left(\vec{B} - \vec{B}_v\right) = 0 , \tag{3.7}$$

while the boundary condition at the conducting wall is

$$\vec{n}_w \times \vec{E}_v = 0. \tag{3.8}$$

Here $\vec{n}_p$ and $\vec{n}_w$ denote the outer normal unit vectors at the plasma boundary and the conducting wall.

To obtain an energy conservation law, Eq. (3.1) is multiplied by $\vec{E}^*$ (the complex conjugate of $\vec{E}$) and integrated over the region V_p. After some rearrangements and using Eq. (3.5) one finds

$$\int_{V_p} dV \frac{\omega}{8\pi} \left(|\vec{B}|^2 - \vec{E}^* \cdot \overleftrightarrow{\varepsilon} \cdot \vec{E} \right) = i \int_{\Sigma_p} d\Sigma \, \hat{\vec{S}} \cdot \vec{n}_p \,, \tag{3.9}$$

where Σ_p is the bounding surface of the region V_p and

$$\hat{\vec{S}} = \frac{c}{8\pi} \vec{E}^* \times \vec{B} \tag{3.10}$$

is a complex Poynting vector whose real part is the actual time-averaged Poynting vector $\vec{S}$.

Likewise from Eq. (3.3) one obtains

$$\int_{V_v} dV \left[\frac{\omega}{8\pi} \left(|\vec{B}_v|^2 - |\vec{E}_v|^2 \right) - \frac{i}{2} \vec{j}_a \cdot \vec{E}_v^* \right] \tag{3.11}$$

$$= -i \int_{\Sigma_p} d\Sigma \, \hat{\vec{S}}_v \cdot \vec{n}_p \,,$$

where the boundary condition (3.8) has been used.

On invoking the matching conditions (3.6) and (3.7) one can combine Eqs. (3.9) and (3.11); the real and imaginary parts of the resulting equation then yield

$$P \equiv -\frac{1}{2}\int_{V_a} dV\, \mathrm{Re}\, \vec{j}_a \cdot \vec{E}_v^* = -\int_{\Sigma_p} d\Sigma\, \vec{S}\cdot\vec{n}_p$$
$$= \int_{V_p} dV\, \frac{\omega}{8\pi}\, \mathrm{Im}\, \vec{E}^* \cdot\!\leftrightarrow \vec{\varepsilon}\cdot \vec{E}, \tag{3.12}$$

$$P_c \equiv -\frac{1}{2}\int_{V_a} dV\, \mathrm{Im}\, \vec{j}_a \cdot \vec{E}_v^* = \int_{V_v} dV\, \frac{\omega}{8\pi}\left(|\vec{B}_v|^2 - |\vec{E}_v|^2\right)$$
$$+ \int_{V_p} dV\, \frac{\omega}{8\pi}\left(|\vec{B}|^2 - \mathrm{Re}\, \vec{E}^* \cdot\!\leftrightarrow \vec{\varepsilon}\cdot \vec{E}\right), \tag{3.13}$$

where V_a is a volume occupied by the antenna current density.

Equation (3.12) expresses a global power balance: the time-averaged power, P, delivered by the antenna is equal to the energy flux through the plasma surface which, in turn, is equal to the power absorbed by the plasma. Equation (3.13) is a conservation law of the time-averaged circulating power P_c.

In order to appreciate the efficiency at which the electromagne-

tic field energy is pumped into the plasma it is convenient to define a quality factor, Q, by the relation

$$Q = \frac{P_c}{P} \quad . \tag{3.14}$$

Note that this quantity is not a cavity Q.

The problem referred to in the title of this section can now be posed as follows:

1) Considering a specific plasma model and geometry, determine an explicit form of the dielectric tensor operator.

2) Imposing a frequency and an antenna current density, find a solution of Eqs. (3.1) and (3.3) satisfying the boundary conditions (3.6) - (3.8).

3) Calculate the power delivered by the antenna, the circulating power and the quality factor.

It should be noted that in most of the cases of practical interest the solutions of Eq. (3.1) can only be found by numerical computations. A powerful procedure for doing this is the finite-element method applied to the weak (Galerkin) variational form of Eq. (3.1). This form can be obtained from Eq. (3.9) by the replacement $\vec{E}^* \to \tilde{\vec{E}}$, where $\tilde{\vec{E}}$ is an arbitrary test function in a suitable functional space.

4. PLASMA MODELS

In order to determine an explicit form of the dielectric tensor operator, defined in the previous section, one has to establish a linear relation between the induced current density and the electric field. This can be done using various plasma models. In this section we shall briefly review the basic equations and the limitations of the most important and frequently used models.

4.1. Fluid Models

In general, the equations of these models apply only when certain requirements are satisfied. Let ν, v_t and ω_c denote the collision frequency, thermal velocity and cyclotron frequency of a species of the plasma. Let further $L_\perp$ and $L_\parallel$ be characteristic scale lengths over which plasma dynamical variables change in the directions perpendicular and parallel to the magnetic field. The conditions of applicability of fluid models can then be stated in the form:

1) Collisional regime

$$\max\left(v_t/L_\parallel\,,\,\omega\right) \ll \nu\,, \tag{4.1}$$

$$v_t/L_\perp \ll \max\left(\omega_c,\nu\right). \tag{4.2}$$

2) Collisionless regime

$$\omega \gg v_t/L_\parallel \gg \nu, \tag{4.3}$$

$$\omega_c \gg v_t/L_\perp \gg \nu, \tag{4.4}$$

$$|\omega - \ell\omega_c| \gg v_t/L_\parallel, \tag{4.5}$$

where l is an integer.

4.1.1 Magnetohydrodynamics (MHD)

This model applies if, in addition to the conditions (4.1) - (4.5), one has

$$c_A \ll c, \tag{4.6}$$

$$\omega \ll \omega_{ci}, \tag{4.7}$$

where c_A is the Alfvén velocity and ω_{ci} is the ion cyclotron frequency. The condition (4.6) allows one to consider the plasma as a single fluid and to neglect the displacement current in Maxwell's equations.

Let ρ_0, p_0, $\vec{B}_0$ and $\vec{j}_0$ represent the equilibrium values of the mass density, pressure, magnetic field and current density. The linearized equations of MHD can then be written in the form

$$\rho_0 \frac{\partial \vec{V}}{\partial t} = -\nabla p + \frac{1}{c}(\vec{j} \times \vec{B}_0 + \vec{j}_0 \times \vec{B}), \tag{4.8}$$

$$\vec{E} + \frac{1}{c}\vec{V} \times \vec{B}_0 = 0, \tag{4.9}$$

$$\frac{\partial p}{\partial t} + \vec{V}\cdot\nabla p_0 + \gamma p_0 \nabla\cdot\vec{V} = 0, \tag{4.10}$$

where $\vec{V}$ is the plasma velocity and γ is the adiabacity index. The equilibrium quantities obey the equations

$$\nabla p_0 = \frac{1}{c}\vec{j}_0 \times \vec{B}_0, \tag{4.11}$$

$$\nabla \times \vec{B}_0 = \frac{4\pi}{c}\vec{j}_0, \tag{4.12}$$

$$\nabla\cdot\vec{B}_0 = 0. \tag{4.13}$$

Note that Eq. (4.9) implies

$$\vec{E}\cdot\vec{B}_0 = 0. \tag{4.14}$$

Consequently, one equation must be omitted from the system of equations (3.1); specifically, it is the component parallel to $\vec{B}_0$. This equation only serves as a means of determining the quantity $\vec{j}\cdot\vec{B}_0$ once the components of $\vec{E}$ perpendicular to $\vec{B}_0$ are known. The point is that this quantity, in turn, cannot be obtained from Eqs. (4.8) - (4.10).

In the MHD literature one usually introduces the plasma displacement $\vec{\xi}$ so that

$$\vec{V} = \frac{\partial \vec{\xi}}{\partial t}. \tag{4.15}$$

Equation (4.10) and Eq. (4.9) combined with Faraday's law can thus be integrated with respect to time. Substitution of the resulting expressions for p

and $\vec{B}$ in Eq. (4.8), where $\vec{j}$ is eliminated in favour of $\vec{B}$ using Ampère's law, yields a single equation for $\vec{\xi}$ [213]:

$$\rho_0 \frac{\partial^2 \vec{\xi}}{\partial t^2} = \vec{F}(\vec{\xi}) \equiv \nabla\left(\vec{\xi}\cdot\nabla p_0 + \gamma p_0 \nabla\cdot\vec{\xi}\right) + \frac{1}{4\pi}\left[\nabla\times\nabla\times\left(\vec{\xi}\times\vec{B}_0\right)\right]\times\vec{B}_0 + \frac{1}{c}\vec{j}_0\times\left[\nabla\times\left(\vec{\xi}\times\vec{B}_0\right)\right]. \tag{4.16}$$

Once a solution of this equation is found, the electric field is simply determined from Eqs. (4.9) and (4.15). If a harmonic time-dependence of $\vec{\xi}$ is considered, this procedure is, of course, equivalent to solving Eq. (3.1).

4.1.2 Cold plasma with an equilibrium current

If the plasma pressure is sufficiently small so that

$$p_0 \ll B_0^2/8\pi \quad , \tag{4.17}$$

the corresponding term in Eq. (4.11) may be neglected. Under these circumstances the plasma equilibrium can be regarded as force-free. Equation (4.10) then implies that the pressure perturbation is negligible as well. Hence the linearized equation of motion in the model in question reads

$$\rho_0 \frac{\partial \vec{V}}{\partial t} = \frac{1}{c}\left(\vec{j}\times\vec{B}_0 + \vec{j}_0\times\vec{B}\right). \tag{4.18}$$

Moreover, if the inequality (4.7) is replaced by a less stringent one

$$\omega \ll \omega_{LH} \,, \tag{4.19}$$

where ω_{LH} is the lower-hybrid frequency, Eq. (4.9) is to be replaced by Ohm's law that includes the Hall term

$$\vec{E} + \frac{1}{c}\vec{V}\times\vec{B}_o = \frac{m_i}{ec\rho_o}\left(\vec{j}\times\vec{B}_o + \vec{j}_o\times\vec{B}\right), \tag{4.20}$$

where e is the electron charge and m_i is the ion mass.

Since in a force-free equilibrium $\vec{j}_0$ is parallel to $\vec{B}_0$, the Ohm's law enforces Eq. (4.14) even in this model. Assuming a harmonic time-dependence of all dynamical variables one can combine Eqs. (4.18) and (4.20) to obtain

$$\vec{j}\times\vec{B}_o = -\vec{j}_o\times\vec{B} - i\omega\rho_o B_o\left(\frac{e}{m_i}\right)^2 \frac{1}{\omega^2-\omega_{ci}^2} \times\left(i\frac{\omega}{\omega_{ci}}\vec{E} - \frac{1}{B_o}\vec{E}\times\vec{B}_o\right), \tag{4.21}$$

where $\omega_{ci} = eB_0 / (m_i\ c)$. Once a particular geometry is specified, it is straightforward from Eq. (4.21) to deduce an explicit form of the dielectric tensor operator pertinent to the present model.

4.1.3 Two fluids

This is the most general fluid model in the sense that the limitations of the two preceeding sections, the inequalities (4.6), (4.17) and (4.19), may be relaxed. Nevertheless, in the context of the present review it is sufficient to consider the

case for which the inequality (4.17) holds. The plasma linear dynamics is then described by the equations of motion for ions and electrons

$$m_j \frac{\partial \vec{V}_j}{\partial t} = q_j \left(\vec{E} + \frac{1}{c} \vec{V}_j \times \vec{B}_o \right), \qquad j = i, e \ , \tag{4.22}$$

where m_j, q_j, and $\vec{V}_j$ are the mass, charge and velocity of species j. The equilibrium velocities of both species are assumed to vanish.

If a harmonic time-dependence of the dynamical variables is considered, Eqs. (4.22) can easily be solved for $\vec{V}_j$. The linear current density can then be calculated from

$$\vec{j} = n_o \sum_j q_j \vec{V}_j \ , \tag{4.23}$$

where n_0 is the equilibrium density of species. Substituting the solutions of Eqs. (4.22) in Eq. (4.23) yields

$$\vec{j} = n_o \sum_j \frac{q_j^2}{m_j} \left[\frac{1}{\omega^2 - \omega_{cj}^2} \vec{e}_{\parallel} \times \left(i\omega \vec{E} \times \vec{e}_{\parallel} + \omega_{cj} \vec{E} \right) + \frac{i}{\omega} \vec{e}_{\parallel} \cdot \vec{E} \, \vec{e}_{\parallel} \right], \tag{4.24}$$

where $\vec{e}_{\parallel} = \vec{B}_0/B_0$ and $\omega_{cj} = q_j B_0/(m_j c)$.

An expression for the dielectric tensor, corresponding to this model, follows from Eq. (4.24) in a trivial manner.

4.1.4 Energy conservation law; Resistivity, viscosity

All the models reviewed so far are ideal since they do not include any dissipative effects. Of course, in order to calculate the energy absorption of the electromagnetic fields in the plasma one needs to take dissipation into account. In the fluid models the energy absorption can be caused by various collisional dissipative mechanisms. In this section we shall briefly discuss the two-fluid model that includes two such mechanisms: resistivity and ion viscosity.

Although the resistivity and viscosity of a plasma in a magnetic field are, in general, tensor quantities (see, for example, Ref. [211]) we shall confine ourselves to the case when they are approximated by scalar coefficients. The linearized equations of motion for ions and electrons can thus be written in the form

$$m_i \frac{\partial \vec{V}_i}{\partial t} = e\left(\vec{E} + \frac{1}{c}\vec{V}_i \times \vec{B}_0\right) - \vec{R} + \frac{\vec{F}}{n_0}, \tag{4.25}$$

$$m_e \frac{\partial \vec{V}_e}{\partial t} = -e\left(\vec{E} + \frac{1}{c}\vec{V}_e \times \vec{B}_0\right) + \vec{R}. \tag{4.26}$$

Here

$$\vec{R} = e\frac{\vec{j}}{\sigma} \tag{4.27}$$

is the friction force due to electron-ion collisions, σ being the electrical conductivity, while

$$\vec{F} = \nabla \cdot (\eta \overleftrightarrow{W}) \tag{4.28}$$

is the friction force density due to ion-ion collisions, η being the ion viscosity coefficient. The rate-of-strain tensor $\overleftrightarrow{W}$ is defined by

$$W_{\alpha\beta} = \frac{\partial V_{i\alpha}}{\partial x_\beta} + \frac{\partial V_{i\beta}}{\partial x_\alpha} - \frac{2}{3}\delta_{\alpha\beta}\nabla\cdot\vec{V}_i \quad . \tag{4.29}$$

It should be noted that the dissipative mechanisms described here can be included in any of the models discussed previously. Thus, for example, if the term $\vec{R}/e$ is added to the right-hand side of Eq. (4.9) one obtains the model which is usually referred to as the resistive MHD.

In order to derive an expression for the energy absorption of the electromagnetic fields in the plasma one must construct an energy conservation law corresponding to Eqs. (4.25) and (4.26). For this purpose Eq. (4.25) is multiplied by $n_0\vec{V}_i$, and Eq. (4.25) by $n_0\vec{V}_e$. Adding the resulting equations yields

$$\frac{1}{2}m_0\frac{\partial}{\partial t}\left(m_i V_i^2 + m_e V_e^2\right) = \vec{j}\cdot\vec{E} - \frac{1}{e}\vec{R}\cdot\vec{j} + \vec{V}_i\cdot\vec{F} \,, \tag{4.30}$$

where the definition (4.23) has been used. Since a harmonic time-dependence of the linear quantities is considered, one is, of course, interested only in the time average of Eq. (4.30). Taking this average and substituting the expressions (4.27) and (4.28) for $\vec{R}$ and $\vec{F}$, Eq. (4.30) can be cast into the form

$$\frac{1}{2}\mathrm{Re}\,\vec{j}\cdot\vec{E}^* = \frac{1}{2\sigma}|\vec{j}|^2 - \frac{1}{2}\nabla\cdot\left(\eta\,\mathrm{Re}\,\overleftrightarrow{W}\cdot\vec{V}_i^*\right)$$

$$+ \frac{\eta}{4}\,tr\left(\overleftrightarrow{W}\cdot\overleftrightarrow{W}^*\right) \quad . \tag{4.31}$$

In obtaining the last term on the right-hand side of Eq. (4.31) we have invoked the property that $\mathrm{tr}\,(\overleftrightarrow{W}) = 0$.

Equation (4.31) expresses a local power balance: the time-averaged power due to the work done by the electric field on the plasma in a volume element is partly dissipated via resistivity and viscosity, and partly transferred through the surface of this element by the energy flux due to viscosity. For further consideration it is convenient to define the local power absorption densities due to resistivity and viscosity as

$$P_r(\vec{x}) = \frac{1}{2\sigma} |\vec{j}|^2 \tag{4.32}$$

and

$$P_v(\vec{x}) = \frac{\eta}{4} \mathrm{tr}\left(\overleftrightarrow{W} \cdot \overleftrightarrow{W}^*\right) . \tag{4.33}$$

Integrating Eq. (4.31) over the volume occupied by the plasma and assuming that $\vec{j} \to 0$ at the plasma boundary one obtains a global power balance

$$\int_{V_p} dV \frac{\omega}{8\pi} \mathrm{Im}\, \vec{E}^* \cdot \overleftrightarrow{\varepsilon} \cdot \vec{E} = \int_{V_p} dV \left(P_r(\vec{x}) + P_v(\vec{x})\right), \tag{4.34}$$

where the definition (3.2) has been used. This equation is to be compared with Eq. (3.12). It should be noted that the quantities $P_r(\vec{x})$ and $P_v(\vec{x})$ are positive-definite since the coefficients σ and η are positive.

4.2. Collisionless Kinetic Models

In general , the conditions of applicability of these models are given by the inequalities

$$\omega \gg \nu \ , \tag{4.35}$$

$$v_t/\nu \gg max\,(L_\perp, L_\parallel). \tag{4.36}$$

For the sake of convenience, in Sections 4.2.1 to 4.2.3 we shall consider

$$\vec{E}_m \equiv \vec{E}, \ \vec{B}_m = \vec{B}_0 + \vec{B}, \ \ \vec{j}_m = \vec{j}_0 + \vec{j} \tag{4.37}$$

as arbitrary nonlinear quantities.

4.2.1 Drift-kinetic equation

This equation holds if, in addition to the conditions (4.35) and (4.36), the following inequalities are satisfied

$$\omega \ll \omega_c \ , \tag{4.38}$$

$$v_t/\omega_c \ll L_\perp \ , \tag{4.39}$$

$$c|\vec{E}_m|/|\vec{B}_m| \ll v_t \,. \tag{4.40}$$

Under these circumstances the guiding centre, at a position $\vec{X}$, of a single particle of a species with charge q and mass m obeys the equations (see, for example, Ref. [210])

$$\frac{dX}{dt} \equiv \vec{v}_g = v_{\parallel}\vec{h} + \vec{v}_E + \frac{1}{\omega_c}\left[\frac{v_\perp^2}{2B_m}\vec{h}\times\nabla B_m + v_{\parallel}^2\vec{h}\times(\vec{h}\cdot\nabla)\vec{h}\right], \tag{4.41}$$

$$\frac{dv_\perp}{dt} = \frac{v_\perp}{2B_m}\left(v_{\parallel}\vec{h}\cdot\nabla B_m + \vec{v}_E\cdot\nabla B_m + \frac{\partial B_m}{\partial t}\right), \tag{4.42}$$

$$\frac{dv_{\parallel}}{dt} = \frac{q}{m}\vec{E}_m\cdot\vec{h} + \frac{v_\perp^2}{2}\nabla\cdot\vec{h} + v_{\parallel}\vec{v}_E\cdot(\vec{h}\cdot\nabla)\vec{h}, \tag{4.43}$$

where

$$\vec{v}_E = \frac{c}{B_m}\vec{E}_m\times\vec{h} \tag{4.44}$$

and $\vec{h} = \vec{B}_m/B_m$, $B_m = |\vec{B}_m|$.

One can now introduce a distribution function $f_g(\vec{X}, v_\perp, v_{\parallel}, t)$ in the phase space $\vec{X}$, $v_\perp$, $v_{\parallel}$ so that $f_g\, d\Gamma$ represents the mean number of particles of the species in question for which the guiding centres lie in a volume element $d\Gamma = 2\pi v_\perp dv_\perp dv_{\parallel} d\vec{X}$. In the collisionless approximation this distribution function must satisfy the Liouville equation

$$\frac{\partial f_g}{\partial t} + \nabla \cdot \left(\vec{v}_g f_g \right) + \frac{1}{v_\perp} \frac{\partial}{\partial v_\perp} \left(v_\perp \frac{dv_\perp}{dt} f_g \right) + \frac{\partial}{\partial v_\parallel} \left(\frac{dv_\parallel}{dt} f_g \right) = 0 \tag{4.45}$$

which expresses the conservation of the number of guiding centres.

Further, by simple differentiation it is easy to show from Eqs. (4.41) - (4.44) that

$$\nabla \cdot \vec{v}_g + \frac{1}{v_\perp} \frac{\partial}{\partial v_\perp} \left(v_\perp \frac{dv_\perp}{dt} \right) + \frac{\partial}{\partial v_\parallel} \frac{dv_\parallel}{dt} = 0. \tag{4.46}$$

Hence Eq. (4.45) can be rewritten in the form

$$\frac{\partial f_g}{\partial t} + \vec{v}_g \cdot \nabla f_g + \frac{dv_\perp}{dt} \frac{\partial f_g}{\partial v_\perp} + \frac{dv_\parallel}{dt} \frac{\partial f_g}{\partial v_\parallel} = 0 \tag{4.47}$$

which states that f_g is constant along a guiding centre trajectory in the phase space. Equation (4.47) is called the drift-kinetic equation.

Let us note that this equation as it stands cannot serve as a starting point for determining the dielectric tensor operator. The reason is that the knowledge of a distribution function f_g is not sufficient for calculating the current components perpendicular to $\vec{B}_n$. The equation is usually used only to determine the power absorbed by the corresponding species in the cases where the electromagnetic field components $\vec{E}_n$ and $\vec{B}_n$ can be regarded as known. Then, multiplying Eq. (4.47) by $m (v_\perp^2 + v_\parallel^2)/2$ and integrating over the whole phase space of the species one obtains

$$\int d\Gamma \frac{m}{2}(v_\perp^2+v_\parallel^2)\frac{\partial f_g}{\partial t} = \int d\Gamma f_g \left(q\vec{E}_n\cdot\vec{v}_g + \frac{m v_\perp^2}{2B_n}\frac{\partial B_n}{\partial t}\right) \qquad (4.48)$$

which can be used to calculate the total absorbed power once f_g is determined in terms of $\vec{E}_n$ and $\vec{B}_n$ from Eq. (4.47).

4.2.2 Vlasov equation

This is the most general equation for describing the dynamics of collisionless plasmas. On denoting by $f(\vec{x}, \vec{v}, t)$ the particle distribution function of a species with charge q and mass m, the Vlasov equation can be stated in the form

$$\frac{\partial f}{\partial t} + \vec{v}\cdot\nabla f + \frac{q}{m}\left(\vec{E}_n + \frac{1}{c}\vec{v}\times\vec{B}_n\right)\cdot\frac{\partial f}{\partial \vec{v}} = 0. \qquad (4.49)$$

If a solution of this equation is obtained the plasma current density is calculated from

$$\vec{j}_n = \sum_s q\int d\vec{v}\,\vec{v} f \ , \qquad (4.50)$$

where the symbol $\sum_s$ denotes the sum over all the plasma species.

Equations (4.49) and (4.50) provide the starting point for determining the dielectric tensor operator of a hot collisionless plasma.

4.2.3 Energy conservation law; local power absorption

In this section we shall be concerned with the problem of calculating the power that is locally absorbed by a plasma species in the case where the plasma dynamics is governed by the Vlasov equation. This problem has been addressed in Refs. [155, 173, 178]. Here we shall follow the argumentation given in Ref. [173].

The mean energy density of the particles that are in a volume element $\langle\vec{x},\vec{x}+d\vec{x}\rangle$ at a time t is given by the quantity

$$\int \frac{mv^2}{2} f \, d\vec{v} . \tag{4.51}$$

In order to ascertain how this quantity varies with time we shall construct an energy balance equation corresponding to Eq. (4.49). For this purpose we multiply (4.49) by $mv^2/2$ and integrate over the velocities. After simple manipulations this yields

$$\int \frac{mv^2}{2} \frac{\partial f}{\partial t} d\vec{v} = q \vec{E}_m \cdot \int \vec{v} f \, d\vec{v} - \int \frac{mv^2}{2} \vec{v} \cdot \nabla f \, d\vec{v} . \tag{4.52}$$

From this equation one can see that the mean energy of the particles in the volume element considered varies with time owing to two effects: the work done by the electric field on these particles (the first term on the right-hand side), and the flux of energy of those particles that stream into or out of the volume element. Thus, if we want to relate a time derivative of quantity (4.51) to the local power absorption we must evaluate it in a frame of reference where

the particle streaming is absent. This can be achieved if we transform equation (4.52) into suitable Lagrangian coordinates.

Let $\vec{x}'$ and $\vec{v}'$ represent the position and velocity of a particle at the time t' as it moves along an unperturbed trajectory (in the absence of the electromagnetic field) with the "initial" conditions $\vec{x}$ and $\vec{v}$ at the time t. Choosing $\vec{x}'$ and $\vec{v}'$ as the new variables we transform equation (4.52) into

$$\int \frac{mv^2}{2}\left(\frac{\partial f}{\partial t}\right)_{\vec{x}',\vec{v}'} d\vec{v} = q\int \vec{E}_m(\vec{x}',t)\cdot\vec{v}'\, f(\vec{x}',\vec{v}',t)\, d\vec{v}, \qquad (4.53)$$

where the relations $v^2 = v'^2$ and $d\vec{v} = d\vec{v}'$ have been used.

We now assume the amplitude of the electromagnetic field to be small. We may then expand the distribution function in powers of $\vec{E}$:

$$f = f_0 + f_1 + f_2 + \dots \quad . \qquad (4.54)$$

Here f_0 describes an equilibrium and f_1 is a solution of the corresponding linear problem. Since a harmonic time-dependence of the field is considered, the lowest order non-vanishing (quasilinear) contribution to the time average of equation (4.53) is given by

$$\tilde{P} \equiv \int \frac{mv^2}{2}\left(\frac{\partial f_2}{\partial t}\right)_{\vec{x}',\vec{v}'} d\vec{v} = q\int \vec{E}(\vec{x}',t)\cdot\vec{v}'\, f_1(\vec{x}',\vec{v}',t)\, d\vec{v}. \qquad (4.55)$$

To make a practical use of equation (4.55) we must perform a time average. Before doing so, however, let us note that the lowest frequency involved in the quantity $\tilde{P}$ is $|\omega - \omega_c|$. For a class of resonant particles we have $|\omega - \omega_c| \sim v_{||}/\lambda_{||}$, where $v_{||}$ is a typical particle velocity component parallel to the magnetostatic field and $\lambda_{||}$ is a characteristic length of the variation of the electromagnetic field in the same direction. Thus, in general, if we perform a time average over the scale $|\omega - \omega_c|^{-1}$, for consistency we have to perform also a space average over the scale $\lambda_{||}$, since a resonant particle of the above-mentioned class traverses this distance during the time $|\omega - \omega_c|^{-1}$. Therefore, without loss of generality we can set

$$\vec{E}(\vec{x},t) = Re\left\{\vec{E}(\vec{x}_\perp)\exp\left[i(k_{||}x_{||} - \omega t)\right]\right\} \tag{4.56}$$

and the same for f_1. Substituting these into Eq. (4.55) and averaging over $x_{||}$ and t we finally obtain a general expression for the local power absorption density as

$$P_L(\vec{x}_\perp) \equiv \langle \tilde{P} \rangle_{x_{||},t} = \frac{q}{2}\int d\vec{w}\, Re\langle \vec{E}^*(\vec{x}_\perp')\cdot\vec{v}' f_1(\vec{x}_\perp', \vec{v}')\rangle_t . \tag{4.57}$$

We now assume that the Larmor radius of the species is much smaller than the characteristic inhomogeneity lengths of macroscopic quantities: density, temperature and magnetostatic field. To the lowest order, i.e., neglecting the explicit gradients of these quantities, the equilibrium distribution function f_0 may then be approximated by a local Maxwellian, f_M, with a temperature T and density n_0. Moreover, to the same order, the particle trajectories may be evaluated assuming a locally uniform magnetostatic field.

Thus, choosing the Cartesian coordinate system with the z-axis along $\vec{B}_0$ we can write

$$\vec{x}_\perp' = \vec{x}_\perp + \frac{v_\perp}{\omega_c}\left[(\sin\alpha - \sin\alpha')\vec{e}_x + (\cos\alpha' - \cos\alpha)\vec{e}_y\right], \tag{4.58}$$

$$\vec{v}' = v_\perp(\cos\alpha'\vec{e}_x + \sin\alpha'\vec{e}_y) + v_z\vec{e}_z, \tag{4.59}$$

$$\alpha' = \alpha + \omega_c(t-t'), \quad v_\perp = (v_x^2 + v_y^2)^{1/2}, \quad \alpha = \operatorname{tg}\frac{v_y}{v_x}. \tag{4.60}$$

To proceed further, we introduce a Fourier transform

$$\left\{\vec{E}(\vec{x}_\perp), f_1(\vec{x}_\perp, \vec{v})\right\} = \int d\vec{k}_\perp e^{i\vec{k}_\perp\cdot\vec{x}_\perp}\left\{\vec{E}(\vec{k}_\perp), f_1(\vec{k}_\perp, \vec{v})\right\}. \tag{4.61}$$

The solution of the linear problem is then easily obtained in the form

$$f_1(\vec{k}_\perp, \vec{v}) = \exp\left[i\xi\sin(\alpha-\psi)\right]\sum_l e^{il(\psi-\alpha)}A_l(\vec{k}_\perp, v_\perp, v_z), \tag{4.62}$$

$$A_\ell(\vec{k}_\perp, v_\perp, v_z) = \frac{iq}{T}\frac{f_M}{\omega - \ell\omega_c - k_z v_z}\left\{v_\perp\left[E_x(\vec{k}_\perp)\right.\right.$$

$$\times\left(\cos\psi\,\frac{\ell}{\xi}J_\ell(\xi) - i\sin\psi\,J'_\ell(\xi)\right) + E_y(\vec{k}_\perp)\left(\sin\psi\,\frac{\ell}{\xi}J_\ell(\xi)\right. \tag{4.63}$$

$$\left.\left.\left. + i\cos\psi\,J'_\ell(\xi)\right)\right] + v_z E_z(\vec{k}_\perp)J_\ell(\xi)\right\},$$

where $\xi = |\vec{k}_\perp|v_\perp/\omega_c$, J_ℓ and J'_ℓ are the Bessel function and its derivative, and $tg\psi = k_y/k_x$. In order to satisfy causality the frequency ω is assumed to have a small, positive, imaginary part.

Upon substituting the expressions (4.58) - (4.63) in Eq. (4.57), carrying out the time average and making some rearrangements one obtains

$$P_L(\vec{x}_\perp) = \frac{\pi q^2}{2T}\int d\vec{w}\, f_M \sum_{\ell,p}\delta(\omega - \omega_c\ell - k_z v_z)$$

$$\times\left|\int d\vec{k}_\perp e^{i\vec{k}_\perp\cdot\vec{x}_\perp}\, e^{i\psi(\ell-p)}J_p(\xi)\left\{v_\perp\left[E_x(\vec{k}_\perp)\left(\cos\psi\,\frac{\ell}{\xi}J_\ell(\xi)\right.\right.\right.\right. \tag{4.64}$$

$$\left.\left. - i\sin\psi\,J'_\ell(\xi)\right) + E_y(\vec{k}_\perp)\left(\sin\psi\,\frac{\ell}{\xi}J_\ell(\xi) + i\cos\psi\,J'_\ell(\xi)\right)\right]$$

$$\left.\left. + v_z E_z(\vec{k}_\perp)J_\ell(\xi)\right\}\right|^2.$$

As one can see from this equation the local power absorption density, for a species close to a local thermodynamical equilibrium, is a positive-definite quantity.

It should be noted that for a weakly-damped travelling wave with a wave vector $\vec{k}_{\perp 0}$, i.e., for $\vec{E}(\vec{k}_\perp) \sim \delta(\vec{k}_\perp - \vec{k}_{\perp 0})$, Eq. (4.64) reduces to

$$P_L = \frac{\omega}{8\pi} \vec{E}^* \cdot \overleftrightarrow{\varepsilon}^a \cdot \vec{E} , \tag{4.65}$$

where $\overleftrightarrow{\varepsilon}^a$ is the anti-Hermitian part of the local dielectric tensor for species in question (see, for example, Ref. [208]).

In many situations of a practical interest the Larmor radius of the species, ρ, appears to be much smaller than a characteristic length, $\lambda_\perp$, of the variation of the electromagnetic field. In such cases one can expand the Bessel functions in Eq. (4.64), to any desired order, to obtain more explicit expressions. In what follows we confine ourselves to accuracy up to $(\rho/\lambda_\perp)^2$ and only retain the terms corresponding to the Cerenkov interaction ($\ell = 0$) since it is this one which is relevant to the subject under review.

Upon expanding the Bessel functions to the required order we invert the resulting expressions from the Fourier space to real space and perform the remaining velocity integrations. This finally yields

$$P_{LC}(\vec{x}_\perp) = \frac{q^2 n_0}{2m} \frac{\pi^{1/2}}{|k_z| v_t} \exp\left[-\left(\frac{\omega}{k_z v_t}\right)^2\right]$$

$$\times \left[\rho^2\left(|(\nabla \times \vec{E})_z|^2 + |(\nabla \times \vec{E})_z - \frac{2\omega\omega_c}{k_z v_t^2} E_z|^2\right)\right.$$

$$\left. + \left(\frac{\omega}{k_z \omega_c}\right)^2 \left(\left|\frac{\partial E_z}{\partial x}\right|^2 + \left|\frac{\partial E_z}{\partial y}\right|^2 + 2\,\mathrm{Re}\left(E_z^* \Delta_\perp E_z\right)\right)\right], \tag{4.66}$$

where

$$v_t^2 = \frac{2T}{m}, \quad \rho^2 = \frac{T}{m\omega_c^2}. \tag{4.67}$$

In equation (4.66) the terms proportional to E_z describe the Landau damping while the remaining terms describe the transit time magnetic pumping.

Let us now return to the energy balance equation (4.52). Substituting the expansion (4.54) for f in this equation, taking the time average and summing over all species we obtain, in the quasilinear approximation,

$$\sum_s \int d\vec{v}\, \frac{mv^2}{2} \left\langle \frac{\partial f_2}{\partial t} \right\rangle_t = \left\langle \vec{j} \cdot \vec{E} \right\rangle_t - \nabla \cdot \sum_s \int d\vec{v}\, \frac{mv^2}{2} \vec{v} \langle f_2 \rangle_t, \tag{4.68}$$

where the definition (4.50) has been used. Further, we integrate Eq. (4.68) over the volume occupied by the plasma assuming that $f_2 \to 0$ at the plasma boundary. This yields a global energy balance in the form

$$\int_{V_p} dV \sum_s \int d\vec{v}\, \frac{mv^2}{2} \left\langle \frac{\partial f_2}{\partial t} \right\rangle_t = \int_{V_p} dV \langle \vec{j} \cdot \vec{E} \rangle_t \,. \tag{4.69}$$

On invoking the property $dV = d\vec{x}'$, Eq. (4.69) can be written as

$$\int_{V_p} dV \sum_s P_L(\vec{x}_\perp) = \int_{V_p} dV \, \frac{\omega}{8\pi} \, \mathrm{Im}\, \vec{E}^* \cdot \overleftrightarrow{\varepsilon} \cdot \vec{E}\,, \tag{4.70}$$

where the definition (3.2) has been used. This equation is to be compared with Eq. (3.12).

5. ANTENNAE: VACUUM FIELDS

This section deals with the modelling of antennae and the solutions of Maxwell's equations, Eqs. (3.3) and (3.5), in the vacuum region surrounding the plasma. In accordance with most of the literature under review the antenna is assumed to be a layer of imposed currents satisfying the constraint (3.4). This assumption implies that the resistive losses in the antenna and an electrostatic coupling between the antenna and the fields are neglected. Examples of the vacuum field calculations that take into account more realistic antenna configurations, electrostatic fields, self-consistent current distribution within antenna elements, Faraday's shields and recesses in metallic walls can be found in Refs. [172, 182, 190, 196, 197, 203].

In order to unburden the notation we dispense with the subscript "v" from the electromagnetic field variables throughout this section. Three different geometries are considered: slab, cylindrical and toroidal.

5.1 Cylindrical (Slab) Geometry

As the modelling of antennae and the expressions for electromagnetic fields in these geometries are rather similar we present them in a parallel way.

On adopting cylindrical ($\vec{e}_r$, $\vec{e}_\theta$, $\vec{e}_z$) and Cartesian ($\vec{e}_x$, $\vec{e}_y$, $\vec{e}_z$) coordinate systems, the antenna current density and electromagnetic fields are Fourier-decomposed into modes exp [i(mθ + k_zz)] and exp [i(k_yy + k_zz)] respectively. A single-mode antenna current density is then assumed to be of the form

$$\vec{j}_a = \left(J_\theta \vec{e}_\theta + J_z \vec{e}_z\right)\delta(r-r_a) + j_f(r)\,\Theta(r-r_a)\,\vec{e}_r \,, \qquad (5.1a)$$

$$\vec{j}_a = \left(J_y \vec{e}_y + J_z \vec{e}_z\right)\delta(x-x_a) + j_f\,\Theta(x-x_a)\,\vec{e}_x \,, \qquad (5.1b)$$

$$j_f(r) = -i\,\frac{r_a}{r}\left(\frac{m}{r_a} J_\theta + k_z J_z\right), \qquad (5.2a)$$

$$j_f = -i\left(k_y J_y + k_z J_z\right), \qquad (5.2b)$$

where δ and Θ are the Dirac and Heaviside functions. The term proportional to δ-function in Eq. (5.1) represents an infinitely-thin current-carrying sheet located at r = r_a (x = x_a) with surface currents J_θ (J_y) and J_z while the term proportional to Θ-function represents a volume current flowing in idealized radial feeders located between the antenna and wall (Figs. 1 and 2, feeders are not shown). The surface currents can be treated as a discontinuity of the oscillating magnetic field whereas the feeder current must be included into Maxwell's equations.

For a single mode it can be shown from Eqs. (3.3) and (3.5) that if E_z and B_z are known, the remaining components of $\vec{E}$ and $\vec{B}$ are determined. They are

$$E_r = \frac{1}{\varkappa^2}\left[\frac{\omega}{c}\left(\frac{m}{r}B_z + \frac{4\pi\tilde{\imath}}{c}j_{ar}\right) - i k_z \frac{dE_z}{dr}\right], \tag{5.3}$$

$$E_\theta = \frac{1}{\varkappa^2}\left(k_z \frac{m}{r}E_z + i\frac{\omega}{c}\frac{dB_z}{dr}\right), \tag{5.4}$$

$$B_r = -\frac{1}{\varkappa^2}\left(i k_z \frac{dB_z}{dr} + \frac{\omega}{c}\frac{m}{r}E_z\right), \tag{5.5}$$

$$B_\theta = \frac{1}{\varkappa^2}\left[k_z\left(\frac{m}{r}B_z + \frac{4\pi\tilde{\imath}}{c}j_{ar}\right) - i\frac{\omega}{c}\frac{dE_z}{dr}\right], \tag{5.6}$$

where

$$\varkappa^2 = k_z^2 - \left(\frac{\omega}{c}\right)^2 . \tag{5.7}$$

The boundary conditions at the antenna are given by

$$\vec{e}_r \times \vec{B}(r_a)\Big|_-^+ = \frac{4\pi}{c}\vec{J}, \tag{5.8}$$

$$\vec{e}_r \times \vec{E}(r_a)\Big|_-^+ = 0, \tag{5.9}$$

where $\Big|_-^+$ denotes the jump across the boundary. The corresponding equations in the slab geometry are obtained from Eqs. (5.3) - (5.9) by the replacements $r \to x$, $\theta \to y$ and $m/r \to k_y$.

The component B_z satisfies the inhomogeneous equation

$$\left[\frac{1}{r}\frac{d}{dr} r \frac{d}{dr} - \left(\mathcal{K}^2 + \frac{m^2}{r^2}\right)\right] B_z = \frac{im}{r}\frac{4\pi}{c} j_{ar} \tag{5.10a}$$

$$\left(\frac{d^2}{dx^2} - k_x^2\right) B_z = i k_y \frac{4\pi}{c} j_{ax}, \tag{5.10b}$$

where

$$k_x^2 = k_y^2 + \mathcal{K}^2, \tag{5.11}$$

while the component E_z satisfies the homogeneous equation (5.10). On introducing the notation $f(r_j) \equiv f_j$ for j = p, a, w (plasma, antenna, wall), we define the following set of fundamental solutions of the homogeneous equation (5.10):

$$F(r) \quad \text{for} \quad r \in \langle r_p, r_w \rangle \quad \text{with} \quad F_w = 0, \; F_w' = 1, \tag{5.12}$$

$$G(r) \text{ for } r \in \langle r_p, r_a \rangle \text{ with } G_a = 0,\ G'_a = 1, \tag{5.13}$$

$$H(r) \text{ for } r \in \langle r_p, r_w \rangle \text{ with } H_w = 1,\ H'_w = 0, \tag{5.14}$$

where the prime denotes differentiation with respect to r. Let further K(r) be a particular solution of the inhomogeneous equation (5.10) satisfying

$$K_w = K'_w = 0. \tag{5.15}$$

The same definitions are used in the case of the slab geometry with $r \rightarrow x$.

The set of functions defined above can be obtained either analytically or by a numerical integration of Eq. (5.10). The analytical expressions are listed below:

$$F(r) = r_w \left[K_m(\varkappa r_w) I_m(\varkappa r) - I_m(\varkappa r_w) K_m(\varkappa r) \right], \tag{5.16a}$$

$$F(x) = \frac{1}{k_x} \sinh \left[k_x (x - x_w) \right], \tag{5.16b}$$

$$G(r) = r_a \left[K_m(\varkappa r_a) I_m(\varkappa r) - I_m(\varkappa r_a) K_m(\varkappa r), \right. \tag{5.17a}$$

$$G(x) = \frac{1}{k_x} \sinh\left[k_x (x - x_a)\right], \tag{5.17b}$$

$$H(r) = r_w \left[I_m'(\alpha r_w) K_m(\alpha r) - K_m'(\alpha r_w) I_m(\alpha r)\right], \tag{5.18a}$$

$$H(x) = \cosh\left[k_x (x - x_w)\right], \tag{5.18b}$$

$$K(r) = im \frac{4\tilde{\pi}}{c} \int_{r_w}^{r} dr' \left[I_m(\alpha r) K_m(\alpha r') - K_m(\alpha r) I_m(\alpha r')\right] j_f(r'), \tag{5.19a}$$

$$K(x) = \frac{i k_y}{k_x^2} \frac{4\tilde{\pi}}{c} j_f \left\{\cosh\left[k_x (x - x_w)\right] - 1\right\}, \tag{5.19b}$$

where I_m and K_m are modified Bessel functions.

We are now in a position to construct the solutions for E_z and B_z in terms of the tangential components of $\vec{E}$ evaluated at the plasma-vacuum interface, which are as yet unknown constants. Invoking the boundary conditions (3.8), (5.8) and (5.9) the desired solutions can be written in the form

$$E_z(r) = \begin{cases} C_1 F(r), & r > r_a \\ C_1 F(r) + i \frac{\omega}{c} \frac{4\tilde{\pi}}{c} J_z G(r), & r < r_a \end{cases}, \tag{5.20}$$

$$C_1 = \frac{1}{F_p}\left(E_z(r_p) - \frac{i\omega}{c}\,\frac{4\pi}{c}\,J_z\,G_p \right), \tag{5.21}$$

$$B_z(r) = \begin{cases} C_2\,H(r) + K(r) & , r > r_a \\ C_3\,H(r) + C_4\,G(r) & , r < r_a \end{cases}, \tag{5.22}$$

$$C_2 = \frac{1}{H'_p}\left[i\frac{c}{\omega}\left(k_z \frac{m}{r_p} E_z(r_p) - \gamma^2 E_\theta(r_p) \right) \right.$$

$$\left. + \frac{1}{H_a}\left(K_a + \frac{4\pi}{c} J_\theta\right)\left(G'_p H'_a - H'_p\right) - K'_a\,G'_p \right], \tag{5.23}$$

$$C_3 = C_2 + \frac{1}{H_a}\left(K_a + \frac{4\pi}{c} J_\theta\right), \tag{5.24}$$

$$C_4 = K'_a - \frac{H'_a}{H_a}\left(K_a + \frac{4\pi}{c} J_\theta\right). \tag{5.25}$$

The constants $E_z(r_p)$ and $E_\theta(r_p)$ will be determined later by means of the boundary conditions (3.6) and (3.7) when the solutions of Maxwell's equations in the plasma region will be considered. For this purpose we shall also need the

tangential components of $\vec{B}$ evaluated at the plasma-vacuum interface. They are easily obtained from Eqs. (5.6) and (5.20) - (5.25) as

$$B_z(r_p) = \frac{1}{H_p'}\left\{ i\frac{c}{\omega} H_p \left(k_z \frac{m}{r_p} E_z(r_p) - \mathcal{R}^2 E_\theta(r_p) \right) \right.$$
$$\left. + R_{ap}\left[H_a' \left(K_a + \frac{4\pi\tilde{\sigma}}{c} J_\theta \right) - H_a K_a' \right] \right\} , \qquad (5.26)$$

$$B_\theta(r_p) = \frac{1}{\mathcal{R}^2}\left\{ i\frac{c}{\omega}\left[\left(\frac{H_p}{H_p'}\left(k_z \frac{m}{r_p}\right)^2 - \left(\frac{\omega}{c}\right)^2 \frac{F_p'}{F_p} \right) E_z(r_p) \right.\right.$$
$$\left. - \frac{H_p}{H_p'} k_z \frac{m}{r_p} \mathcal{R}^2 E_\theta(r_p) \right] + R_{ap}\left[\left(\frac{\omega}{c}\right)^2 \frac{F_a}{F_p} \frac{4\pi\tilde{\sigma}}{c} J_z \qquad (5.27)$$
$$\left. + k_z \frac{m}{r_p} \frac{1}{H_p'} \left(H_a' \left[K_a + \frac{4\pi\tilde{\sigma}}{c} J_\theta \right] - H_a K_a' \right) \right] \right\} ,$$

where $R_{ap} = r_a/r_p$. In the slab geometry, the expressions corresponding to Eqs. (5.20)-(5.27) are obtained by setting $R_{ap} = 1$ and the replacements $r \to x$, $\theta \to y$ and $m/r_p \to k_y$ in Eqs. (5.20) - (5.27). In the region $x < 0$, one has to set $\vec{J} = 0$ and $x \to -x$.

Having determined the vacuum electromagnetic fields one can calculate the complex power delivered by the antenna, Eqs. (3.12) and (3.13). One obtains

$$\tilde{P} \equiv P - iP_c = \tilde{\sigma} r_a L_z \frac{\omega}{c\mathcal{R}^2}\left\{ i J_\theta \left(C_2 H_a' + K_a' \right) - \frac{\omega}{c} J_z C_1 F_a \right.$$
$$\left. - j_f(r_a)\left[m \int_{r_a}^{r_w} \frac{dr}{r}\left(C_2 H(r) + K(r) \right) + i\frac{4\pi\tilde{\sigma}}{c} r_a j_f(r_a) \ln\frac{r_w}{r_a} \right] \right\} , \qquad (5.28a)$$

$$\tilde{P} = \frac{L_y L_z}{2} \frac{\omega}{c\,\mathcal{R}^2} \left[\left(i J_y + \frac{k_y}{k_x^2} j_f \right) \left(C_2 H_a' + K_a' \right) \right.$$

$$\left. - \frac{\omega}{c} J_z C_1 F_a + \frac{4\pi i}{c} \left(\frac{\mathcal{R}}{k_x} \right)^2 |j_f|^2 (\chi_w - \chi_a) \right] , \tag{5.28b}$$

where L_z and L_y are the dimensions of the system in the z and y directions.

Let us note that for a pure helical antenna without feeders, i.e. with $j_f(r)$ or j_f equal to zero, or for an antenna with $J_z = 0$ one can define the total current in the antenna to be

$$I \equiv J_\theta \int_{-\pi/(2k_z)}^{\pi/(2k_z)} dz \exp(i k_z z) = \frac{2}{k_z} J_\theta , \tag{5.29}$$

and introduce the antenna impedance Z by the relation

$$Z = \frac{2\tilde{P}}{I^2} . \tag{5.30}$$

Concluding this section we should like to mention that the expressions presented here, which have been incorporated in the most recent version of the numerical code ISMENE [171], reduce to those previously obtained in various

limiting cases: slab geometry [62, 65, 81, 165], cylindrical geometry — pure helical antenna [75, 93, 96, 107, 112, 121, 123, 128, 135], cylindrical geometry — antenna with feeders [36, 111, 142, 162, 166]. Moreover, notice that we have only considered single-mode travelling wave antennae. The Fourier decomposition of current density in more realistic antennae (finite length, standing wave) can be found in Refs. [36, 104, 142, 157, 162].

5.2 Toroidal Geometry

This geometry has been considered in Refs. [109, 166].

For the description of the antenna configuration, a toroidal coordinate system (ρ, θ, φ) is used, where ρ denotes the distance from the magnetic axis, θ is the poloidal angle and φ is the toroidal angle (Fig. 3). The antenna is modelled by a current-carrying sheet with a current density

$$\vec{j}_a = \delta(a)\nabla a \times \nabla b, \tag{5.31}$$

where

$$a \equiv \rho - \rho_a(\theta) = 0 \tag{5.32}$$

defines an antenna surface Σ_a and b is a current potential. For a single-mode helical antenna, the potential is assumed to be

$$b = -b_0 \exp\left[i(m\theta + n\varphi)\right] , \tag{5.33}$$

where b_0 is a constant related to the total antenna current by

$$I = 2b_0 . \tag{5.34}$$

In the references cited, only the plasma models with $\vec{E} \cdot \vec{B}_0 = 0$ in the plasma are treated. For such models the boundary conditions (3.6) at the plasma-vacuum interface can be replaced by

$$\vec{n}_p \cdot \vec{B}\Big|_-^+ = 0 . \tag{5.35}$$

It is then sufficient to determine only the magnetic field component of the vacuum electromagnetic oscillations. Moreover, the treatment is confined to the case of negligible displacement current.

The relevant equations, which follow from Eqs. (3.3) and (3.5), are thus

$$\nabla \times \vec{B} = 0 , \tag{5.36}$$

$$\nabla \cdot \vec{B} = 0 , \tag{5.37}$$

with the boundary conditions at the antenna

$$\vec{n}_a \times \vec{B}\Big|_-^+ = \frac{4\pi}{c}\vec{n}_a \times \nabla b, \tag{5.38}$$

$$\vec{n}_a \cdot \vec{B}\Big|_-^+ = 0, \tag{5.39}$$

where $\vec{n}_a$ is the outer normal unit vector at the antenna surface. The boundary condition at the wall, which follows from Eq. (3.8), is

$$\vec{n}_w \cdot \vec{B} = 0 \ . \tag{5.40}$$

The aim is to establish a relation between $\vec{n}_p \bullet \vec{B}$ and $\vec{n}_p \times \vec{B}$ at the plasma-vacuum interface. This allows one to match the vacuum solutions onto the solutions of Maxwell's equations in the plasma region via the boundary conditions (3.7) and (5.35). To this end, the magnetic potential is introduced by

$$\vec{B} = \nabla \Phi \ . \tag{5.41}$$

Equation (5.36) is thus satisfied identically and Eq. (5.37) implies

$$\Delta \underline{\phi} = 0, \tag{5.42}$$

while the boundary conditions (5.38) - (5.40) written in terms of the potential are

$$\underline{\phi}(\vec{x}_a)\Big|_-^+ = \frac{4\pi}{c} b(\vec{x}_a), \tag{5.43}$$

$$\vec{n}_a \cdot \nabla \underline{\phi}(\vec{x}_a)\Big|_-^+ = 0, \tag{5.44}$$

$$\vec{n}_w \cdot \nabla \underline{\phi}(\vec{x}_w) = 0. \tag{5.45}$$

Equation (5.42) is solved by means of the Green's function technique. The desired relation is then obtained in the form

$$\underline{\phi}(\vec{x}_p) = Q_{pp}\, \vec{n}_p \cdot \nabla \underline{\phi}(\vec{x}_p) + \underline{\phi}_e(\vec{x}_p), \tag{5.46}$$

where

$$Q_{pp} = M_{pp}^{-1}\left[E_{pp} + (2\hat{\underline{I}} - D_{pw}) D_{ww}^{-1} E_{wp}\right], \tag{5.47}$$

$$M_{pp} = D_{pp} - 2\hat{\underline{I}} + (2\hat{\underline{I}} - D_{pw}) D_{ww}^{-1} D_{wp} \tag{5.48}$$

and

$$\underline{\Phi}_e(\vec{x}_p) = M_{pp}^{-1}\left[\left(D_{pw} - 2\hat{I}\right)D_{ww}^{-1}D_{wa} + 2\hat{I} - D_{pa}\right]\frac{4\tilde{\pi}}{c}b(\vec{x}_a). \tag{5.49}$$

Here, $\hat{I}$ is the unit operator, and the integral operators $D_{\mu\nu}$ and $E_{\mu\nu}$, where $\mu,\nu = p, a, w$, are defined by

$$D_{\mu\nu}f(\vec{x}_\nu) = \frac{1}{2\tilde{\pi}}\int_{\Sigma_\nu} d\Sigma'\left[f(\vec{x}') - f(\vec{x}_\nu)\right]\vec{n}_\nu\cdot\nabla' G(\vec{x}_\mu, \vec{x}'), \tag{5.50}$$

$$E_{\mu\nu}f(\vec{x}_\nu) = \frac{1}{2\tilde{\pi}}\int_{\Sigma_\nu} d\Sigma'\, G(\vec{x}_\mu, \vec{x}')\vec{n}_\nu\cdot\nabla' f(\vec{x}'), \tag{5.51}$$

where

$$G(\vec{x},\vec{x}') = \frac{1}{|\vec{x}-\vec{x}'|}. \tag{5.52}$$

The complex power emitted by the antenna is shown to be

$$\tilde{P} = \frac{i\omega}{2c}\int_{\Sigma_a} d\Sigma\; b^*(\vec{x}_a)\,\vec{n}_a\cdot\vec{B}(\vec{x}_a), \tag{5.53}$$

where

$$\vec{n}_a\cdot\vec{B}(\vec{x}_a) = T_{pa}^{-1}\left[\left(V_{pp} - U_{pp}Q_{pp}\right)\vec{n}_p\cdot\nabla\underline{\Phi}(\vec{x}_p) - U_{pp}\underline{\Phi}_e(\vec{x}_p)\right] \tag{5.54}$$

and

$$U_{pp} = D_{pp} - 2\hat{I} + (2\hat{I} - D_{pa}) D_{aa}^{-1} D_{ap} \,, \tag{5.55}$$

$$T_{pa} = E_{pa} + (2\hat{I} - D_{pa}) D_{aa}^{-1} E_{aa} \,, \tag{5.56}$$

$$V_{pp} = E_{pp} + (2\hat{I} - D_{pa}) D_{aa}^{-1} E_{ap} \,. \tag{5.57}$$

Expressions (5.46) - (5.57) are evaluated numerically.

6. DIELECTRIC TENSOR OPERATORS

6.1 Slab Geometry

In this geometry the equilibrium magnetic field is assumed to be uniform, $\vec{B}_0 = B_0 \vec{e}_z$, B_0 = const, while the plasma equilibrium quantities in general vary in the x direction. For the description of the plasma dynamics the following two models are considered:

Two fluids

We confine ourselves to the case for which the inequalities (4.6) and (4.19) hold. On combining Eqs. (3.2) and (4.24), and neglecting terms of O (m_e/m_i) we can then write the dielectric tensor in the form

$$\varepsilon_{xx} = \varepsilon_{yy} = \varepsilon_1 \equiv \left(\frac{c}{c_A}\right)^2 \frac{1}{1 - (\omega/\omega_{ci})^2} \quad , \tag{6.1}$$

$$\varepsilon_{xy} = -\varepsilon_{yx} = i\varepsilon_2 \equiv i \frac{\omega}{\omega_{ci}} \varepsilon_1 \quad , \tag{6.2}$$

$$\varepsilon_{zz} = \varepsilon_3 \equiv -\frac{\omega_{pe}^2}{\omega^2} \quad , \tag{6.3}$$

where

$$C_A^2 = \frac{B_o^2}{4\pi m_i n_o} \quad , \quad \omega_{pe}^2 = \frac{4\pi e^2 n_o}{m_e} \quad . \tag{6.4}$$

The remaining components of the tensor are equal to zero.

Expressions (6.1) - (6.3) can easily be generalized for the case when the resistive term, Eq. (4.27), is included in Eq. (4.22). One finds that the expressions corresponding to Eqs. (6.1) - (6.3) are obtained by the replacements

$$\varepsilon_1 \rightarrow \left(\frac{c}{c_A}\right)^2 \frac{1 - i\,\frac{\nu_{ei}}{\omega_{ce}}\,\frac{\omega}{\omega_{ci}}}{\left(1 - i\,\frac{\nu_{ei}}{\omega_{ce}}\,\frac{\omega}{\omega_{ci}}\right)^2 - \left(\frac{\omega}{\omega_{ci}}\right)^2} \quad , \tag{6.5}$$

$$\varepsilon_2 \rightarrow \left(\frac{c}{c_A}\right)^2 \frac{\frac{\omega}{\omega_{ci}}}{\left(1 - i\,\frac{\nu_{ei}}{\omega_{ce}}\,\frac{\omega}{\omega_{ci}}\right)^2 - \left(\frac{\omega}{\omega_{ci}}\right)^2} \quad , \tag{6.6}$$

$$\varepsilon_3 \rightarrow - \frac{\omega_{pe}^2}{\omega(\omega + i\nu_{ei})} \quad , \tag{6.7}$$

where ν_{ei} is the electron-ion collision frequency, which is related to the electrical conductivity by

$$\sigma = \frac{e^2 n_o}{m_e \nu_{ei}} \quad . \tag{6.8}$$

The local power absorption density due to resistivity can be calculated using either Eq. (4.32) or Eq. (4.65), which are equivalent in view of Eq. (4.31).

An expression for the dielectric tensor that would include the effects of ion viscosity has not been obtained as yet. Nevertheless, one can calculate the local power absorption density due to viscosity in an approximate way. On obtaining $\vec{E}$ from Maxwell's equations in the absence of viscosity terms, one can determine the ion velocity, $\vec{V}_i$, from Eq. (4.22) and then evaluate the power absorption using the expression (4.33). This procedure, of course, makes sense only if the absorption is weak.

It is worth noting that the dielectric tensor of the present model is not an operator. It can therefore easily be transformed into other geometries.

Hot collisionless plasma

In order to establish a relation between the induced current density and the electric field one has to solve the linearized Eq. (4.49). On performing the Fourier decomposition this equation simplifies to

$$i(\omega - k_z v_z) f_1 - (i k_y v_y + v_x \frac{\partial}{\partial x}) f_1 - \omega_c \vec{v} \times \vec{e}_z \cdot \frac{\partial f_1}{\partial \vec{v}}$$

$$= \frac{q}{m} \left[\vec{E} + \frac{1}{i\omega} \vec{v} \times (\nabla \times \vec{E}) \right] \cdot \frac{\partial f_0}{\partial \vec{v}} \,, \qquad (6.9)$$

where Eq. (3.5) has been used.

The equilibrium distribution function obeys

$$v_x \frac{\partial f_0}{\partial x} + \omega_c \vec{v} \times \vec{e}_z \cdot \frac{\partial f_0}{\partial \vec{v}} = 0 , \tag{6.10}$$

which is satisfied if

$$f_0 = F(v_\perp, v_z, X = x + \frac{v_y}{\omega_c}) , \tag{6.11}$$

F being an arbitrary function.

On introducing the following two small parameters

$$\delta_f \sim \left| \frac{\partial \vec{E}}{\partial x} \right| \frac{\rho}{|\vec{E}|} \sim k_y \rho , \tag{6.12}$$

$$\delta_p \sim \left| \frac{\partial f_0}{\partial x} \right| \frac{\rho}{|f_0|} , \tag{6.13}$$

---

equation (6.9) can be solved by a perturbation method. The solution valid up to δ^2_f and δ^2_p has been obtained in Ref. [174]. Knowing f_1 in terms of $\vec{E}$ one can calculate the induced current density from the linear part of Eq. (4.50). To this end, one needs to specify the distribution function F. In the reference cited this function has been assumed to be a Maxwellian with n_0 and T being arbitrary functions of X. On carrying out the velocity integrations in Eq. (4.50) and recalling the definition (3.2) one then obtains a final expression for the dielectric tensor operator.

For the sake of brevity we shall use the notation

$$\tilde{Z}_\ell = \frac{\omega_p^2}{\omega - \ell\omega_c} Z\left(\frac{\omega - \ell\omega_c}{|k_z| v_t}\right), \tag{6.14}$$

$$Z_\ell = \frac{T}{m} \tilde{Z}_\ell , \tag{6.15}$$

where

$$Z(x) = x \exp(-x^2)\left[2\int_0^x \exp(x'^2)\,dx' - i\pi^{1/2}\right] \tag{6.16}$$

is the plasma dispersion function as defined in Ref. [212] and ω_p is the plasma frequency of the species in question. In the present review we shall write the expression for the dielectric operator ignoring all terms of O (δ^2_p) and only retaining the terms of O (δ_p) corresponding to the Cerenkov interaction. We thus have

$$\overleftrightarrow{\varepsilon} = \frac{d}{dx}\overleftrightarrow{\alpha}\frac{d}{dx} + \overleftrightarrow{\beta}\frac{d}{dx} + \frac{d}{dx}\overleftrightarrow{\beta}^{+} + \overleftrightarrow{\gamma} , \tag{6.17}$$

where

$$\overleftrightarrow{\alpha} = \begin{pmatrix} \alpha_{xx} & \alpha_{xy} & 0 \\ -\alpha_{xy} & \alpha_{yy} & 0 \\ 0 & 0 & \alpha_{zz} \end{pmatrix} \tag{6.18}$$

with

$$\alpha_{xx} = \frac{1}{2\omega\omega_c^2}\left(Z_2 + Z_{-2} - Z_1 - Z_{-1}\right),$$

$$\alpha_{xy} = \frac{i}{2\omega\omega_c^2}\left(Z_2 - Z_{-2} - 2Z_1 + 2Z_{-1}\right),$$

$$\alpha_{yy} = \frac{1}{2\omega\omega_c^2}\left(Z_2 + Z_{-2} - 3Z_1 - 3Z_{-1} + 4Z_0\right),$$

$$\alpha_{zz} = \frac{1}{2\omega\omega_c^2 k_z^2}\left[(\omega-\omega_c)^2\tilde{Z}_1 + (\omega+\omega_c)^2\tilde{Z}_{-1} - 2\omega^2\tilde{Z}_0\right],$$

$$\overleftrightarrow{\beta} = \begin{pmatrix} 0 & \beta_{xy} & \beta_{xz} \\ 0 & 0 & \beta_{yz} \\ 0 & 0 & 0 \end{pmatrix}, \quad \overleftrightarrow{\beta}^{+} = \begin{pmatrix} 0 & 0 & 0 \\ \beta_{xy} & 0 & 0 \\ \beta_{xz} & -\beta_{yz} & 0 \end{pmatrix} \tag{6.19}$$

with

$$\beta_{xy} = \frac{ik_y}{\omega\,\omega_c^2}\left(Z_1 + Z_{-1} - 2Z_0\right),$$

$$\beta_{xz} = \frac{i}{2\omega\omega_c k_z}\left[(\omega-\omega_c)\tilde{Z}_1 - (\omega+\omega_c)\tilde{Z}_{-1}\right],$$

$$\beta_{yz} = \frac{1}{2\omega\omega_c k_z}\left[(\omega-\omega_c)\tilde{Z}_1 + (\omega+\omega_c)\tilde{Z}_{-1} - 2\omega\tilde{Z}_0\right],$$

and

$$\gamma_{xx} = \gamma_{xx}^{(0)} - k_y^2 \alpha_{yy} ,$$

$$\gamma_{xy} = -\gamma_{yx} = \gamma_{xy}^{(0)} - k_y^2 \alpha_{xy} ,$$

$$\gamma_{xz} = -\gamma_{zx} = -i k_y \beta_{yz} ,$$

$$\gamma_{yy} = \gamma_{xx}^{(0)} - k_y^2 \alpha_{xx} ,$$

$$\gamma_{yz} = \gamma_{zy} = i k_y \beta_{xz} + \frac{1}{\omega \omega_c k_z} \frac{d}{d\nu} \left(\omega_p^2 - \omega \tilde{Z}_o \right), \qquad (6.20)$$

$$\gamma_{zz} = \gamma_{zz}^{(0)} - k_y^2 \alpha_{zz} + \frac{k_y}{\omega \omega_c k_z^2} \frac{d}{d\nu} \left(\omega \tilde{Z}_o - \omega_p^2 \right),$$

$$\gamma_{xx}^{(0)} = 1 - \frac{1}{2\omega} \left(\tilde{Z}_1 + \tilde{Z}_{-1} \right),$$

$$\gamma_{xy}^{(0)} = \frac{i}{2\omega} \left(\tilde{Z}_{-1} - \tilde{Z}_1 \right),$$

$$\gamma_{zz}^{(0)} = 1 + \frac{2}{(k_z v_t)^2} \left(\omega_p^2 - \omega \tilde{Z}_o \right) .$$

It should be noted that in writing Eqs. (6.18) - (6.20) the symbol denoting the sum over the plasma species has been omitted in order to simplify notation.

As can be seen from Eqs. (6.17) - (6.20) the dielectric tensor operator is of a Hermitian form, i.e. exhibits certain symmetry properties. On the other hand, it does not satisfy the Onsager reciprocity relation, since $\gamma_{ik}(-B_o) \neq \gamma_{ki}(B_o)$. The

reason for this symmetry breaking is the fact that the unperturbed state of the system in question, described by the distribution function F, is not a state of a thermodynamical equilibrium, but only a steady state.

For an evaluation of the local power absorption by a plasma species via the Cerenkov interaction, which would be consistent with Eqs. (6.17) - (6.20), the expression (4.66) must be generalized to include terms of O (δ_p). This can easily be done by using the expression for f_1 obtained in Ref. [174]. On substituting this in Eq. (4.57) we find that Eq. (4.66) is to be replaced by

$$P_L(x) = \frac{1}{8\pi^{1/2}|k_z|}\left[\rho^2\left(\left|\frac{dE_y}{dx} - ik_y E_x\right|^2 + \left|\frac{dE_y}{dx} - ik_y E_x - \frac{2\omega\omega_c}{k_z v_t^2}E_z\right|^2\right)\right.$$

$$+ \left(\frac{\omega}{k_z\omega_c}\right)^2\left(\left|\frac{dE_z}{dx}\right|^2 + 2\,Re\left(E_z^*\frac{d^2E_z}{dx^2}\right) - k_y^2|E_z|^2 + \frac{d|E_z|^2}{dx}\frac{d}{dx}\right) \qquad (6.21)$$

$$\left. - \frac{\omega}{\omega_c}\frac{k_y}{k_z^2}|E_z|^2\frac{d}{dx}\right]\frac{\omega_p^2}{v_t}\exp\left[-\left(\frac{\omega}{k_z v_t}\right)^2\right].$$

According to Eq. (3.9) the local power balance in the plasma is given by

$$\frac{dS_x}{dx} + \frac{\omega}{8\pi}\,Im\left(\vec{E}^*\cdot\overleftrightarrow{\varepsilon}\cdot\vec{E}\right) = 0. \qquad (6.22)$$

Equations (6.17) - (6.21) allow one to cast this balance into a more explicit and interpretable form. On dispensing with the dissipative parts of the plasma dispersion functions that correspond to cyclotron resonances — which are of no

interest for the frequency range considered — and making some re-arrangements one obtains

$$\frac{d}{dx}\left(S_x + S_T\right) + \sum_s P_L(x) = 0, \tag{6.23}$$

where

$$S_T = \frac{\omega}{8\pi} Im\left[\vec{E}^* \cdot \overleftrightarrow{\alpha} \cdot \frac{d\vec{E}}{dx} + \vec{E}^* \cdot \overleftrightarrow{\beta}^+ \cdot \vec{E}\right.$$
$$\left. + 2\beta_{yz} Re\left(E_y E_z^*\right) - \alpha_{zz} \frac{d|E_z|^2}{dx}\right] \tag{6.24}$$

is the energy flux density due to coherent finite-Larmor-radius motion of the plasma particles in the electric field or, briefly, the kinetic flux.

6.2 Cylindrical Geometry

In this geometry all equilibrium quantities are assumed to vary in the r direction. The equilibrium magnetic field is given by

$$\vec{B}_o = B_{o\theta}(r)\vec{e}_\theta + B_{oz}(r)\vec{e}_z \quad , \tag{6.25}$$

which is the most general form compatible with Eq. (4.13). Using Eq. (6.25) we define the quantities b_θ and b_z such that

$$\vec{e}_{\parallel} = \frac{\vec{B}_o}{B_o} \equiv b_\theta \vec{e}_\theta + b_z \vec{e}_z \quad , \tag{6.26}$$

and introduce a local magnetic coordinate system $(\vec{e}_r, \vec{e}_\perp, \vec{e}_\parallel)$ where

$$\vec{e}_\perp = \vec{e}_\parallel \times \vec{e}_r \quad . \tag{6.27}$$

For the description of the plasma dynamics we consider the following two models:

Cold plasma with an equilibrium current

We project Eq. (4.21) on the magnetic coordinate system and eliminate $\vec{j}_0$ in favour of $\vec{B}_0$, and $\vec{B}$ in favour of $\vec{E}$ via Eqs. (4.12) and (3.5). On Fourier-decomposing the resulting expression and combining it with Eq. (3.2) we find, after some manipulation, the dielectric tensor in the form

$$\begin{aligned}
\varepsilon_{rr} &= \varepsilon_1 , \\
\varepsilon_{r\perp} &= -\varepsilon_{\perp r} = i\left[\varepsilon_2 - \left(\frac{c}{\omega}\right)^2 k_\parallel \frac{b_z^2}{r}\frac{d}{dr}\left(r\frac{b_\theta}{b_z}\right)\right], \\
\varepsilon_{\perp\perp} &= \varepsilon_1 - \left(\frac{c}{\omega}\right)^2 \frac{b_z^2}{r}\frac{d}{dr}\left(r\frac{b_\theta}{b_z}\right)\frac{b_\theta^2}{r}\frac{d}{dr}\left(r\frac{b_z}{b_\theta}\right),
\end{aligned} \tag{6.28}$$

where

$$k_\parallel = b_\theta \frac{m}{r} + b_z k_z , \tag{6.29}$$

and the quantities ε_1 and ε_2 are given by Eqs. (6.1) and (6.2).

Expressions equivalent to Eq. (6.28) have been obtained in Refs. [56, 135, 151] and for the case $|b_\theta| << 1$ in Refs. [119, 126]. In the limit $\omega/\omega_{ci} \to 0$, Eq. (6.28) reduces to the dielectric tensor of force-free MHD [106].

Hot collisionless plasma

From Eqs. (6.17) - (6.20) it is in general not possible to infer the form of the dielectric tensor operator pertinent to the cylindrical geometry. It has been therefore necessary to repeat the derivation in analogy to that of Ref. [174]. The essential features of the derivation are outlined in the Appendix. The results have briefly been reported in Ref. [178]. A limiting form of the operator for the cylindrical geometry has been derived (in a heuristic fashion) from the slab model in Ref. [107].

We restrict ourselves to the same accuracy as in Eqs. (6.17) - (6.20). Moreover, we assume $|b_\theta| << 1$ and retain only terms of $O(|b_\theta|)$. We can then write

$$\overleftrightarrow{\mathcal{E}} = \frac{1}{r}\frac{d}{dr} r \overleftrightarrow{\alpha} \frac{d}{dr} + \overleftrightarrow{\beta}\frac{d}{dr} + \frac{1}{r}\frac{d}{dr} r \overleftrightarrow{\beta}^{+} + \overleftrightarrow{\gamma} \tag{6.30}$$

where, in the magnetic coordinates, the tensors $\overleftrightarrow{\alpha}$, $\overleftrightarrow{\beta}$, $\overleftrightarrow{\beta}^{+}$ and $\overleftrightarrow{\gamma}$ have the same structure and symmetry properties as in the slab geometry. Their components are given by

$$\alpha_{rr} = \alpha_{xx}\,, \quad \alpha_{r\perp} = \alpha_{xy}\,, \quad \alpha_{\perp\perp} = \alpha_{yy}\,, \quad \alpha_{\parallel\parallel} = \alpha_{zz}\,, \tag{6.31}$$

$$\beta_{r\perp} = ik_\perp(\alpha_{xx} - \alpha_{yy})\,, \quad \beta_{r\parallel} = \beta_{xz}\,, \quad \beta_{\perp\parallel} = \beta_{yz}\,, \tag{6.32}$$

and

$$\gamma_{rr} = \gamma_{xx}^{(0)} - \left(\frac{\alpha_{xx}}{r^2} + k_\perp^2 \alpha_{yy} - \frac{2i}{r} k_\perp \alpha_{xy}\right),$$

$$\gamma_{r\perp} = \gamma_{xy}^{(0)} - \left[\alpha_{xy}\left(\frac{1}{r^2} + k_\perp^2\right) + \frac{i k_\perp}{r}\left(\alpha_{xx} + \alpha_{yy}\right)\right] - i\left(\frac{c}{\omega}\right)^2 \frac{k_\parallel}{r} \frac{d}{dr}(r b_\theta),$$

$$\gamma_{r\parallel} = -i k_\perp \beta_{yz},$$

$$\gamma_{\perp\perp} = \gamma_{xx}^{(0)} - \left(\frac{\alpha_{yy}}{r^2} + k_\perp^2 \alpha_{xx} - \frac{2i}{r} k_\perp \alpha_{xy}\right) + \frac{2}{\omega \omega_c^2} \frac{1}{r} \frac{d}{dr} Z_o \tag{6.33}$$

$$\gamma_{\perp\parallel} = i k_\perp \beta_{xz} + \frac{1}{\omega \omega_c k_\parallel} \frac{d}{dr}\left(\omega_p^2 - \omega \tilde{Z}_o\right),$$

$$\gamma_{\parallel\parallel} = \gamma_{zz}^{(0)} - k_\perp^2 \alpha_{zz} + \frac{k_\perp}{\omega \omega_c k_\parallel^2} \frac{d}{dr}\left(\omega \tilde{Z}_o - \omega_p^2\right),$$

where k_z in the arguments of the plasma dispersion functions is to be replaced by $k_\parallel$, and

$$k_\perp = \frac{m}{r} b_z - k_z b_\theta \,. \tag{6.34}$$

The analogues of Eqs. (6.21), (6.23) and (6.24) for the geometry in question read

$$P_L(r) = \frac{1}{8\sqrt{\pi}^{1/2}} \left\{ \rho^2 \left(\left| \frac{1}{r} \frac{d}{dr} r E_\perp - i k_\perp E_r \right|^2 + \left| \frac{1}{r} \frac{d}{dr} r E_\perp - i k_\perp E_r \right. \right.\right.$$

$$\left.\left. - \frac{2\omega\omega_c}{k_\parallel v_t^2} E_\parallel \right|^2 \right) + \left(\frac{\omega}{k_\parallel \omega_c}\right)^2 \left[\left| \frac{dE_\parallel}{dr} \right|^2 + 2 \mathrm{Re}\left(E_\parallel^* \frac{1}{r} \frac{d}{dr} r \frac{dE_\parallel}{dr} \right) \right. \tag{6.35}$$

$$\left. - k_\perp^2 |E_\parallel|^2 + \frac{d|E_\parallel|^2}{dr} \frac{d}{dr} \right] - \frac{\omega}{\omega_c} \frac{k_\perp}{k_\parallel^2} |E_\parallel|^2 \frac{d}{dr} \Bigg\} \frac{\omega_p^2}{|k_\parallel| v_t}$$

$$\times \exp\left[- \left(\frac{\omega}{k_\parallel v_t}\right)^2 \right],$$

$$\frac{1}{r}\frac{d}{dr}r\left(S_r + S_T\right) + \sum_S P_L(r), \tag{6.36}$$

and

$$S_T = \frac{\omega}{8\pi}\,\mathrm{Im}\left[\vec{E}^*\cdot\overleftrightarrow{\alpha}\cdot\frac{d\vec{E}}{dr} + \vec{E}^*\cdot\overleftrightarrow{\beta}^+\cdot\vec{E} + \frac{\alpha_{\perp\perp}}{r}|E_\perp|^2\right.$$

$$\left. + 2\beta_{\perp\parallel}\,\mathrm{Re}\left(E_\perp E_\parallel^*\right) - \alpha_{\parallel\parallel}\frac{d}{dr}|E_\parallel|^2\right]. \tag{6.37}$$

It is important to note that Maxwell's equations (3.1) in conjunction with Eq. (6.30) must be supplemented by appropriate regularity conditions at r = 0. They can be written as

$$E_r = E_\perp = \frac{dE_\parallel}{dr} = 0, \quad \text{for} \quad |m| \neq 1 \tag{6.38}$$

and

$$E_r + im\,E_\perp = \frac{d}{dr}\left(E_r + im\,E_\perp\right) = E_\parallel = 0, \text{for } |m| = 1. \tag{6.39}$$

Using these conditions it is straightforward to show that $S_r = S_T = 0$ at r = 0.

Concluding this section we should like to mention that various limiting cases of Eqs. (6.30) - (6.33) have previously been cbtained in Refs. [9, 37, 51, 93, 96, 107, 112, 160, 161, 183].

6.3 Toroidal Geometry

In this geometry we only consider systems with axisymmetric equilibria whose dynamics are described by the cold plasma model with an equilibrium current [166]. The equilibrium magnetic field in such systems is of the form

$$\vec{B}_0 = \nabla\varphi \times \nabla\psi + B_T R \nabla\varphi , \tag{6.40}$$

where ψ is the poloidal flux function, B_T is the toroidal field and R is the distance from the symmetry axis. The equilibrium plasma density is assumed to be an arbitrary function of ψ.

Using Eq. (6.40) we introduce a local magnetic coordinate system ($\vec{e}_\psi$, $\vec{e}_\perp$, $\vec{e}_\parallel$) where

$$\vec{e}_\psi = \frac{\nabla\psi}{|\nabla\psi|} , \quad \vec{e}_\perp = \vec{e}_\parallel \times \vec{e}_\psi , \quad \vec{e}_\parallel = \frac{\vec{B}_0}{B_0} . \tag{6.41}$$

On projecting Eq. (4.21) on the magnetic coordinate system and eliminating $\vec{j}_0$ in favour of $\vec{B}_0$, and $\vec{B}$ in favour of $\vec{E}$ via Eqs. (4.12) and (3.5) we obtain, after some transformations, the dielectric tensor operator in the form

$$\begin{aligned}
\varepsilon_{\psi\psi} &= \varepsilon_1 , \quad \varepsilon_{\perp\perp} = \varepsilon_1 + \mu \vec{e}_\perp \cdot (\nabla \times \vec{e}_\perp), \\
\varepsilon_{\psi\perp} &= i\,\varepsilon_2 + \mu \left[(\nabla_\parallel \lg \frac{B_0}{|\nabla\psi|}) - \nabla_\parallel \right], \\
\varepsilon_{\perp\psi} &= -i\,\varepsilon_2 + \mu \left[\nabla_\parallel - (\nabla_\parallel \lg |\nabla\psi|) \right],
\end{aligned} \tag{6.42}$$

where

$$\mu = \left(\frac{c}{\omega}\right)^2 \frac{\vec{B}_0 \cdot \nabla \times \vec{B}_0}{B_0^2} \quad , \quad \nabla_{\parallel} = \vec{e}_{\parallel} \cdot \nabla \,, \tag{6.43}$$

and the quantities ε_1 and ε_2 are given by Eqs. (6.1) and (6.2).

Let us note that for force-free equilibria Eqs. (4.12) and (4.13) imply

$$\nabla_{\parallel} \mu = 0 \,. \tag{6.44}$$

On using this property and Eq. (4.13) one can easily show that the operator (6.42) is Hermitian.

7. LOW-FREQUENCY WAVES

In this section we shall review the properties of electromagnetic waves in the frequency range $\omega < \omega_{ci}$. We first introduce some basic concepts and the classification of different types of waves in unbounded plasmas. We then proceed to discuss spectral characteristics of electromagnetic oscillations in bounded systems.

7.1 Unbounded Homogeneous Plasmas

For the description of waves in these plasmas we adopt the slab geometry and employ the expressions for the dielectric tensor presented in Section 6.1.

7.1.1 Dispersion relations; Dampings

For homogeneous plasmas Maxwell's equations (3.1) are differential equations with constant coefficients. We may therefore seek their solutions in the form of plane waves, i.e. proportional to $\exp(i\vec{k}\cdot\vec{x})$ where $\vec{k}$ is the wave vector. Equations (3.1) then reduce to the algebraic equations

$$\left[k^2\overleftrightarrow{I} - \vec{k}\vec{k} - \left(\frac{\omega}{c}\right)^2\overleftrightarrow{\varepsilon}\right]\cdot\vec{E} = 0, \tag{7.1}$$

which have a nontrivial solution if, for a given $\vec{k}$, ω satisfies the dispersion equation

$$D(\vec{k},\omega) \equiv \det\left[k^2\overleftrightarrow{I} - \vec{k}\vec{k} - \left(\frac{\omega}{c}\right)^2\overleftrightarrow{\varepsilon}\right] = 0. \tag{7.2}$$

Since $\overleftrightarrow{\varepsilon}$ in general contains dissipative terms the solutions of the dispersion equation are complex. The imaginary part of a solution can be readily found if it is small compared with the real part; this is possible if the dissipative terms are small. Setting $\omega = \omega_k - i\gamma_k$ one easily obtains

$$\gamma_k = Im\, D(\vec{k},\omega_k)\left(\frac{\partial Re\, D(\vec{k},\omega_k)}{\partial \omega_k}\right)^{-1}, \tag{7.3}$$

where ω_k satisfies

$$Re\, D(\vec{k},\omega_k) = 0. \tag{7.4}$$

The quantities ω_k and γ_k are usually referred to as the dispersion relation and the damping rate. In what follows we shall only discuss the waves for which Eqs. (7.3) and (7.4) apply.

We begin by considering the waves in a cold plasma whose dynamics are described by the dielectric tensor of the two-fluid model, Eqs. (6.1) - (6.3). As one can see from these expressions, $|\varepsilon_3| >> \varepsilon_1, \varepsilon_2$ for $\omega<\omega_{ci}$. Equation (7.2) may thus be approximated by

$$\varepsilon_1 N_\perp^4 + \varepsilon_3 (N_z^2 - \varepsilon_1) N_\perp^2 + \varepsilon_3 \left[(N_z^2 - \varepsilon_1)^2 - \varepsilon_2^2\right] = 0, \tag{7.5}$$

where

$$N_\perp^2 = \left(\frac{k_\perp c}{\omega}\right)^2 , \quad N_z^2 = \left(\frac{k_z c}{\omega}\right)^2 , \quad k_\perp^2 = k^2 - k_z^2 . \tag{7.6}$$

We now take various limits of Eq. (7.5).

In the MHD limit ($\omega/\omega_{ci} \to 0$, $m_e \to 0$) we have $\varepsilon_2 \to 0$, $\varepsilon_3 \to \infty$, and Eq.(7.5) simplifies to

$$(N_z^2 - \varepsilon_1)(N_\perp^2 + N_z^2 - \varepsilon_1) = 0. \tag{7.7}$$

Nullifying the left bracket yields the dispersion relation of the Alfvén wave (also called the shear or torsional Alfvén wave)

$$\omega_k^2 = C_A^2 k_z^2 , \tag{7.8}$$

while nullifying the other bracket yields the dispersion relation of the fast magnetoacoustic wave (also called the compressional Alfvén wave)

$$\omega_k^2 = C_A^2 k^2 . \tag{7.9}$$

The Alfvén wave has the property that $B_z = 0$.

Assuming $\omega/\omega_{ci} \neq 0$ and $m_e \to 0$, which corresponds to the model of Section 4.1.2 in the absence of the equilibrium current, we have

$$(N_z^2 - \varepsilon_1)(N_\perp^2 + N_z^2 - \varepsilon_1) - \varepsilon_2^2 = 0. \tag{7.10}$$

The solutions of this equation can be written in the form [214]

$$\left(\omega_k^2\right)^{\pm} = \frac{1}{2} C_A^2 k^2 \left\{ 1 + \frac{k_z^2}{k^2} + \left(\frac{k_z C}{\omega_{pi}}\right)^2 \right.$$

$$\left. \pm \left[\left(1 + \frac{k_z^2}{k^2} + \left(\frac{k_z C}{\omega_{pi}}\right)^2 \right)^2 - 4 \frac{k_z^2}{k^2} \right]^{1/2} \right\} . \tag{7.11}$$

These are finite-ω/ω_{ci} generalizations of the dispersion relations of the fast magnetoacoustic wave (plus sign) and the Alfvén wave (minus sign). As ω approaches ω_{ci} they may be approximately separated into

$$\omega_k^2 = C_A^2 k^2 \left(1 + \frac{k_z^2}{k^2} \right) \tag{7.12}$$

and

$$\omega_k^2 = \omega_{ci}^2 \left[1 - \left(\frac{\omega_{pi}}{k_z C}\right)^2 \left(1 + \frac{k_z^2}{k^2} \right) \right] . \tag{7.13}$$

One can see that Eq. (7.12) is not greatly different from Eq. (7.9). Thus the fast magnetoacoustic wave is not much affected by the finite ω/ω_{ci} values. On the other hand, Eq. (7.13) differs considerably from Eq. (7.8). The wave associated with this dispersion relation is therefore called the ion cyclotron wave [208]. As Eq. (7.13) shows, this wave can propagate only if $\omega < \omega_{ci}$.

Taking $m_e \neq 0$ and $\omega/\omega_{ci} \rightarrow 0$, Eq. (7.5) may be approximately factorized as

$$\left(N_z^2 - \varepsilon_1 + N_\perp^2 \frac{\varepsilon_1}{\varepsilon_3}\right)\left(N_\perp^2 + N_z^2 - \varepsilon_1\right) = 0. \tag{7.14}$$

We observe that the second bracket is the same as that in Eq. (7.7). Hence the finite m_e has no influence on the dispersion relation of the fast magnetoacoustic wave. Nullifying the first bracket yields

$$\omega_k^2 = \frac{C_A^2 k_z^2}{1 + \frac{k_\perp^2 C^2}{\omega_{pe}^2}}\,, \tag{7.15}$$

which is the finite-m_e modification of the dispersion relation of the Alfvén wave. The associated wave was discussed for the first time in Refs. [69, 86] where it was termed "electrostatic surface wave" and "cold plasma surface wave". We prefer to call it the quasi-electrostatic surface wave since it has the property that only $B_z = 0$ and not $\vec{B} = 0$.

Let us now consider the effects of collisional dissipation on the waves discussed above. For the sake of simplicity we confine ourselves to the case $\omega/\omega_{ci} << 1$. The damping due to resistivity can be determined from Eq. (7.14) if we replace the quantities ε_1 and ε_3 according to Eqs. (6.5) and (6.7). For $\omega << \nu_{ei}$ one then finds that the damping rates of the Alfvén wave and the fast magnetoacoustic wave are the same and given by [206, 211]

$$\gamma_k = \frac{\nu_{ei}}{2} \frac{c^2}{\omega_{pe}^2} k^2\,, \quad \frac{c^2 k^2}{\omega_{pe}^2} \ll 1\,. \tag{7.16}$$

For $\omega >> \nu_{ei}$ the damping rate of the quasi-electrostatic surface wave is easily shown to be

$$\gamma_k = \frac{\nu_{ei}}{2} \frac{1}{1 + \frac{\omega_{pe}^2}{k_\wedge^2 c^2}} \quad . \tag{7.17}$$

We shall not review the derivation of the damping due to viscosity, as it is beyond the framework of the present paper. It can be found in Refs. [206, 211]. For $\nu_{ii} << \omega_{ci}$, where ν_{ii} is ion-ion collision frequency, it has been shown [211] that the damping rate of the Alfvén wave is given by

$$\gamma_k = \frac{3}{20} \nu_{ii} \rho_i^2 \left(k_\wedge^2 + 4 k_z^2 \right), \tag{7.18}$$

while that of the fast magnetoacoustic wave is

$$\gamma_k = \frac{1}{12} \frac{v_{ti}^2}{\nu_{ii}} k_\wedge^2 \, . \tag{7.19}$$

For $\nu_{ii} >> \omega_{ci}$, which is the case when Eq. (4.28) applies, it has been shown [206] that the damping rates of both waves are the same and given by

$$\gamma_k = \frac{1}{4} \frac{v_{ti}^2}{\nu_{ii}} k^2 . \tag{7.20}$$

We note that in this case the viscosity coefficient is approximately [211]

$$\eta = \frac{n_0 T_i}{\nu_{ii}} \quad . \tag{7.21}$$

Let us finally treat the waves in a hot collisionless plasma whose dynamics is described by the dielectric tensor given by Eqs. (6.17) - (6.20). We only consider the case $\omega/\omega_{ci} << 1$ and assume $kv_{ti} << \omega << k_z v_{te}$. On choosing a coordinate system in which $k_y = 0$, the relevant components of the dielectric tensor may then be obtained from Eqs. (6.17) - (6.20) in the form

$$\begin{aligned}
\varepsilon_{xx} &= \left(\frac{c}{c_A}\right)^2 \left(1 - \frac{3}{4} k_\perp^2 \rho_i^2\right), \\
\varepsilon_{yy} &= \left(\frac{c}{c_A}\right)^2 \left(1 + i\tilde{\pi}^{1/2} \frac{m_e}{m_i} \frac{k_\perp^2 v_{te}}{|k_z| \omega}\right), \\
\varepsilon_{yz} &= -i \frac{\omega_{pi}^2}{\omega \omega_{ci}} \frac{k_\perp}{k_z} \left(1 + i\tilde{\pi}^{1/2} \frac{\omega}{|k_z| v_{te}}\right), \\
\varepsilon_{zz} &= \frac{2\omega_{pe}^2}{k_z^2 v_{te}^2} \left(1 + i\tilde{\pi}^{1/2} \frac{\omega}{|k_z| v_{te}}\right) - \frac{\omega_{pi}^2}{\omega^2} \quad .
\end{aligned} \tag{7.22}$$

In writing Eq. (7.22) we have only retained the dissipative terms due to the Cerenkov interaction of the waves with the electrons, the ion contributions being exponetially small. It is easily seen that $|\varepsilon_{zz}| >> |\varepsilon_{xx}|, |\varepsilon_{yy}|, |\varepsilon_{yz}|$. The dispersion equation (7.2) may therefore be written approximately as

$$\left(N_z^2 - \varepsilon_{xx} + \frac{\varepsilon_{xx}}{\varepsilon_{zz}} N_\perp^2\right)\left(N_\perp^2 + N_z^2 - \varepsilon_{yy} - \frac{\varepsilon_{yz}^2}{\varepsilon_{zz}}\right) = 0. \tag{7.23}$$

It is straightforward to show that the real part of the second bracket in Eq. (7.23) is the same as that for the cold plasma (cf. Eq. (7.7)). Thus the dispersion relation of the fast magnetoacoustic wave is unaltered by the thermal motion of particles provided $v_{ti} << c_A$. The imaginary part yields the wave damping rate [212, 214]

$$\gamma_k = \frac{\pi^{1/2}}{4} \frac{m_e}{m_i} \frac{v_{te}}{C_A} \frac{k_\perp^2}{k|k_z|} \omega_k . \tag{7.24}$$

Setting to zero the first bracket in Eq. (7.23) one obtains the dispersion relation and damping rate of the kinetic Alfvén wave [72, 73]

$$\omega_k^2 = C_A^2 k_z^2 \left[1 + k_\perp^2 \rho_i^2 \left(\frac{3}{4} + \frac{T_e}{T_i}\right)\right], \tag{7.25}$$

$$\gamma_k = \frac{1}{2}\left(\frac{\pi}{2}\right)^{1/2} \left(\frac{m_e}{m_i}\right)^{1/2} \frac{k_\perp^2 C_A^2}{\omega_{ci}^2} |k_z| C_s \tag{7.26}$$

where $c_s = (T_e/m_i)^{1/2}$. It is worth mentioning that this wave has the property that $B_z \approx 0$.

For a plasma with $T_e >> T_i$, the first bracket yields another solution of Eq. (7.23), corresponding to the ion acoustic wave. Its dispersion relation and damping rate are given by [73]

$$\omega_k^2 = \frac{C_s^2 k_z^2}{1 + \frac{k_\perp^2 C_s^2}{\omega_{ci}^2}} , \tag{7.27}$$

$$\gamma_k = \frac{\pi}{2}^{1/2} \frac{\omega_k^2}{|k_z| v_{te}} \frac{1}{1 + \frac{k_\perp^2 c_s^2}{\omega_{ci}^2}} \,. \tag{7.28}$$

We note that the expressions (7.27) and (7.28) may be obtained using the electrostatic approximation, i.e. assuming $\vec{B} = 0$.

7.1.2 Equation of energy transfer; Group velocity; Wave energy

Owing to dissipative effects the energy associated with the waves diminishes in time and is absorbed by the plasma particles. If the energy absorption is weak the dynamics of this process may be described by means of an equation of energy transfer. Such an equation can be obtained starting from the general form of Poynting's theorem

$$\frac{\partial}{\partial t} \frac{1}{8\pi} \left(E^2 + B^2 \right) + \nabla \cdot \frac{c}{4\pi} \left(\vec{E} \times \vec{B} \right) + \vec{j} \cdot \vec{E} = 0. \tag{7.29}$$

On setting

$$\vec{E}(\vec{x},t) = Re \left\{ \vec{E}_s(\vec{x},t) \exp \left[i(\vec{k} \cdot \vec{x} - \omega_k t) \right] \right\} \tag{7.30}$$

and assuming

$$\left|\frac{\partial \vec{E}_s}{\partial t}\right| \frac{1}{|\vec{E}_s|\omega_k} \sim \left|\frac{\partial \vec{E}_s}{\partial \vec{x}}\right| \frac{1}{|\vec{E}_s|k} \sim \left|\frac{\varepsilon^a_{\alpha\beta}}{\varepsilon^h_{\alpha\beta}}\right| \ll 1, \tag{7.31}$$

where $\varepsilon_{\alpha\beta}{}^h$ and $\varepsilon_{\alpha\beta}{}^a$ are the Hermitian and anti-Hermitian parts of the dielectric tensor, Eq. (7.29) may be reduced to [208, 212]

$$\frac{\partial W}{\partial t} + \nabla \cdot \vec{T} + \frac{\omega_k}{8\pi} \varepsilon^a_{\alpha\beta} E^*_\alpha E_\beta = 0. \tag{7.32}$$

Here W is the wave energy density and $\vec{T}$ is the wave energy flux density; these are given by the expressions

$$W = \frac{\partial(\omega_k^2 \varepsilon^h_{\alpha\beta})}{\omega_k \partial \omega_k} \frac{E^*_\alpha E_\beta}{16\pi}, \tag{7.33}$$

$$\vec{T} = \vec{S} - \omega_k \frac{\partial \varepsilon^h_{\alpha\beta}}{\partial \vec{k}} \frac{E^*_\alpha E_\beta}{16\pi}. \tag{7.34}$$

In writing Eqs. (7.32) - (7.34) we have dispensed with the subscript "s".

Equation (7.32) may be further simplified if one introduces the group velocity $\vec{v}_g = \partial\omega_k/\partial\vec{k}$ and the damping rate, Eq. (7.3) for the waves. On making use of Eq. (7.1) it can then be shown that

$$\vec{T} = \vec{v}_g W \tag{7.35}$$

and

$$\frac{\omega_k}{8\pi} \varepsilon^a_{\alpha\beta} E^*_\alpha E_\beta = 2\gamma_k W. \tag{7.36}$$

The equation of energy transfer can thus be written in the form

$$\frac{\partial W}{\partial t} + \vec{v}_g \cdot \nabla W + 2\gamma_k W = 0. \tag{7.37}$$

In a steady state this equation is an analogue of Eqs. (6.23) and/or (6.36).

7.2 Bounded Cold Homogeneous Plasmas

We shall now treat the electromagnetic oscillations of a cold cylindrical plasma whose dynamics are described by the dielectric tensor of the two-fluid model, Eqs. (6.1) - (6.3). We confine ourselves to the case of free oscillations, i.e. we set $\vec{j}_a = 0$. Various cases of forced oscillations have been investigated in Refs. [10, 22, 30, 34 - 36, 208].

For a homogeneous plasma the most convenient way to write Maxwell's equations (3.1) is to eliminate E_r and E_θ in favour of E_z and B_z via Eq. (3.5). On Fourier-decomposing the resulting equations one finds [209]

$$\left\{\varepsilon_1\left[\left(\frac{c}{\omega}\right)^2\Delta_\perp - N_z^2\right] + \varepsilon_1^2 - \varepsilon_2^2\right\}B_z + i N_z \varepsilon_2 \varepsilon_3 E_z = 0, \tag{7.38}$$

$$\left[\varepsilon_1\left(\frac{c}{\omega}\right)^2\Delta_\perp + \varepsilon_3(\varepsilon_1 - N_z^2)\right]E_z - i N_z \varepsilon_2 B_z = 0, \tag{7.39}$$

where

$$\Delta_\perp = \frac{1}{r}\frac{d}{dr} r \frac{d}{dr} - \frac{m^2}{r^2} \quad . \tag{7.40}$$

If E_z and B_z are known, E_r and E_θ are given by the relations

$$\frac{\omega}{c}\left[(N_z^2 - \varepsilon_1)^2 - \varepsilon_2^2\right]E_r = (N_z^2 - \varepsilon_1)\left(\frac{m}{r}B_z - i N_z E_z'\right) + \varepsilon_2\left(\frac{i m}{r} N_z E_z - B_z'\right), \tag{7.41}$$

$$\frac{\omega}{c}\left[\left(N_z^2-\varepsilon_1\right)^2-\varepsilon_2^2\right]E_\theta = \left(N_z^2-\varepsilon_1\right)\left(\frac{m}{r}N_z E_z + iB_z'\right) - \varepsilon_2\left(\frac{im}{r}B_z + N_z E_z'\right). \tag{7.42}$$

Assuming E_z and B_z to be proportional to $J_m(k_r r)$ [6], Eqs. (7.38) and (7.39) reduce to algebraic equations which have a nontrivial solution if $N_\Lambda^2 = (k_r c/\omega)^2$ satisfies Eq. (7.5). Since the latter is a quadratic equation in k_r^2 the general solution of Eqs. (7.38) and (7.39), regular at r = 0, may be written in the form

$$E_z = \sum_{j=1}^{2} a_j J_m(k_{rj} r), \tag{7.43}$$

$$B_z = \frac{i}{N_z \varepsilon_2}\sum_{j=1}^{2} a_j\left[\varepsilon_1 N_{rj}^2 + \varepsilon_3\left(N_z^2-\varepsilon_1\right)\right]J_m(k_{rj} r), \tag{7.44}$$

where a_j are constants to be determined by the boundary conditions. In what follows we shall distinguish the two configurations : $r_p = r_w$ (frequently called the completely filled plasma waveguide) and $r_p \neq r_w$ (the partially filled plasma waveguide).

When $r_p = r_w$ the boundary condition (3.8) applies. Combining Eqs. (7.42) - (7.44) and (3.8) one obtains the dispersion equation [209]

$$D_1\frac{J_m'(k_{r1}r_p)}{J_m(k_{r1}r_p)} - D_2\frac{J_m'(k_{r2}r_p)}{J_m(k_{r2}r_p)} + \frac{m}{r_p}\varepsilon_1\varepsilon_2\left(N_{r2}^2 - N_{r1}^2\right) = 0, \tag{7.45}$$

where

$$D_j = (N_z^2 - \varepsilon_1)\left[\varepsilon_1 N_{rj}^2 + \varepsilon_3 (N_z^2 - \varepsilon_1)\right] + N_z^2 \varepsilon_2^2 . \tag{7.46}$$

The dispersion equation considerably simplifies in the limit $\varepsilon_2 \to 0$. Equations (7.38) and (7.39) then uncouple and the oscillations can be divided into two types: in one $B_z = 0$, and in the other $E_z = 0$. For the former Eq. (3.8) implies

$$J_m (k_r r_p) = 0, \tag{7.47}$$

while for the latter it follows from Eqs. (3.8) and (7.42.) that

$$J_m' (k_r r_p) = 0. \tag{7.48}$$

Equations (7.47) and (7.48) give rise in each case to an infinite set of discrete values for k_r. The frequency spectra of the oscillations are then obtained by substituting the corresponding discrete values of k_r for $k_\wedge$ in Eqs. (7.15) and (7.9) respectively. In the general case, when $\varepsilon_2 \neq 0$, the $B_z = 0$ and $E_z = 0$ oscillations are coupled and to obtain their frequency spectra one has to solve Eq. (7.45) together with Eq. (7.5).

For the partially filled waveguide the general dispersion equation is very complicated [209]. We shall therefore consider only the most important limiting case $\varepsilon_3 \to \infty$. We then have $E_z = 0$ and may choose $B_z = J_m (k_r r)$ where $k_r^2 = k_\wedge^2$ is given by Eq. (7.10). Expressing E_θ in terms of B_z via Eq. (7.42) the solution in the plasma region can be matched to that in the vacuum region, Eq. (5.26), using the boundary conditions (3.6) and (3.7). One thus obtains the dispersion equation [96, 128, 129, 209]

$$\frac{J_m'(k_r r_p)}{J_m(k_r r_p)} + \frac{m}{r_p}\frac{\varepsilon_2}{\varepsilon_1 - N_z^2} + \frac{k_r^2}{k_z^2}\frac{H_p'}{H_p} = 0, \tag{7.49}$$

where (cf. Eq. (5.18a))

$$\frac{H_p'}{H_p} = \frac{I_m'(k_z r_w)K_m'(k_z r_p) - I_m'(k_z r_p)K_m'(k_z r_w)}{I_m'(k_z r_w)K_m(k_z r_p) - I_m(k_z r_p)K_m'(k_z r_w)} \cdot \tag{7.50}$$

We have dropped the displacement current in Eq. (7.50). If $k_r^2 < 0$ the function J_m in Eq. (7.49) is to be replaced by I_m ($|k_r| r_p$). For $r_w \to \infty$ (the plasma cylinder surrounded by vacuum) Eq. (7.50) reduces to [206]

$$\frac{H_p'}{H_p} = \frac{K_m'(k_z r_p)}{K_m(k_z r_p)} \cdot \tag{7.51}$$

Equation (7.49) has been analysed in Refs. [126, 128, 129] (see also Ref. [164]) and for the case $r_w \to \infty$, $m = 0$ in Ref. [2(8]. Analogues of Eq. (7.49) for the slab geometry have been investigated in Refs. [120, 130]. In the discussion below we shall closely follow Ref. [129].

It is easy to solve Eq. (7.49) numerically. A numerical solution is shown in Fig. 4 for the case $\omega_{pi} r_p/c = 2$ and $r_w/r_p = 1.5$ which are typical values of a small tokamak. The eigenfrequencies are shown for $m = +1$ and $m = -1$ as a function of k_z.

Analytical solutions of Eq. (7.49) can be obtained for $m \neq 0$ in the limit $k_z r_p << 1$. The expression (7.50) then simplifies to

$$\frac{H_p'}{H_p} \approx -\frac{|m|}{r_p}\,\frac{(r_w/r_p)^{2|m|}-1}{(r_w/r_p)^{2|m|}+1}\,, \tag{7.52}$$

and Eq. (7.49) may be approximately satisfied either by $k_r >> k_z$ or by $k_r \sim k_z$.

In the first case one finds (cf. Eqs. (7.9) and (7.12))

$$\omega^2 = c_A^2 k_r^2\,, \tag{7.53}$$

where the discrete values of k_r are given by

$$J_m(k_r r_p) = 0. \tag{7.54}$$

These are the frequencies of the radial eigenmodes of the fast magnetoacoustic wave (F). For $|m| = 1$ and $\omega_{pi} r_p/c = 2$ the first zero of Eq. (7.54), $k_r r_p = 3.83$, yields $\omega/\omega_{ci} = 1.91$. In Fig. 4 this mode is denoted with F_2 as the second radial eigenmode of the fast wave. As long as $k_z r_p \lesssim 1$ this mode and all the higher ones are practically identical for $m = \pm 1$. And the same is true for the modes with $|m| \geq 2$.

The first radial eigenmodes of the fast wave F_1 are obtained in the limit $k_r \sim k_z$. Making the approximation $J'_m / J_m \approx |m|/(k_r r_p)$ and assuming $\omega/\omega_{ci} << 1$, Eq. (7.49) yields

$$\omega = \omega_o \left(1 + \mathrm{sign}(m)\frac{\omega_o}{2\omega_{ci}}\right), \tag{7.55}$$

where

$$\omega_o^2 = C_A^2 k_z^2 \left(1 + \frac{(r_w/r_p)^{2|m|} + 1}{(r_w/r_p)^{2|m|} - 1}\right). \tag{7.56}$$

Equations (7.52) and (7.56) hold even for $r_w \to \infty$ as can be seen from Eq. (7.51). Taking this limit and $\omega/\omega_{ci} \to 0$ in Eqs. (7.55) and (7.56) one finds

$$\omega = \sqrt{2}\, C_A k_z \,. \tag{7.57}$$

This is the surface eigenmode frequency as given by MHD theory [217]. In the MHD limit the two modes for $m \gtrless 0$ behave identically and like an eigenmode of the fast wave. It seems therefore natural to identify the first radial eigenmode of the fast magnetoacoustic wave F_1 with the surface eigenmode S.

In Fig. 4 only the mode F_1, $m = -1$ has been labelled with S for the following reason. For small k_z the wave fields of F_1 are global functions as opposed to those of the surface mode in slab geometry where they are confined to the neighbourhood of the plasma-vacuum interface. It is only for $k_z r_p \gtrsim 1$ that the mode F_1 , $m = -1$ has surface-mode character as can be seen from Fig. 5. The mode F_1 , $m = 1$ has global wave fields for all values of k_z. The surface-mode character of F_1 , $m = -1$ in cylindrical geometry is clearly related to the fact that it merges with the Alfvén resonance $\varepsilon_1 - N_z^2 = 0$, denoted by A_∞ (at $k_z r_p = 1.5$ in the case of Fig. 4). The value of k_z where S and A_∞ merge depends on r_w as we shall see in Fig. 6.

Let us, however, first finish the discussion of Fig. 4 by describing the global eigenmodes of the Alfvén wave (cf. Eq. (7.11) with the minus sign). As can be seen from Fig. 4 there is no physical interest to obtain analytical solutions for small k_z because the whole class is extremely densely packed; in

the MHD limit the solutions are even infinitely degenerate. For $k_z r_p > 1.5$ the eigenfrequencies of the lowest radial modes (only A_1, $m = \pm 1$ are shown; all the higher modes, A_s, $s > 1$, lie between A_1 and A_∞) are distinctly detached from the accumulation point A_∞. In the case shown the largest distances have been found around $k_z r_p \approx 3.5$. The relative distances $(\omega_\infty - \omega_s)/\omega_\infty$ are 7.2 %, 3.2 % and 1.7 % for the modes $s = 1, 2, 3$, $m = -1$ and 3.6 %, 1.8 %, 1.1 % for $m = 1$. It is interesting to note, that the set of A_s, $m = 1$ seems to contain one mode more than $m = 1$, namely the mode A_1. All the other modes can, in fact, be put into a close one-to-one correspondence, A_{s+1} $(m = -1) \approx A_s$ $(m = 1)$, with respect to frequency and radial wavenumber k_r (not shown). At small k_z the surface mode S has been identified as an eigenmode of the fast wave; at high k_z it now appears as a part of the Alfvén wave. This is, however, from a purist's point of view, somewhat misleading. Strictly speaking, the mode lies always <u>above</u> A_∞ and should, therefore, not be identified with any eigenmode of the Alfvén wave.

The behaviour of the surface mode as a function of k_z and of the radius of the conducting wall, r_w, has been investigated in detail. The most striking result is shown in the upper part of Fig. 6. The radial wavelength k_r changes from real to imaginary as k_z grows. This fact explains the change (Fig. 5) from a global waveform at $k_z r_p = 0.4$ to the surface waveform at $k_z r_p = 1.5$: at $k_z r_p = 0.4$ the eigenfunction for B_z is given by $J_1(\sqrt{.15}\, r/r_p)$ whereas at $k_z r_p = 1.5$ B_z is given by an exponentially growing $I_1(|k_r|\, r)$. We note the strong effect of the conducting wall. The smaller the vacuum gap the higher are the axial phase velocities ω/k_z at small values of k_z (see lower part of Fig. 6). This fact is well described by Eq. (7.56) which for $k_z r_p \lesssim 0.4$ approximates the exact result within 10 %. From Eq. (7.56) we conclude that the phase velocities of the mode F_1, $m = 1$ show the same tendency to increase, when the wall is approached to the plasma, as those of the surface mode.

7.3 Bounded Cold Inhomogeneous Plasmas

We shall now discuss the spectral characteristics of electromagnetic oscillations in bounded inhomogeneous systems whose dynamics are described by the dielectric tensor of the cold plasma model with an equilibrium current, Eqs. (6.28) and/or (6.42).

7.3.1 Discrete and continuous spectra

Cylindrical geometry

For an inhomogeneous cylindrical plasma the most elegant way to write Maxwell's equations (3.1) is to eliminate E_r in favour of $B_\parallel$ via Eq. (3.5). To this end, we Fourier-decompose Eqs. (3.1) and (3.5) and project them on the magnetic coordinate system. The elimination of E_r then yields [64, 106, 119]

$$A\frac{1}{r}\frac{d}{dr}rE_\perp = Gk_\perp E_\perp + \frac{i\omega}{c}\left(A-k_\perp^2\right)B_\parallel \quad , \tag{7.58}$$

$$A\frac{dB_\parallel}{dr} = \frac{c}{i\omega}\left(G^2-A^2\right)E_\perp - Gk_\perp B_\parallel \quad , \tag{7.59}$$

where

$$A = \left(\frac{\omega}{c_A}\right)^2 \frac{1}{1-(\omega/\omega_{ci})^2} - k_\parallel^2 \quad , \tag{7.60}$$

$$G = \left(\frac{\omega}{c_A}\right)^2 \frac{\omega/\omega_{ci}}{1-(\omega/\omega_{ci})^2} - \frac{2}{r}b_\theta k_\parallel \quad . \tag{7.61}$$

If $E_\perp$ is known, E_r is given by the relation

$$(A-k_\perp^2)E_r = i\left(\frac{k_\perp}{r}\frac{d}{dr}r - G\right)E_\perp \tag{7.62}$$

In writing Eqs. (7.58) - (7.62) we have confined ourselves to the most important limiting case $|b_\theta| << 1$. The corresponding equations for an arbitrary b_θ can be found in Ref. [151], and their analysis for a specific case with $\omega/\omega_{ci} = 0$ in Ref. [150].

Equations (7.58) and (7.59) considerably simplify in the case $b_\theta = \omega/\omega_{ci} = m = 0$. It is then advantageous to eliminate $B_\parallel$ in favour of $E_\perp$ and one obtains [52]

$$\left(\frac{d}{dr}\frac{1}{r}\frac{d}{dr}r + A\right)E_\perp = 0, \tag{7.63}$$

while Eq. (7.62) reduces to

$$AE_r = 0. \tag{7.64}$$

Equation (7.63) describes the axisymmetric modes of the fast magnetoacoustic wave. Their frequency spectrum for a parabolic density profile has been obtained in Ref. [52]. It was shown that the spectrum is not much different from that for the case of a homogeneous density [208].

Equation (7.64), which is uncoupled from Eq. (7.63), describes the axisymmetric modes of the Alfvén wave. Assuming that $A = 0$ has a simple zero at $r = r_s$ the solution of Eq. (7.64) can be written in the form [54]

$$E_r = \bar{E}_r \, \delta(r - r_s), \tag{7.65}$$

where $\bar{E}_r$ is an arbitrary constant. The associated frequency is given by [52]

$$\omega^2 = C_A^2(r_s) k_z^2 . \tag{7.66}$$

Since one can construct a singular solution of this type for each value of ω in the range

$$\min C_A^2(r) \leq (\omega/k_z)^2 \leq \max C_A^2(r) , \tag{7.67}$$

one sees that Eq. (7.64) possesses a continuous spectrum of eigenvalues given in Eq. (7.67). The associated eigenfunctions, Eq. (7.65), are singular, of course.

Another case, when Eqs. (7.58) and (7.59) simplify, is $m = k_z = 0$. Again, the elimination of $B_{\|}$ yields

$$\left[\frac{d}{dr}\frac{1}{r}\frac{d}{dr}r + \left(\frac{\omega}{C_A}\right)^2\right] E_\perp = 0, \tag{7.68}$$

and

$$E_r = -i \frac{\omega}{\omega_c} E_\perp . \tag{7.69}$$

These equations describe the purely radial eigenmodes of the fast magnetoacoustic wave. Their analysis, for various cases, can be found in the work on magnetoacoustic resonance [18, 41, 43, 45].

In their completeness Eqs. (7.58) and (7.59) can only be analysed numerically. The results of such an analysis will be presented in Section 7.3.2.

Here we shall discuss some general properties of these equations and consider a special case for which their solution can be obtained analytically.

If $A \neq 0$ for the parameters of interest, Eqs. (7.58) and (7.59) still possess discrete spectra associated with the eigenmodes of the fast magnetoacoustic wave and the global eigenmodes of the Alfvén wave [54, 57, 63, 67, 106, 113, 122, 129, 132, 141, 183]. These spectra, as we shall see shortly, are not much different from those presented in Section 7.2.

Let us now assume that $A = 0$ has a simple zero at $r = r_s$. The solution of Eqs. (7.58) and (7.59) can then be written as [54, 57, 63, 96, 103, 217]

$$\mathcal{B}_{\parallel} = \begin{cases} C_1 F_1(r) + C_2 F_2(r) \quad , & r > r_s \, , \\ C_3 F_1(r) + C_2 F_2(r) \quad , & r < r_s \, , \end{cases} \tag{7.70}$$

where C_1, C_2, C_3 are arbitrary constants. The functions F_1 and F_2 are the regular and singular fundamentals, respectively, with the properties

$$F_1 \to 1 \, , \quad F_2 \to \lg|r - r_s| \, , \quad \text{for } r \to r_s \, . \tag{7.71}$$

An expression similar to Eq. (7.70) is also true for $E_\perp$. In the case when $G = 0$ the fundamentals have the properties

$$F_1 \to (r - r_s)^2 \, , \quad F_2 \to \text{const} + (r - r_s)^2 \lg|r - r_s| \, , \tag{7.72}$$

while the fundamentals corresponding to $E_\perp$ retain the properties (7.71). The fact that the constants C_1 and C_3 are independent across the singularity

preclude any one-to-one relation between ω and the wavenumber. Thus, the frequency associated with the singular solution (7.70) is given by

$$\omega^2 = \omega_A^2(r_s) \equiv \frac{C_A^2(r_s) k_\parallel^2(r_s)}{1 + C_A^2(r_s) k_\parallel^2(r_s)/\omega_{ci}^2}, \tag{7.73}$$

which follows from Eq. (7.60). Since one can construct a singular eigenfunction of type (7.70) for each value of ω in the range

$$\min \omega_A^2(r) \leq \omega^2 \leq \max \omega_A^2(r), \tag{7.74}$$

one sees that Eqs. (7.58) and (7.59) possess a continuous spectrum of eigenvalues given in Eq. (7.74). The associated modes are called the singular eigenmodes of the Alfvén wave [54, 217].

Finally, we consider the case of a uniform density and uniform axial current, i.e. n_0 = const. and b_θ/r = const. An approximate solution of Eqs. (7.58) and (7.59) can then be obtained in terms of Bessel functions. On repeating the same procedure as that leading to Eq. (7.49) one obtains the dispersion equation

$$\frac{J_m'(k_r r_p)}{J_m(k_r r_p)} + k_\perp(r_p)\frac{G}{A} + \frac{H_p'}{H_p}\frac{A^2 - G^2}{k_\parallel^2 A} = 0, \tag{7.75}$$

where

$$k_r^2 = \frac{A^2 - G^2}{A} + 2k_\parallel \frac{b_\theta}{r}\left(m - \frac{G}{A}\right). \tag{7.76}$$

Assuming $k_r \sim k_{||} << 1/r_p$ and $\omega/\omega_{ci} << 1$, Eqs. (7.75) and (7.76) yield the dispersion relation of the surface eigenmode modified by the presence of a uniform axial current [135, 141]

$$\omega = \omega_0 \left[1 + \mathrm{sign}(m)\left(\frac{1}{2}\frac{\omega_0}{\omega_{ci}} - \frac{b_\theta}{r} k_{||} \frac{c_A^2}{\omega_0^2}\right)\right], \tag{7.77}$$

where ω_0 is given by Eq. (7.56) with the replacement $k_z \to k_{||}$.

Toroidal geometry

The analogues of Eqs. (7.58) and (7.59) for the geometry in question may be written in the form [70, 71, 105, 110, 115, 143, 169, 188, 191]

$$\frac{|\nabla\psi|}{B_0} \nabla_\psi \frac{B_0}{|\nabla\psi|} E_\perp = -\frac{\Delta\psi}{|\nabla\psi|} E_\perp + \frac{i\omega}{c} B_{||} + |\nabla\psi| \nabla_\perp \frac{E_\psi}{|\nabla\psi|}, \tag{7.78}$$

$$\frac{i\omega}{c} B_0 \nabla_\psi \frac{B_{||}}{B_0} = -\left[|\nabla\psi| \nabla_{||} \frac{B_0}{(\nabla\psi)^2} \nabla_{||} \frac{|\nabla\psi|}{B_0} + \left(\frac{\omega}{c}\right)^2 \varepsilon_1\right] E_\perp$$

$$+ \left\{i\left(\frac{\omega}{c}\right)^2 \varepsilon_2 + \left[\vec{e}_\perp \cdot (\nabla \times \vec{e}_\perp) - \left(\frac{\omega}{c}\right)^2 \mu\right] |\nabla\psi| \nabla_{||} \frac{1}{|\nabla\psi|}\right\} E_\psi, \tag{7.79}$$

and

$$\hat{A} E_\psi = \left\{\frac{B_0}{|\nabla\psi|} \nabla_{||} \frac{|\nabla\psi|}{B_0} \left[\left(\frac{\omega}{c}\right)^2 \mu - \vec{e}_\perp \cdot (\nabla \times \vec{e}_\perp)\right] - i\left(\frac{\omega}{c}\right)^2 \varepsilon_2\right\} E_\perp + \frac{i\omega}{c} B_0 \nabla_\perp \frac{B_{||}}{B_0}, \tag{7.80}$$

where

$$\nabla_\psi = \vec{e}_\psi \cdot \nabla \quad , \quad \nabla_\perp = \vec{e}_\perp \cdot \nabla \ . \tag{7.81}$$

The surface operator $\hat{A}$ is given by

$$\hat{A} = \frac{B_0}{|\nabla\psi|} \nabla_\parallel \frac{(\nabla\psi)^2}{B_0} \nabla_\parallel \frac{1}{|\nabla\psi|} + \left(\frac{\omega}{c}\right)^2 \varepsilon_1 \ . \tag{7.82}$$

For a given equilibrium, one can formally solve E_ψ in terms of $E_\perp$ and $B_\parallel$ from Eq. (7.80) by inverting the operator $\hat{A}$. Substituting the result in Eqs. (7.78) and (7.79) yields then equations for $E_\perp$ and $B_\parallel$. Admissible regular solutions must be periodic in both θ and φ directions (see Section 5.2), and satisfy the boundary conditions (3.6) and (3.7). If the inverse of $\hat{A}$ exists for all the magnetic surfaces ψ = const., Eqs. (7.78) and (7.79) possess discrete spectra associated with the eigenmodes of the fast magnetoacoustic wave and the global eigenmodes of the Alfvén wave [169].

The above procedure fails if the inverse of $\hat{A}$ does not exist for a given ω at a certain $\psi = \psi_s$ surface. Then Eqs. (7.78) and (7.79) have radial singularity and non-square-integrable solutions with spatial singularity at $\psi = \psi_s$ are possible [70, 71]. If, at some set of ψ, nontrivial single-valued periodic solutions in θ and φ can be found for the equation

$$\hat{A} E_\psi = 0, \tag{7.83}$$

then the corresponding set of eigenvalues ω forms the continuous spectrum associated with the singular eigenmodes of the Alfvén wave.

In most of the literature under review, Eq. (7.83) has been investigated in the limit $\omega/\omega_{ci} = 0$: numerical solutions have been obtained in Refs. [77, 134,

169], approximate analytical solutions in Refs. [105, 115, 169, 188] and a WKB solution in Ref. [170]. The case of finite ω/ω_{ci} has been considered in Refs. [143, 191, 198]. An analogue of Eq. (7.83) for non-axisymmetric systems has been discussed in Refs. [88, 116, 127, 163]. Below we shall briefly review the results obtained in Refs. [105, 115, 169] and [143, 198].

Consider a large-aspect-ratio circular tokamak and employ the toroidal coordinate system (see Section 5.2). In the limit $\rho/R_0 << 1$, the flux surfaces become concentric circles, and one can use the following conventional model for the equilibrium field:

$$\vec{B}_0 = \left(0, \frac{\varsigma}{q_s R_0}, 1\right) \frac{B_0}{1+\varsigma\cos\theta/R_0}, \tag{7.84}$$

where R_0 is the major radius of the magnetic axis and q_s is the safety factor. Equation (7.83) then reduces to

$$\left[\nabla_\parallel\left(1+\frac{\varsigma}{R_0}\cos\theta\right)\nabla_\parallel + \left(\frac{\omega}{c_A}\right)^2\left(1+\frac{\varsigma}{R_0}\cos\theta\right)^3\right] E_\psi = 0, \tag{7.85}$$

where

$$\nabla_\parallel = \frac{1}{R_0}\left(\frac{1}{q_s}\frac{\partial}{\partial\theta} + \frac{1}{1+\varsigma\cos\theta/R_0}\frac{\partial}{\partial\varphi}\right). \tag{7.86}$$

Since φ is an ignorable angle one may set

$$E_\psi = e^{in\varphi}\sum_m f_m e^{im\theta}. \tag{7.87}$$

Substituting this in Eq. (7.85) yields coupled equations for the functions f_m. The aim is now to obtain, using a perturbation method, the eigenvalues of these equations valid up to ρ/R_0.

In the lowest order one finds

$$\omega^2 = \left(\frac{C_A}{R_0}\right)^2 \left(\frac{m}{q_s} + n\right)^2. \tag{7.88}$$

This eigenvalue is at least two-fold degenerate since the modes (m, n) and (-m, -n) are both linearly independent solutions for the same eigenvalue. Additional degeneracy will occur between modes (m, n) and (m', n) whenever

$$\left(\frac{m}{q_s} + n\right)^2 = \left(\frac{m'}{q_s} + n\right)^2. \tag{7.89}$$

This condition can be satisfied exactly only on rational surfaces and approximately on the neighbouring surfaces.

It can be shown that in the first order, the effect of toroidicity is to couple degenerate, or nearly degenerate, modes with poloidal wavenumbers differing by one. Thus, considering the coupling between two modes m and m-1 which satisfy Eq. (7.89) on a particular rational surface, q_r, one obtains

$$\omega^2 = \left(\frac{C_A}{R_0}\right)^2 \left(\frac{m}{q_r} + n\right)^2 \left(1 \pm 2\frac{\rho}{R_0}\right). \tag{7.90}$$

As can be seen from this expression the effect of toroidicity is to create a gap in the continuous spectra around the surface q_r. It has been shown in Ref. [169] (see also Ref. [200]) that such a gap, for a particular equilibrium, gives rise to the toroidicity-induced global eigenmodes of the Alfvén wave. The associated frequencies, which lie inside the gap, form a discrete spectrum.

In the case of finite ω/ω_{ci}, explicit solutions of Eq. (7.83) have been obtained in the WKB approximation [143, 198]. The corresponding relationship for the eigenvalues may be written in the form

$$m+n\bar{q} = \pm \frac{\omega}{c}\frac{1}{2\pi}\int_0^{2\pi} d\chi\, J B_0\, \varepsilon_1^{1/2} \quad , \quad \bar{q} = \frac{1}{2\pi}\int_0^{2\pi} \frac{J B_\tau}{R}\, d\chi \, , \tag{7.91}$$

where J is the Jacobian of an orthogonal coordinate system ψ, χ, φ.

Equation (7.91) may only be valid for $\varepsilon_1 > 0$, i.e. at the magnetic surfaces that do not intersect the line $\omega = \omega_{ci}$. Numerical computations [193] carried out using the code LION indicate that all the surfaces intersecting the line $\omega = \omega_{ci}$ are singular surfaces.

7.3.2 Collective modes; Alfvén resonance damping

In the foregoing section, ω has been considered a real number. As a consequence, Eqs. (7.58) and (7.59) are singular at the Alfvén spatial resonance, Eq. (7.73). An alternative approach is to regularize this singularity by adding a small, positive, imaginary part to ω. This procedure, which guarantees causality, is similar to that used in regularizing the linearized Vlasov equation. As a result, the eigenvalue problem associated with Eqs. (7.58) and (7.59) becomes complex. The eigenvalues, which form a discrete set,

correspond to a set of oscillating, damped eigenmodes. It should be emphasized, however, that these modes are no longer the eigenmodes of the original spectral problem, discussed in the previous section, but the collective modes of the time-asymptotic plasma response to either an initial perturbation, in an initial-value problem [60, 80, 111], or to an external perturbation (an imposed antenna current), in a steady-state forced-oscillation problem (see e.g. Refs. [61, 62, 65, 75, 84, 87]). The relation between the two approaches and the corresponding mathematical subtleties are discussed in Ref. [217] and in the references cited therein (see also Refs. [87, 111]).

From the practical point of view there are two procedures for analysing the complex-eigenvalue problem. One is to construct a dispersion equation (analytically or numerically) of type (7.75) and solve for its complex zeros [60, 82, 96, 120, 138]. Another involves the calculation of the power delivered by an antenna as a function of the applied frequency [75, 111, 113, 119, 129]. Any peak that appears indicates the existence of a collective mode or a global eigenmode of the original spectral problem. Below we shall illustrate both these procedures.

Following Ref. [138] let us consider a case when the frequency and damping rate of a collective mode can be determined analytically using the first procedure. Take the limit $b_\theta = \omega/\omega_{ci} = 0$ and the following profile of the plasma density

$$n_0(r) = \begin{cases} n_0 = \text{const}, & 0 \le r \le r_e, \\ n_0 \dfrac{r_p - r}{r_p - r_e}, & r_e \le r \le r_p. \end{cases} \tag{7.92}$$

Assuming $k_z (r_p - r_e) \equiv \delta << k_z r_p << 1$, Eqs. (7.58) and (7.59) then reduce to

$$A \frac{1}{r} \frac{d}{dr} r E_\perp = \frac{\omega}{ic} \frac{m^2}{r^2} B_\parallel \,, \tag{7.93}$$

$$\frac{dB_\parallel}{dr} = \frac{ic}{\omega} A E_\perp \,. \tag{7.94}$$

In the region of the constant density the solution of these equations is again expressed in terms of Bessel functions. In the region of the inhomogeneous density the solution is obtained as a series in the small parameter δ. On matching these solutions to each other and te that in the vacuum region (assuming $r_w \to \infty$) one finds, with the accuracy up to $O(\delta)$, the dispersion equation

$$A(r_e) - k_z^2 = |m| \int_{r_e}^{r_p} \frac{dr}{r} \left[\frac{k_z^2 A(r_e)}{A(r)} - A(r) \right]. \tag{7.95}$$

An approximate solution of Eq. (7.95) yields the frequency and damping rate of the collective surface eigenmode

$$\omega_k^2 = 2 C_A^2 k_z^2 \quad , \quad \gamma_k = \frac{\pi}{8} \frac{|m|}{r_e} (r_p - r_e) |\omega_k| \,. \tag{7.96}$$

As can be seen from Eq. (7.95) the damping arises from the presence of the Alfvén spatial resonance. It may therefore be called the Alfvén resonance damping. The physical interpretation of this damping can be best understood in a steady-state forced problem. It represents a rate at which the energy is accumulated around the resonance layer [83, 87, 111]. To an external observer it appears as an energy absorption.

Let us now turn our attention to the second procedure. Its formulation will be presented in Section 9. Here we shall only discuss the results obtained numerically in Ref. [129]. The first case shown is (Fig. 7) that of a parabolic density profile, $n_0(r) = n_0 [1 - 0.99 (r/r_p)^2]$, with no axial current. The other parameters are the same as those used for Fig. 4. As a consequence of the inhomogeneous density we now have a continuous spectrum of the Alfvén wave (in the original spectral problem), in addition to discrete spectra. In Fig.7, the lower and upper bounds of the continuum, $\omega_A (r = 0)$ and $\omega_A (r = r_p)$, are shown with broken lines. Only the most important collective and/or global modes (F_1, m = 1; S and A_1, m = -1) are represented. The frequencies of F_1 and S are somewhat higher than in Fig. 4, which is consistent with the fact that the average density for the parabolic profile is lower by a factor of two compared with the constant density profile. These modes F_1 and S therefore appear to be related to the eigenmodes F_1 and S which have been discussed in Fig. 4. However, for those values of k_z where they lie inside the continuum they have a complex frequency; the imaginary part is not shown in Fig. 7. We conclude from this figure that the modes F_1 and S ignore, as far as the real part of frequency is concerned, the difference between a collective mode and a global eigenmode.

This conclusion remains more or less true even in the much more complicated case of a current-carrying plasma cylinder (Fig. 8). In addition to the parabolic density profile we have now included a peaked current profile ~ $[1 - (r/r_p)^2]^4$ which results in $b_\theta = 0.06 \{1 - [1 - (r/r_p)^2]^5\} r_p^2/r^2$. For an aspect ratio of 3.3 this field yields a safety factor of 1 on the axis and 5 at the plasma edge. The current makes the Alfvén continuum non-monotonous in r. We show therefore the lower bound $\min \omega_A(r)$ of the continuum in addition to $\omega_A (r = 0)$

and ω_A ($r = r_p$). Due to the current the solutions depend on the sign of k_z. We remark that the current merely shifts the two branches of the surface mode S by a small amount (cf. Eq. (7.77)). The small shift in k_z is approximately equal to that observed for $\omega_A(r = r_p)$. Apart from this small shift the dispersion relations of F_1 (not shown) and S seem to be unaffected by the current. In Figs. 7 and 8 they coincide up to values of $k_z r_p$ of the order of one. The deviation at higher values is accompanied by the appearance of an imaginary part of ω (not shown) of the order of the real part.

The global eigenmodes of the Alfvén wave are distinctly separated from the continuum in the whole range of negative k_z values, but have completely disappeared from the positive range of k_z. In the negative range of k_z it looks as if the continuum, under the influence of the current, has withdrawn from the global Alfvén modes, whereas in the positive range of k_z the continuum has moved downwards hiding these modes.

The most striking new feature, however, is the existence of unstable eigenmodes. The graph has been obtained by plotting the imaginary part of ω of the unstable eigenmodes; their real frequency is practically zero as one would expect from MHD. The absolute value of the growth rates and the marginal stability points are not correctly given in Fig. 8 because the approximation used in the derivation of Eqs. (7.58) and (7.59), namely first order in b_θ, is insufficient. The results are nevertheless easily interpretable. The mode A_1 is known in MHD as the external kink mode. In Fig. 8 its growth rate turns out to be roughly twice the correct MHD result. The range of instability is a bit too large in Fig. 8. Ideal MHD theory gives $0 \lesssim k_z r_p \lesssim .3$. The modes A_s, $s \geq 2$, are called internal kink modes.

7.4 Bounded Hot Plasmas

It has been noted in Section 7.1.1 that in low-beta plasmas (cf. Eq. (4.17)) the dispersion relation of the fast magnetoacoustic wave is unaltered by the thermal motion of particles. The spectral characteristics of this wave in hot plasmas remain therefore essentially the same as in cold plasmas. On the other hand, the Alfvén wave is dramatically modified by hot-plasma effects: it becomes the kinetic Alfvén wave. It is therefore of importance to ascertain the properties of this wave in bounded systems.

The problem of the spectral characteristics of the kinetic Alfvén wave has been addressed for cylindrical plasmas using various approximations for treating the ions: cold-ion model [123, 132, 144], the effects of finite Larmor radius to the second order [139, 161, 175] and to all orders [156]. Here we shall briefly review some of the results obtained in Ref. [156].

Consider a weakly-inhomogeneous, cylindrical plasma whose dynamics are described by the dielectric tensor operator given by Eqs. (6.30) - (6.33). Since $B_{\parallel}$ of the kinetic Alfvén wave is negligible one may use a two-potential approximation to represent the wave electric field [73]. Thus we set

$$\vec{E} = \left(\frac{\partial \phi_1}{\partial r} , i k_{\perp} \phi_1 , i k_{\parallel} \phi_2 \right) , \tag{7.97}$$

where ϕ_1 and ϕ_2 are the potentials. To derive the appropriate wave equations for the potentials we note that Eq. (3.1) implies

$$\nabla \cdot \overleftrightarrow{\varepsilon} \cdot \vec{E} = 0. \tag{7.98}$$

On substituting the representation (7.97) in Eq. (7.98) and the parallel component of Eq. (3.1), and making some rearrangements, one obtains [156]

$$\phi_2 = \frac{T_e/T_i}{(1-\Gamma)[1-(\omega/\omega_{ci})^2]} \rho_i^2 \Delta_\perp \phi_1 , \tag{7.99}$$

$$\left\{\left(\frac{\omega}{c_A}\right)^2 - k_\parallel^2\left[1-\left(\frac{\omega}{\omega_{ci}}\right)^2\right] + \Delta_\perp \rho_i^2\left[\frac{T_e}{T_i}\frac{k_\parallel^2}{1-\Gamma} + \frac{3}{4}\left(\frac{\omega}{c_A}\right)^2 \frac{1}{1-(\omega/2\omega_{ci})^2}\right]\right\}\Delta_\perp \phi_1 = 0, \tag{7.100}$$

where $\Gamma \equiv \Gamma(\omega/|k_\parallel| v_{te})$ and the operator $\Delta_\perp$ is given by Eq. (7.40). In deriving Eqs. (7.99) and (7.100) we have also used the fact that $\omega >> |k_\parallel| v_{ti}$ for low-beta plasmas. The generalizations of these equations that take into account ion Larmor radius terms to all orders and more general profiles of the equilibrium quantities can be found in Ref. [156].

In the limit $T_i \to 0$, $T_e \to 0$, $m_e \to 0$ Eq. (7.99) yields $\phi_2 = 0$ while Eq. (7.100) reduces to

$$\left[\omega^2 - \omega_A^2(r)\right]\Delta_\perp \phi_1 = 0, \tag{7.101}$$

which is a singular equation describing the Alfvén continuum. Thus, as can be seen from Eq. (7.100), the effects of finite ion Larmor radius to the second order and/or parallel electron dynamics remove the Alfvén continuum and replace it

by a discrete spectrum of the kinetic Alfvén wave. Such a spectrum can easily be found in the two following cases.

Consider a completely filled plasma waveguide. The boundary condition (3.8) and Eq. (7.97) imply

$$\phi_1 = \phi_2 = 0 \qquad at \quad r = r_p . \tag{7.102}$$

Assuming uniform equilibrium profiles, Eqs. (7.99) and (7.100) can be solved in terms of Bessel functions. The discrete spectrum is then given by

$$\omega^2 = \frac{c_A^2 k_\parallel^2}{1+(c_A k_\parallel/\omega_{ci})^2}\left[1 + k_r^2 \rho_i^2\left(\frac{T_e}{T_i} + \frac{3}{4+3(c_A k_\parallel/\omega_{ci})^2}\right)\right], \tag{7.103}$$

where the discrete values of the radial wavenumber k_r are solutions of the equation

$$J_m(k_r r_p) = 0, \tag{7.104}$$

which follows from Eq. (7.102). In deriving Eq. (7.103) we have assumed $\omega << |k_\parallel| v_{te}$ and neglected the Landau damping.

Another simple case is that of weakly-nonuniform equilibrium profiles. A WKB analysis of Eq. (7.100) then yields the following relationship for the eigenvalues

$$\int_0^{r_p} \frac{dr}{\rho_i} \left\{ \frac{(\omega/c_A k_\parallel)^2 + (\omega/\omega_{ci})^2 - 1}{T_e/T_i + \frac{3}{4}(\omega/c_A k_\parallel)^2 \left[1 - (\omega/2\omega_{ci})^2\right]^{-1}} \right\}^{1/2} = l\pi, \tag{7.105}$$

where l is a large, positive integer.

It has been shown in Ref. [156] that the inclusion of ion Larmor radius terms to all orders does not destroy the second-order discrete spectrum, presented here, provided $k_\parallel \neq 0$. Moreover, the second-order spectrum has been found to be a good approximation to the full spectrum even for quite high values of the radial wave number.

8. MAGNETIC PUMPING

In this section we shall review the heating rates for various schemes in which the energy of an excited electromagnetic field is directly absorbed by plasma species. Since in such schemes the energy absorption is expected to be rather global the heating rates may be estimated by assuming the equilibrium plasma to be uniform and currentless.

8.1 Gyro-Relaxation

In this scheme the energy of electromagnetic field is pumped into the energy of perpendicular plasma motion. The resulting anisotropy is then relaxed via ion-ion collisions, which leads to the ion heating. The heating rate for this process has been investigated using different models: single particle [1, 2, 3, 4], fluid [11, 13, 26] and the drift-kinetic Boltzmann equation [5, 48]. The results obtained may be summarized by the following approximate formula

$$\frac{dT_i}{dt} \approx 0.1 \frac{\omega^2 \nu_{ii}}{\omega^2 + \nu_{ii}^2} T_i \left| \frac{B_\parallel}{B_0} \right|^2, \qquad (8.1)$$

where $B_\parallel$ has been assumed to be a constant independent of spatial coordinates (low-frequency cutoff field). It is straightforward to see from Eq. (8.1) that the heating rate over the oscillation period is maximized at $\omega \approx \nu_{ii}$.

It should be noted that the fluid limit of Eq. (8.1) can be obtained by assuming that the electromagnetic energy is transported into the plasma via the excitation of the fast magnetoacoustic wave which is damped owing to the ion viscosity. Indeed, invoking the energy conservation, Eq. (7.37) implies

$$n_0 \frac{dT_i}{dt} = -\frac{dW}{dt} = 2\gamma_k W, \tag{8.2}$$

where W, according to Eq. (7.33), may be expressed as

$$W = \frac{1}{8\pi} |B_\parallel|^2 \frac{k^2}{k_\wedge^2}, \tag{8.3}$$

and γ_k is given by Eq. (7.19). Using Eq (7.9) we can rewrite Eq. (7.19) as

$$\gamma_k \approx 0.1 \frac{v_{ti}^2}{\nu_{ii}} \left(\frac{\omega}{C_A}\right)^2 \frac{k_\wedge^2}{k^2} . \tag{8.4}$$

Subsituting Eqs. (8.3) and (8.4) into Eq. (8.2) then yields

$$\frac{dT_i}{dt} \approx 0.1 \frac{\omega^2}{\nu_{ii}} T_i \left|\frac{B_\parallel}{B_0}\right|^2, \tag{8.5}$$

which is just the fluid limit of Eq. (8.1).

8.2 Transit Time Pumping

This heating method is based on the collisionless damping of electromagnetic fields due to the Cerenkov resonance. The field energy can be transported into the plasma in different ways depending on the excitation frequency, which is considered to be much smaller than ω_{ci}, and the type of pumping.

8.2.1 Compressional pumping

In this scheme the energy of electromagnetic field is pumped into the energy of some kind of compressional plasma motion. The interaction of such perturbations with the resonant particles may be adequately described employing the slab or cylindrical geometry. The pertinent heating rates can thus be obtained from Eqs. (6.21) or (6.35). In what follows we shall make use of Eq. (6.35) and distinguish three cases:

a) For $\omega \sim k_{\|} v_{ti}$ the energy is absorbed by the ions. Using Eq. (3.5) we can rewrite Eq. (6.35) approximately as

$$P_i = \frac{1}{8\pi^{1/2}} \frac{\rho_i^2 \omega_{pi}^2}{|k_{\|}| v_{ti}} \left(\frac{\omega}{c}\right)^2 \exp\left[-\left(\frac{\omega}{k_{\|} v_{ti}}\right)^2\right] \times \left(|B_{\|}|^2 + \left|B_{\|} - \frac{c}{i\omega} \frac{2\omega\omega_{ci}}{k_{\|} v_{ti}} E_{\|}\right|^2\right). \tag{8.6}$$

With $E_{\|} = 0$ the expression (8.6) is equivalent to that derived in Refs. [4, 5]. The effect of $E_{\|} \neq 0$ has been considered in Refs. [8, 9, 11, 37]. To derive an explicit expression for P_i in this case one must relate $E_{\|}$ to $B_{\|}$. This can easily be done by substituting Eqs. (6.30) - (6.33) into Eq. (7.98) and again using Eq. (3.5). With the relevant accuracy one finds

$$E_{\|} = -B_{\|} \frac{i\omega}{c} \frac{k_{\|} v_{ti}^2}{2\omega\omega_{ci}} \frac{Z}{T_i/T_e + 1 - Z}, \tag{8.7}$$

where $Z \equiv Z\left(\frac{\omega}{|k_{\|}| v_{ti}}\right)$. Inserting Eq. (8.7) in Eq. (8.6) and making some rearrangements one obtains

$$P_i = \frac{\pi^{1/2}}{2} n_0 T_i \frac{\omega^2}{|k_\parallel| v_{ti}} \exp\left[-\left(\frac{\omega}{k_\parallel v_{ti}}\right)^2\right] \left|\frac{B_\parallel}{B_0}\right|^2 \times \left[1 + \frac{(1+T_i/T_e)^2}{|T_i/T_e + 1 - Z|^2}\right]. \tag{8.8}$$

The order of magnitude estimate for the heating rate is then given by

$$\frac{dT_i}{dt} \sim \omega T_i \left(\frac{\tilde{B}}{B_0}\right)^2, \tag{8.9}$$

where $\tilde{B}$ is the amplitude of the oscillating magnetic field in the vacuum. Comparing Eq. (8.9) with Eq. (8.1) we may conclude that the transit time pumping is at least one order of magnitude more efficient than the gyro-relaxation.

b) For $T_e >> T_i$ and $\omega \sim k_\parallel c_s$ the pumping field excites the ion-accoustic wave which is damped by the electron Landau damping. Since the direct contribution of $B_\parallel$ - terms to Eq. (6.35) turns out to be negligible one has

$$P_e = \frac{1}{4\pi^{1/2}} \frac{\omega^2 \omega_{pe}^2}{|k_\parallel|^3 v_{te}^3} |E_\parallel|^2. \tag{8.10}$$

Using the same procedure as that leading to Eq. (8.7) $E_\parallel$ is now expressed in terms of $B_\parallel$ as

$$E_\parallel = -B_\parallel \left(\frac{2}{\pi}\right)^{1/2} \frac{k_\parallel c_s^2}{c\,\omega_{ci}} \left(\frac{m_i}{m_e}\right)^{1/2}. \tag{8.11}$$

Substitution of Eq. (8.11) into Eq. (8.10) then yields [8, 27, 37]

$$P_e = \frac{\omega}{(2\pi)^{1/2}} \left(\frac{m_i}{m_e}\right)^{1/2} n_0 T_e \left|\frac{B_\parallel}{B_0}\right|^2 . \tag{8.12}$$

In comparison with Eq. (8.9) this result represents an enhancement in the absorbed power by a factor of the order $(T_e/T_i)\,(m_i/m_e)^{1/2}$.

c) The pumping field excites the fast magnetoacoustic wave whose energy is absorbed by the electrons. Assuming $v_{te} >> c_A$ one finds

$$E_\parallel = -i B_\parallel \frac{k_\parallel c_S^2}{c\,\omega_{ci}} . \tag{8.13}$$

Inserting Eq. (8.13) in Eq. (6.35) thus yields [25, 51]

$$P_e = \frac{\pi^{1/2}}{2} \frac{\omega^2}{|k_\parallel| v_{te}} n_0 T_e \left|\frac{B_\parallel}{B_0}\right|^2 . \tag{8.14}$$

If ω is close to an eigenfrequency of the plasma column (magnetoacoustic resonance) $B_\parallel$ may be estimated using Eq. (7.24) to be

$$B_\parallel \sim \tilde{B} \frac{m_i}{m_e} \frac{c_A}{v_{te}} . \tag{8.15}$$

Combining Eqs. (8.14) and (8.15) one obtains the order of magnitude estimate [27, 51]

$$P_e \sim \omega \frac{c_A}{v_{te}} \frac{m_i}{m_e} \tilde{B}^2 . \tag{8.16}$$

We note that the heating rate given by Eq. (8.16) is by a factor of the order $(B_0^2/n_0T_e)^{3/2}$ larger than that given by Eq. (8.12).

8.2.2 Torsional and toroidal-drift pumping

In this scheme, which is specific to toroidal systems, the pumping field excites torsional plasma perturbations that can interact not only with the parallel particle motion but also with toroidal particle drift in the inhomogeneous magnetostatic field. To obtain the pertinent heating rates it is convenient to make use of the drift-kinetic equation, Eq. (4.47).

We adopt a cylindrical coordinate system $(\vec{e}_R, \vec{e}_\varphi, \vec{e}_z)$ in a toroidal configuration with z as the symmetry axis. The magnetostatic field is assumed to be of the form

$$\vec{B}_0 = B_T \frac{R_0}{R} \vec{e}_\varphi \,, \tag{8.17}$$

while the unperturbed distribution function of a plasma species is taken to be a uniform Maxwellian. The solution of the linearized Eq. (4.47) is then obtained as

$$f_{g1} = i \frac{q}{T} f_M \frac{E_\varphi v_\parallel + E_z (v_\perp^2/2 + v_\parallel^2)/R\omega_c}{\omega - n v_\parallel/R - k_z (v_\perp^2/2 + v_\parallel^2)/R\omega_c} \,, \tag{8.18}$$

where the perturbations have been decomposed into modes exp [$i(n\varphi + k_z z)$] and B_φ has been set to zero. Substituting expression (8.18) into Eq. (4.48) and carrying out the time average yields the power absorption density

$$P_L(R) = \frac{\pi q^2}{2T}\int d\vec{w}\, f_M\, \delta\left(\omega - \frac{n v_\parallel}{R} - \frac{k_z}{R\omega_c}\left[\frac{v_\perp^2}{2} + v_\parallel^2\right]\right)$$

$$\times \left| E_\varphi v_\parallel + E_z \frac{1}{R\omega_c}\left(\frac{v_\perp^2}{2} + v_\parallel^2\right)\right|^2, \qquad (8.19)$$

which is an analogue of Eq. (4.64).

The following two cases may now be distinguished:

---

a) For $\omega \sim \frac{n}{R} v_{ti}$ (torsional pumping [19 - 21]) the last term in the argument of the Dirac function may be neglected and Eq. (8.19) implies

$$P_i = \frac{\pi^{1/2} e^2 n_0}{2 T_i} \frac{R}{|n| v_{ti}} \exp\left[-\left(\frac{R\omega}{n v_{ti}}\right)^2\right]\left[\frac{v_{ti}^2}{2}\left(\frac{\rho_i}{R}\right)^2 |E_z|^2 + \left|\frac{\omega R}{n} E_\varphi + \frac{E_z}{\omega_{ci}}\left(\frac{\omega^2 R}{n^2} + \frac{v_{ti}^2}{2R}\right)\right|^2\right]. \qquad (8.20)$$

The component E_φ can be expressed in terms of E_z using the equation of charge quasineutrality. Since the electrons may be considered adiabatic [11] this equation takes the form

$$E_\varphi \frac{e n_0}{T_e} = -i \frac{n}{R}\int f_{g1}^{ion}\, d\vec{w}. \qquad (8.21)$$

Inserting expression (8.18) in Eq. (8.21) one obtains

$$E_\varphi = \frac{n E_z}{R\omega_{ci}} \frac{1}{T_i/T_e + 1 - Z}\left[(Z-1)\frac{R\omega}{n^2} + \frac{v_{ti}^2}{2R\omega} Z\right], \tag{8.22}$$

where $Z \equiv Z(\omega R/|n|v_{ti})$. Combining Eqs. (8.20) and (8.22) then yields

$$P_i = \frac{\pi^{1/2}}{2} n_0 T_i \frac{\omega^2 R}{|n|^3 v_{ti}} \exp\left[-\left(\frac{R\omega}{n v_{ti}}\right)^2\right] \left|\frac{B_R}{B_0}\right|^2$$

$$\times \left(1 + \left|\frac{1 + \frac{T_i}{T_e}\left[1 + 2\left(\frac{\omega R}{n v_{ti}}\right)^2\right]}{\frac{T_i}{T_e} + 1 - Z}\right|^2\right), \tag{8.23}$$

where E_z has been eliminated in favour of B_R using Eq. (3.5). If $|B_\parallel|$ and $|B_R|$ are of the same order, the heating rates given by Eqs. (8.8) and (8.23) are of the same order as well. However, on performing an optimization it has been shown [19] that the torsional pumping can be by a factor R_0/r_p more efficient than the compressional pumping.

b) For $n = 0$ and $\omega \sim k_z v_{ti}\rho_i/R$ (toroidal-drift pumping [38, 39]) Eq. (8.21) implies $E_\varphi = 0$, and Eq. (8.19) yields

$$P_i = 4\pi^{1/2} n_0 T_i \omega x^5 e^{-x^2} \mathrm{Re}\, Z(x) \left|\frac{\xi_R}{R}\right|^2,$$

$$x = \frac{1}{v_{ti}}\left(\frac{\omega\omega_{ci} R}{|k_z|}\right)^{1/2}, \tag{8.24}$$

where E_z has been eliminated in favour of ξ_R using Eqs. (4.9) and (4.15). Noting that $|\xi_R/R| \sim \tilde{B}/B_0$ it is easy to show that this heating rate can be a few times larger than that given by Eq. (8.23).

9. ALFVEN RESONANCE HEATING

In this section we shall review the heating schemes for which the frequency of an excited electromagnetic field lies within the continuous spectrum of the Alfvén wave or just below its minimum (see Eqs. (7.73) and (7.74)). Since in such schemes the inhomogeneity of an equilibrium plasma and the presence of an equilibrium current play an essential role it is in general difficult to treat the entire linear problem, formulated in Section 3, by analytical means. As already mentioned in that section a starting point for a numerical treatment is the weak variational form of Eq. (3.1). The two most important cases of such form, considered in the literature under review, may be expressed as follows:

a) Cylindrical geometry - Hot collisionless plasma (Eq. 6.30))

$$\int_{r_0}^{r_p+0} r\,dr\left[\left(\frac{c}{\omega}\right)^2(\nabla\times\tilde{\vec{E}})\cdot(\nabla\times\vec{E})+\frac{d\tilde{\vec{E}}}{dr}\cdot\overleftrightarrow{\alpha}\cdot\frac{d\vec{E}}{dr}+\frac{d\tilde{\vec{E}}}{dr}\cdot\overleftrightarrow{\beta}^{+}\cdot\vec{E}-\tilde{\vec{E}}\cdot\overleftrightarrow{\beta}\cdot\frac{d\vec{E}}{dr}\right.$$

$$\left.-\tilde{\vec{E}}\cdot\overleftrightarrow{\gamma}\cdot\vec{E}\right]=\tilde{\vec{E}}\cdot\left(\overleftrightarrow{\alpha}\cdot\frac{d\vec{E}}{dr}+\overleftrightarrow{\beta}^{+}\cdot\vec{E}\right)r\Big|_{r=r_0} \tag{9.1}$$

$$-\left(\frac{c}{\omega}\right)^2\left[\tilde{\vec{E}}\times(\nabla\times\vec{E})\right]_r r\Big|_{r=r_0}+i\frac{c}{\omega}\left(\tilde{\vec{E}}\times\vec{B}\right)_r r\Big|_{r=r_p+0},$$

where $\vec{B}$ in the last term is given by Eqs. (5.26) and (5.27), and $r_0 \to 0$.

b) Toroidal geometry - Cold plasma with an equilibrium current

$$\int_{V_p} dV\left[\left(\frac{c}{\omega}\right)^2(\nabla\times\tilde{\vec{E}})\cdot(\nabla\times\vec{E})-\tilde{\vec{E}}\cdot\overleftrightarrow{\varepsilon}\cdot\vec{E}\right]=-i\frac{c}{\omega}\int_{\Sigma_p}d\Sigma\oint\vec{B}_0\cdot\nabla\frac{\tilde{E}_\perp}{B_0}, \tag{9.2}$$

where $\overleftrightarrow{\varepsilon}$ is given by Eq. (6.42) and Φ by Eq. (5.46).

For numerical purposes Eqs. (9.1) and (9.2) are approximated by the finite-element method. The details of the procedure can be found in Refs. [165, 166, 178].

Once the solutions of Eqs. (9.1) and (9.2) are obtained the power absorption can be calculated using Eqs. (5.28a) and (5.53).

9.1 Resonance Absorption

It has been noted in Section 7.3.2 that if an excited wave field meets the condition for the Alfvén spatial resonance its energy is absorbed around the resonance layer owing to the Alfvén resonance damping. Provided that certain other conditions are met (they will be discussed in Section 9.2) this property of the cold plasma (or MHD) model can be used to calculate the total absorbed power without specifying a dissipation mechanism. One thus obtains what is referred to as the resonance absorption. The following two cases may be distinguished.

9.1.1 Surface modes

In this scheme the electromagnetic energy is transported into the plasma via the excitation of the first radial, $m \neq 0$ modes of the fast magnetoacoustic wave. The work on the resonance absorption of such modes may be divided into the following categories depending on the methods and plasma models used:

analytical — MHD [61, 62, 65, 77, 89, 98], cold plasma [96, 135, 136, 147, 153],
numerical — MHD [75, 83, 84, 87, 103, 109, 111], cold plasma [56, 119, 126, 130, 145, 171, 172].

The essential features of the analytical estimates can be illustrated on a simple representative example for which the results may be obtained in a closed and explicit form. Consider again the case described in Section 7.3.2, Eqs. (7.92) - (7.94). In the region $r_e \le r \le r_p$, the solution of Eqs. (7.93) and (7.94) (matched to the solution of these equations in the region of the constant density) may be written in the form

$$E_\perp = B_\parallel(r_p)\,\frac{\omega}{ic}\,\frac{|m|}{r}\left(\frac{1}{A(r_e)} + |m|\int_{r_e}^{r}\frac{dr'}{r'A(r')}\right), \tag{9.3}$$

$$B_\parallel = B_\parallel(r_p). \tag{9.4}$$

According to Eq. (3.12) the total absorbed power is given by

$$P = -2\tilde{\pi} r_p L_z S_r(r_p). \tag{9.5}$$

Substitution of Eqs. (9.3) and (9.4) into Eq. (9.5) then yields

$$P = \frac{\tilde{\pi}}{4} L_z \omega m^2 \left(\frac{r_p}{r_e} - 1\right)\left(\frac{c_A}{\omega}\right)^2 |B_\parallel(r_p)|^2, \quad \omega^2 > k_z^2 c_A^2. \tag{9.6}$$

Comparing Eq. (9.6) with Eq. (8.9) we may conclude that the resonance absorption is by a factor of the order B_0^2/n_0T_i more efficient than the transit

time pumping. Moreover, Eq. (9.6) indicates that the absorbed power is of the same order of magnitude as the circulating power.

In order to make expression (9.6) explicit one has to relate $B_{\|}(r_p)$ to an antenna current. This can easily be done by substituting Eqs. (9.3) and (9.4) into Eq. (5.26). Considering a pure helical antenna and assuming $r_w \to \infty$ one finds

$$B_{\|}(r_p) = \frac{\omega^2 - k_z^2 C_A^2}{D}\left(\frac{r_p}{r_a}\right)^{|m|}\frac{4\tilde{\pi}}{c} J_\theta \,, \tag{9.7}$$

where

$$D = \omega^2 - 2k_z^2 C_A^2 + i\tilde{\pi}|m|\left(\frac{r_p}{r_e} - 1\right)\left(1 - \frac{k_z^2 C_A^2}{\omega^2}\right)k_z^2 C_A^2 \,. \tag{9.8}$$

As can be seen from Eq. (9.8) the amplitude of $B_{\|}(r_p)$ is strongly enhanced if ω coincides with the frequency of the surface eigenmode, Eq. (7.96). Combining Eqs. (9.6) - (9.8) then yields

$$P = 2\tilde{\pi}\omega L_z \frac{r_e}{r_p - r_e}\left[\left(\frac{r_p}{r_a}\right)^{|m|}\frac{I}{c}\right]^2 , \tag{9.9}$$

where Eq. (5.29) has been used. In general, Eq. (9.7) indicates that the absorbed power decreases as the distance between the antenna and plasma increases. A further reduction of the power is brought about by the presence of a wall ($r_w \neq \infty$) owing to the excitation of image currents. Using Eq. (5.26) it can easily be shown that the power is reduced by the factor

$$\left[\frac{1 - (r_a/r_w)^{2|m|}}{1 - (r_p/r_w)^{2|m|}}\right]^2 \tag{9.10}$$

Let us now turn our attention to the numerical work. We begin by reviewing the results obtained using an MHD cylindrical code [84]. The characteristics of the system considered are chosen as follows: $n_0(r) = n_0 [1 - 0.99 (r/r_p)^2]$, $\vec{j_0} = \vec{e_z} \bar{j_0}\ c B_0 (0) [1 - (r/r_p)^2]^{\alpha} / 4\pi r_p$, pure helical antenna with m = 1 and $I = r_p c B_0 (0) / 4\pi$, $r_a = 1.2 r_p$ and $r_w = 1.5 r_p$. The quantities n_0, $B_0(0)$ and r_p are scaled out, and the free parameters $\bar{j_0}$, α, ω and k_z are varied within certain ranges. The results are presented in terms of P/P_N, where $P_N = L_z r_p c_A(0) B_0^2(0) / 4\pi$.

A typical result is shown in Fig. 9 for the case $\bar{j_0} = 0.6$ and $\alpha = 2$. Plotted in this figure are the absorbed power (solid lines) and quality factor, Eq. (3.14), (dashed lines) versus k_z for the three fixed positions of the resonance surface: $r_s = 0.3 r_p$, $r_s = 0.5 r_p$ and $r_s = 0.8 r_p$ It is easily seen that for each surface the absorbed power has a maximum, $M(r_s)$, at a definite value of k_z. At the same time, the corresponding quality factor is reasonably small, which implies a good coupling. Moreover the plot indicates that for given characteristics of the system (except for ω and k_z) there exists an optimal resonance surface associated with a maximal absorbed power, max $M(r_s)$. In order to find the position of this surface, $M(r_s)$ is plotted versus r_s as shown in Fig. 10. One sees that for the case considered the optimal surface is located at $r_s \approx 0.4 r_p$. The corresponding value of k_z is found to be $k_z r_p \approx 2.5$. It has been shown that when this optimum occurs ω coincides approximately with the frequency of the surface eigenmode.

The dependence of the optimal absorbed power on the characteristics of the plasma equilibrium has been investigated. Figure 10 shows the quantity $M(r_s)$ versus r_s for different values of $\bar{j_0}$ in the case where $\alpha = 2$. One notices that for a

fixed current profile, the position of the optimal resonance surface is shifted towards the plasma axis when the current increases. At the same time the optimal absorbed power is enhanced. The dependence of the quantity $M(r_s)$ upon the current profile, the total current being fixed, is demonstrated in Fig. 11. It is seen that the optimal resonance surface is shifted towards the plasma axis when the current profile is steeper. For a very peaked current the energy absorption appears to be equally good for all inner surfaces.

The effects of toroidal geometry on the above picture of resonance absorption have been investigated in Refs. [87, 109]. It is shown that for a circular cross-section the overall coupling is much the same as that obtained from the cylindrical model except for some additional resonance surfaces which may be excited due to the interaction of different poloidal modes (cf. Section 7.3.1). However, non-circular cross-sections may introduce additional, larger deviations. As an example, ellipticity is discussed in detail using the Solov'ev equilibrium which, in the coordinate system of Section 8.2.2, is described by

$$\psi = \frac{\psi_s}{\rho_p^2 R_o^2}\left[\frac{R^2 z^2}{(1+\varepsilon)^2} + \frac{1}{4}\left(R^2 - R_o^2\right)^2\right], \qquad (9.11)$$

where ψ_s is the flux at the plasma surface which is inversely proportional to q_o, the safety factor on the axis, ρ_p is a length characterizing the plasma minor radius and ε is a dimensionless parameter which measures the ellipticity of the cross-section. To separate elliptical and purely toroidal effects, a large-aspect-ratio torus is considered, $\rho_p / R_o = 0.0055$, with $q_o = 0.02$ and a (m = 1, n = 100) excitation. In Fig.12, the flux-surface-averaged ψ-component of the Poynting vector is plotted versus the radial coordinate, $s = (\psi/\psi_s)^{1/2}$, for

different values of ε. This graph shows evidence of an edge absorption problem. One sees that for a modest ellipticity of $\varepsilon = 0.25$, 7% of the energy is deposited in the immediate neighbourhood of the plasma edge. For an ellipticity of the order of 0.5, which is approximately that of JET, 25% of the energy is deposited near the edge. For even higher ellipticities, more than 50% of the energy goes to the plasma edge.

The importance of the finite ω/ω_{ci} effects on the resonance absorption of the surface modes has been demonstrated in Ref. [119] using the cold plasma model with an equilibrium current in the cylindrical geometry. An illustrative example is shown in Fig. 13 for the case $\bar{j}_0 = 0.6$, $\alpha = 2$, $m = -1$ and $k_z r_p = -2.5$, the characteristics of the system considered being the same as in the MHD limit (see above). Plotted in this figure is the absorbed power versus the position of the resonance surface for different values of ω/ω_{ci}. One observes that a dramatic modification of the MHD picture occurs already for rather small values of ω/ω_{ci}. A distinct maximum at $\omega/\omega_{ci} = 0.075$ corresponds to the resonance with the surface eigenmode.

9.1.2 Cavity modes

In this scheme the electromagnetic energy is transported into the plasma via the excitation of higher radial, $m \neq 0$ modes and all $m = 0$ modes (there is no surface mode for $m = 0$) of the fast magnetoacoustic wave. On using simplified models, analytical estimates of the resonance absorption of such modes have been obtained in Refs. [81, 82, 86, 114, 157]. Numerical computations based on more realistic models have been carried out in Refs. [119, 157]. Below we present some representative examples obtained in Ref. [119] using the cold plasma model with an equilibrium current in the cylindrical geometry.

The characteristics of the system considered are again the same as in the foregoing section. In order to assess the main differences between the resonance absorption of cavity modes and that of surface modes, the resonances of absorbed power corresponding to the excitation of the first and second radial eigenmodes are followed in the ωk_z-space. Figure 14 shows the absorbed power (a), the resonance width (b) and the position of resonance surface (c) versus k_z for the case $\bar{j}_0 = 0.6$, $\alpha = 2$, $m = 1$ and $\omega/\omega_{ci} = 0$. The resonance width $\Delta\omega$ is defined as the full width at half power and the quantity $\omega/\Delta\omega$ can be interpreted as the cavity Q. One may note the following typical features. The power deposited by the cavity mode appears to be much higher than that deposited by the surface mode. On the other hand, the resonance width of the second mode is much narrower than that of the first one, implying a high cavity Q (hence the term cavity mode). The most important issue, however, are the positions of resonance surface. The power of the cavity mode is deposited near the plasma edge.

The finite ω/ω_{ci} effects on the resonance absorption of cavity modes are illustrated in Fig. 15. The parameters used are the same as in Fig. 14 except that $\omega/\omega_{ci} = 0.3$. Plotted in this figure are also the same quantities as in Fig. 14 but only for the second radial eigenmode. Comparing Figs. 14 and 15 one may conclude that the ω/ω_{ci} effects tend to reduce the absorbed power and to broaden the resonance width. The position of resonance surface appears not to be affected significantly.

9.2 Mode Conversion and Global Alfvén Eigenmode Resonance

To obtain a physical picture of the resonance absorption and to treat more general cases for which the cold plasma approximation breaks down, one has to use more realistic plasma models that include dissipation mechanisms. Such models also allow one to calculate the absorption of global eigenmodes of the Alfvén wave and, in general, the radial profiles of power deposition.

If the plasma considered is hot enough such that $\omega \lesssim k_{\|} v_{te}$, an appropriate model to be used is the one described by the dielectric tensor operator given by Eqs. (6.30)-(6.33). For relatively colder plasmas with $\omega >> k_{\|} v_{te}$, it is sufficient to adopt the two-fluid model that includes collisional dissipation (for example Eqs. (6.5)-(6.7)) [53, 138].

Let us first elucidate the physical mechanism of the resonance absorption in hot plasmas. This problem has been addressed analytically in Refs. [51, 66, 72, 73, 92, 96, 148, 160]. Here we shall follow the argumentation given in Ref. [73].

Consider the region near the resonance layer where the electromagnetic field may approximately be described by Eq. (7.100) in the slab geometry. Generalizing this equation for the case of arbitrary profiles of the equilibrium quantities we obtain

$$\frac{d^2}{dx^2}\rho_i^2\left[\frac{T_e}{T_i}+\frac{3}{4}\left(\frac{\omega}{k_z c_A}\right)^2\right]\frac{d^2\phi_1}{dx^2}+\frac{d}{dx}\left[\left(\frac{\omega}{k_z c_A}\right)^2-1\right]\frac{d\phi_1}{dx}=0. \qquad (9.12)$$

In writing Eq. (9.12) we have assumed $\omega << \omega_{ci}$, $k_y << d/dx$ and neglected the Landau damping.

To proceed further we expand the equilibrium quantities in Taylor series about the resonance point $x = x_s$, where $\omega^2 = k_z^2 c_A^2(x_s)$, and retain only the leading-order terms. Introducing the notation $L^{-1} = d \lg n_0/dx$, $\bar{\rho}^2 = \rho_i^2 (T_e/T_i+3/4)$ and $\xi = (x - x_s)/\bar{\rho}^{2/3} L^{1/3}$ we reduce Eq. (9.12) to a simple form

$$\frac{d^2 E_x}{d\xi^2} + \xi E_x = \left(\frac{L}{\bar{\rho}}\right)^{2/3} E_0 , \tag{9.13}$$

where E_0 is an integration constant representing the source field associated with the fast magnetoacoustic wave.

The general solution of Eq. (9.13) can be expressed in terms of the Airy functions. Here, however, we are only interested in the asymptotic solution for $|\xi| >> 1$. To determine it we must specify appropriate boundary conditions. If the resonance layer is far enough from the plasma centre and/or the damping is sufficiently strong so that the wave propagating towards high-density side is absorbed before reaching the centre, the pertinent boundary condition for $\xi > 0$ is to accept only the outgoing wave. For $\xi < 0$ the boundary condition is simply that the field be finite at $\xi \to -\infty$. The asymptotic solution can then be written as

$$E_x = \begin{cases} \left(\frac{L}{\bar{\rho}}\right)^{2/3} E_0 \left\{ \frac{1}{\xi} - \frac{\pi^{1/2}}{\xi^{1/4}} \exp\left[i\left(\frac{2}{3}\xi^{3/2} + \frac{\pi}{4}\right)\right]\right\}, & \xi > 0 \\ \left(\frac{L}{\bar{\rho}}\right)^{2/3} \frac{E_0}{\xi} , & \xi < 0 . \end{cases} \tag{9.14}$$

The term containing the exponential function represents the kinetic Alfvén wave while the remaining terms represent the field of the fast magnetoacoustic wave.

Thus, in hot plasmas the resonance absorption is a manifestation of the mode conversion of the fast magnetoacoustic wave into the kinetic Alfvén wave which is then absorbed by the electrons via the Landau damping. Since the solution for $\xi < 0$ in Eq. (9.14) is identical to that obtained under the cold plasma approximation, the total absorbed power remains unchanged from the previous resonance-absorption calculations. If, however, the kinetic Alfvén wave reaches the plasma centre, the above picture breaks down and the absorption must be calculated using the hot plasma model.

An argumentation similar to that just described can also be put forward for the case when $\omega >> k_{||} v_{te}$ at the resonance layer. In this case the fast magnetoacoustic wave is found to be mode-converted into the quasi-electrostatic surface wave, Eq. (7.15), which propagates towards the low-density side. If this wave does not reach the plasma edge, once again the total absorbed power is the same as that obtained from the cold plasma calculations.

In general, the quantitative description of Alfvén resonance heating schemes by means of the hot plasma model can only be accomplished numerically. The results of such treatments, using various approximations to Eqs.(6.30)-(6.33), have been reported in Refs. [85, 90, 92, 94, 104, 107, 112, 121, 123, 139, 154, 161, 162, 168, 175, 177, 181-184, 201, 202, 204].Below we present some representative examples obtained using the numerical code ISMENE [178],which is based on Eqs.(6.30)-(6.33) in their completeness (see also Eq. (9.1)).

Let us first consider the frequency range of surface modes which is typical for plasmas of a medium size tokamak (TCA [179]). The characteristics of the system used for the computations are chosen as follows: deuterium plasma, $R_0 = 65$ cm, $r_p = 18$ cm, $k_z = -0.03$ cm^{-1}, $m = -1$, $\omega = 1.9 \times 10^7$ sec^{-1}, $n_0(r) = n_0 [1 - 0.98 (r/r_p)^2]^{0.7}$, $T_{e,i} = T_{eo,io} [1 - 0.84 (r/r_p)^2]^2$ with $T_{eo} = 800$ eV and $T_{io} = 500$ eV, $B_{oz} = 15$ kG, $j_{oz}(r) = j_{oz} [1 - (r/r_p)^2]^2$ with an amplitude j_{oz} such that the total current is 120 kA. As a result of these parameters the safety factor has the values $q(0) = 1$ and $q(r_p) = 3$.

Shown in Fig. 16 is the total absorbed power versus the density on the axis. One can distinguish essentially four different excitation regimes denoted by GEAW, KAW, CONT and SQEW. The waveforms, Im E_r, and the profiles of power deposition, Eq. (6.35), corresponding to these regimes, are plotted versus radius in Fig. 17.

At the lowest density, $n_0 = 2.61 \times 10^{13}$ cm^{-3}, the plasma responds with a high quality resonance owing to the excitation of the fundamental global eigenmode of the Alfvén wave (GEAW). Having its frequency below the minimum of the Alfvén continuum, this mode can correctly be situated even with the cold plasma model (see Section 7.3.2). However, as mentioned earlier, the power absorbed at this resonance can only be obtained from the hot plasma model. We note that the corresponding power deposition profile is rather broad, Fig. 17(b).

The next peak denoted by KAW (kinetic Alfvén wave) is situated within the Alfvén continuum and cannot be found there with the cold plasma model. This resonance is due to the excitation of a standing kinetic Alfvén wave which is established between the mode-conversion layer and the plasma centre, Fig.

17(a). In this regime the absorption profile is also rather broad as can be seen from Fig. 17(b).

At higher densities, indicated by CONT (continuum) in Figs. 16 and 17, the mode-converted kinetic Alfvén wave does not reach the plasma centre and therefore cannot establish a standing wave. Under these conditions, as discussed earlier, the total absorbed power can be calculated using the cold plasma model. To obtain the corresponding power deposition profile, however, one has to use the hot plasma model. Notice that in this case the absorption is somewhat localized near the conversion layer, Fig. 17(b).

Finally, at high densities the total absorbed power exhibits a peak denoted by SQEW (surface quasi-electrostatic wave). In this regime, the conversion layer is situated near the plasma edge, where $\omega >> k_{||} v_{te}$, so that the fast magnetoacoustic wave is mode-converted into the surface quasi-electrostatic wave, which establishes a standing wave between the conversion layer and the plasma edge. Once again the power absorbed at this resonance can only be obtained from the hot plasma model. The corresponding absorption profile is very narrow and situated close to the plasma edge.

In large tokamaks, Alfvén resonance heating may also be accomplished by using the frequency range of cavity modes that lies below the ion cyclotron frequency. The overall picture of this scheme within the context of the hot plasma model is similar to that of the frequency range of surface modes. There may be, however, one noteworthy exception if the applied frequency coincides with the eigenfrequency of a cavity mode. It has been noted in Section 9.1.2 that in this case the Alfvén resonance layer (the mode-conversion layer in the present context) is situated near the plasma edge. It can then occur that the

power absorbed near the resonance layer via the mode conversion is smaller than that absorbed directly via the magnetic pumping in the plasma interior (cf. Eq. (8.16)). An example of such a case is presented in Fig. 18 for the following PLT characteristics: hydrogen plasma, $R_o = 130$ cm, $r_p = 40$ cm, $k_z = -7{,}7 \times 10^{-2}$, $\omega = 1.6 \times 10^{8}$ sec^{-1}, $n_o = 10^{14}$ cm^{-3}, $T_{eo} = T_{io} = 2$ keV, $B_{oz} = 40$ kG, the remaining parameters being the same as those for TCA. Shown in Fig. 18 are: (a) the real parts of the wave electric field components and (b) the power deposition profile and the total energy flux, $S_r + S_T$, versus radius. The kinetic flux, S_T, is calculated using Eq. (6.24). Figure 18 (b) clearly demonstrates a predominance of the magnetic pumping over the mode conversion.

10. RELATION TO HEATING IN THE ION CYCLOTRON RANGE OF FREQUENCIES

The frequency range considered for the use of Alfvén resonance heating schemes in present-day devices does not lie far below the ion cyclotron frequency. It could therefore be expected that these schemes have certain features in common with those in the ion cyclotron range of frequencies. In this section we shall very briefly comment on the relation between these two kinds of heating schemes.

In most of the scenarios of both kinds the electromagnetic energy is transported from the antenna into the plasma via the excitation of the fast magnetoacoustic wave. As far as the electrons are concerned this wave may undergo two types of interaction:

1) Its energy is directly dissipated through the Cerenkov resonance.

2) The wave is mode-converted into a quasi-electrostatic wave whose energy is then absorbed via the Landau damping.

The first type of interaction is the same in both kinds of heating schemes. As for the second type, however, there is a slight difference: while in the low-frequency range the fast magnetoacoustic wave is mode-converted into the kinetic Alfvén wave, in the ion cyclotron range of frequencies this wave is mode-converted into an ion Bernstein wave.

Regarding the ions there is a considerable difference between the two kinds of schemes. In the Alfvén resonance heating the electromagnetic field

does not interact with the ions at all (except possibly via collisions). On the other hand, in the ion cyclotron range of frequencies the interaction of the wave field with the ions is mostly rather strong. One can distinguish two generic cases:

1) The first or higher harmonic heating in a single-ion-species plasma. In this regime the energy of the fast magnetoacoustic wave is absorbed through the first or higher harmonic cyclotron damping. The coupling to the Bernstein wave is weak, but nonetheless has an important influence on the absorption.

2) The minority fundamental heating in a multiple-ion-species plasma. In this regime the fast magnetoacoustic wave is mode-converted into the Bernstein wave at the ion-ion hybrid resonance (an analogue of the Alfvén resonance) which, if the minority ions are sufficiently dilute, occurs near the fundamental cyclotron layer of the minority ions. This wave is then absorbed through the fundamental cyclotron damping.

It is worth pointing out that, in the slab geometry, the description of heating in the ion cyclotron range of frequencies can be accomplished using the hot plasma model presented in this review.

11. CONCLUSIONS

The present state of affairs in the linear theory of magnetic pumping and Alfvén resonance heating has been assessed.

One of the main conclusions is that the Alfvén resonance heating schemes are in general superior to the magnetic pumping schemes. In the former, the absorbed power may attain the magnitude comparable to that of the circulating power while in the latter it is typically much less. An exception is the case in which the applied frequency is close to the frequency of an eigenmode of the fast magnetoacoustic wave. The power absorbed by the electrons via Cerenkov resonance can then be comparable for both types of schemes.

Further, it appears that an accurate description of plasma heating by low-frequency waves can only be accomplished by numerical computations. The most advanced tools in this respect are cylindrical codes based on the hot plasma model. On the other hand, the codes which treat a tokamak in toroidal geometry are less advanced: the physics involved is at most that of the cold plasma model. Thus, what is missing at present is a toroidal kinetic code.

As far as nonlinear theory is concerned, only a few aspects have been addressed up to now: modifications of linear damping rates due to finite wave amplitudes have been estimated in Refs. [12, 55, 216] using the quasilinear approximation and in Refs. [15, 21, 25, 100, 124] using a single-wave approximation; parametric instabilities have been treated in Refs. [73, 74, 95, 97]. Thus, one may state that a comprehensive picture of nonlinear effects is not available as yet.

The results of experiments that have been performed so far may be very briefly summarized as follows. In regard to the antenna impedance (its overall value and the positions of peaks corresponding to the excitation of eigenmodes) there is a good agreement between theory and experiment (see, for example, Refs. [145, 179]). In the plasma, the mode conversion of the fast magnetoacoustic wave into the kinetic Alfvén wave has been seen experimentally [194, 195], but there has been no demonstration of significant heating as yet.

Appendix

DIELECTRIC TENSOR OPERATOR OF A HOT, INHOMOGENEOUS, CURRENT-CARRYING PLASMA COLUMN

In this Appendix we outline the derivation of the operator presented in Section 6.2, Eqs. (6.20) - (6.33).

The starting point is the linearized Vlasov equation, Eq. (4.49):

$$\left(\frac{\partial}{\partial t}+\vec{v}\cdot\nabla\right)f_1+\frac{q}{mc}\vec{v}\times\vec{B}_0\cdot\frac{\partial f_1}{\partial\vec{v}}=-\frac{q}{m}\left(\vec{E}+\frac{1}{c}\vec{v}\times\vec{B}\right)\cdot\frac{\partial f_0}{\partial\vec{v}}\ , \qquad \text{(A.1)}$$

where $\vec{B}_0$ is given by Eq. (6.25) and the equilibrium distribution function satisfies

$$\vec{v}\cdot\nabla f_0+\frac{q}{mc}\vec{v}\times\vec{B}_0\cdot\frac{\partial f_0}{\partial\vec{v}}=0\ . \qquad \text{(A.2)}$$

We adopt the magnetic coordinate system, Eqs. (6.26) and (6.27), and set

$$\vec{v}=v_\perp\left(\vec{e}_r\cos\alpha+\vec{e}_\perp\sin\alpha\right)+v_\parallel\vec{e}_\parallel\ . \qquad \text{(A.3)}$$

Moreover, we assume $|b_\theta| \ll 1$ and confine ourselves in the subsequent analysis to the first order approximation in $|b_\theta|$. Equation (A.2) is thus transformed into

$$v_\perp\left(\cos\alpha\,\frac{\partial f_0}{\partial r}-\frac{\sin\alpha}{r}\,\frac{\partial f_0}{\partial\alpha}\right)-\omega_c\,\frac{\partial f_0}{\partial\alpha}=0\ , \qquad \text{(A.4)}$$

with ω_c being constant. The solution of Eq. (A.4) valid up to first order in δ_p (cf. Eq. (6.13)), which is the approximation we wish to consider, is given by

$$f_o = F + \sin\alpha \, \frac{v_\perp}{\omega_c} \frac{\partial F}{\partial r} \, , \tag{A.5}$$

where F is an arbitrary function of $v_\perp$, $v_\parallel$ and r. For our purposes it is sufficient to consider only

$$F = F(v', r) \, , \qquad v' = \left[v_\perp^2 + (v_\parallel - u)^2 \right]^{1/2} \, , \tag{A.6}$$

where u is a drift velocity related to the equilibrium current.

Likewise, performing the Fourier decomposition Eq. (A.1) is transformed into

$$\omega_c \frac{\partial f_1}{\partial \alpha} + i(\omega - k_\parallel v_\parallel) f_1 + v_\perp \left[\sin\alpha \left(\frac{1}{r} \frac{\partial}{\partial \alpha} - i k_\perp \right) - \cos\alpha \frac{\partial}{\partial r} \right] f_1$$

$$= A \equiv \frac{q}{m} \left[\vec{E} + \frac{1}{i\omega} \vec{v} \times (\nabla \times \vec{E}) \right] \cdot \frac{\partial f_o}{\partial \vec{v}} \, , \tag{A.7}$$

where $\vec{B}$ has been eliminated via Faraday's law and the quantities $k_\parallel$ and $k_\perp$ are defined by Eqs. (6.26) and (6.34). The aim is now to obtain , using a perturbation method, the solution of Eq. (A.7) valid up to δ_p and $\delta^2 f$ (cf. Eq. (6.12)).

Since f_1 must be periodic in α we can write it as a Fourier series

$$f_1 = \sum_{l=-\infty}^{+\infty} \tilde{f}_l \, e^{il\alpha} \,, \tag{A.8}$$

and the same is true for A. Inserting the expression (A.5) into the right-hand side of Eq. (A.7) we can separate order by order and perform the Fourier series decomposition. Before doing this, however, it is convenient to transform Eq. (A.7) into a frame of reference moving with the velocity u. We then have

$$A_l^{(0)} = \frac{q}{m}\frac{1}{v'}\frac{\partial F}{\partial v'}\left\{\frac{v_\perp}{2}\left[E_r(\delta_1+\delta_{-1})+iE_\perp(\delta_{-1}-\delta_1)\right]+v_\parallel E_\parallel \delta_0\right\}, \tag{A.9}$$

$$\begin{aligned} A_l^{(1)} = \frac{q}{m}\Bigg\{&\frac{1}{v'}\frac{\partial^2 F}{\partial v'\partial r}\frac{v_\perp}{\omega_c}\left[\frac{v_\perp}{4}\left\{iE_r(\delta_{-2}-\delta_2)+E_\perp(2\delta_0-\delta_2-\delta_{-2})\right\}\right. \\ &\left.+\frac{i}{2}v_\parallel E_\parallel(\delta_{-1}-\delta_1)\right]+\frac{1}{\omega_c}\frac{\partial F}{\partial r}\left(1-\frac{k_\parallel v_\parallel}{\omega}\right)E_\perp\delta_0 \\ &-\frac{uk_\parallel}{\omega}\frac{1}{v'}\frac{\partial F}{\partial v'}\frac{v_\perp}{2}\left[E_r(\delta_1+\delta_{-1})+iE_\perp(\delta_{-1}-\delta_1)\right]\Bigg\}, \end{aligned} \tag{A.10}$$

$$A_l^{(2)} = \frac{q}{m}\frac{1}{\omega_c\omega}\frac{\partial F}{\partial r}\left[v_\parallel E_\parallel k_\perp\delta_0+\frac{v_\perp}{2}\left(k_\perp E_r+i\frac{dE_\perp}{dr}\right)(\delta_1+\delta_{-1})\right], \tag{A.11}$$

where $\delta_{\mathfrak{L}'} \equiv \delta_{\mathfrak{L}',\mathfrak{L}}$ is Kronecker's delta. In writing the expressions (A.9) - (A.11) we have omitted contributions that are not needed in subsequent calculations.

Finally, substituting the expression (A.8) into Eq. (A.7) and separating different orders we obtain a recursion relation

$$i\Omega_{-\ell}\,\tilde{f}_{\ell}^{(j)} = \frac{v_\perp}{2}\left(L_\ell^+\,\tilde{f}_{\ell-1}^{(j-1)} + L_\ell^-\,\tilde{f}_{\ell+1}^{(j-1)}\right) + A_\ell^{(j)}\,, \qquad \text{(A.12)}$$

where

$$\Omega_\ell = \omega - k_\parallel(v_\parallel + u) - \ell\omega_c\,, \qquad \text{(A.13)}$$

and

$$L_\ell^{\pm} = \frac{\partial}{\partial r} \pm k_\perp + \frac{1}{r}(1 \mp \ell)\,. \qquad \text{(A.14)}$$

For j= 0, the recursion relation simplifies to

$$\tilde{f}_{\ell}^{(0)} = \frac{A_\ell^{(0)}}{i\Omega_{-\ell}}\,, \qquad \text{(A.15)}$$

and after a little algebra

$$\tilde{f}_{\ell}^{(1)} = -\frac{1}{\Omega_{-\ell}}\left[\frac{v_\perp}{2}\left(L_\ell^+\,\frac{A_{\ell-1}^{(0)}}{\Omega_{-\ell+1}} + L_\ell^-\,\frac{A_{\ell+1}^{(0)}}{\Omega_{-\ell-1}}\right) + iA_\ell^{(1)}\right],$$

$$\tilde{f}_{\ell}^{(2)} = \frac{1}{\Omega_{-\ell}}\left[i\left(\frac{v_\perp}{2}\right)^2\left(L_\ell^+ L_{\ell-1}^+\,\frac{A_{\ell-2}^{(0)}}{\Omega_{-\ell+1}\,\Omega_{-\ell+2}} + L_\ell^+ L_{\ell-1}^-\,\frac{A_\ell^{(0)}}{\Omega_{-\ell}\,\Omega_{-\ell+1}}\right.\right. \qquad \text{(A.16)}$$

$$\left.\left. + L_\ell^- L_{\ell+1}^+\,\frac{A_\ell^{(0)}}{\Omega_{-\ell}\,\Omega_{-\ell-1}} + L_\ell^- L_{\ell+1}^-\,\frac{A_{\ell+2}^{(0)}}{\Omega_{-\ell-1}\,\Omega_{-\ell-2}}\right)\right.$$

(A.17)

$$-\frac{v_\perp}{2}\left(L_\ell^+ \frac{A_{\ell-1}^{(1)}}{\Omega_{-\ell+1}} + L_\ell^- \frac{A_{\ell+1}^{(1)}}{\Omega_{-\ell-1}}\right) - i A_\ell^{(2)} \Bigg].$$

Having found f_1 to the desired order we can calculate the induced current density. According to Eq. (4.50) we have

$$\vec{j} = \pi \sum_s q \int_0^\infty v_\perp dv_\perp \int_{-\infty}^{+\infty} dv_\parallel \left\{ v_\perp \left[(\tilde{f}_1 + \tilde{f}_{-1}) \vec{e}_r + i (\tilde{f}_1 - \tilde{f}_{-1}) \vec{e}_\perp \right] + 2 (v_\parallel + u) \tilde{f}_0 \vec{e}_\parallel \right\}. \tag{A.18}$$

Once the current is known the dielectric tensor operator can be determined from the relation (3.2).

In order to perform the velocity integration in Eq. (A.18) we need to specify the equilibrium distribution function F(v',r). For our purposes we assume this function to be a Maxwellian with n_0 and T being arbitrary functions of r. We now combine Eqs. (A.9) - (A.11) with Eqs. (A.15) - (A.17). On substituting the resulting expressions into Eq. (A.18) we can easily evaluate the integrals over $v_\perp$. In fact, only a few $v_\perp$-moments of the Maxwellian are involved. The integration over $v_\parallel$, however, is more complicated. We have first to decompose various products of the denominators Ω^{-1}_ℓ in terms of irreducible fractions. When this is achieved all the integrals in question can be represented by the plasma dispersion function and its derivatives.

For the ion species we set u = 0 and for the electrons we neglect u compared with v_t and $\omega/k_{\parallel}$ everywhere except for the last term in Eq. (A.10). Moreover, from the terms of O (δ_p) we only retain those corresponding to the Cerenkov interaction. After considerable manipulations, we thus arrive at the expressions given by Eqs. (6.30) - (6.33).

ACKNOWLEDGEMENTS

We are indebted to Dr. E. Canobbio who initiated this project.

This work was supported in part by the Swiss National Science Foundation.

REFERENCES

MAGNETIC PUMPING

[1] BUDKER, G.I., in Plasma Physics and Problems of Controlled Thermonuclear Reactions, Vol. 1, AN USSR, Moscow (1958) 122.

[2] SPITZER, Jr., L., WITTEN, L., On the Ionization and Heating of a Plasma, U.S. Atomic Energy Commission, Report No. NYO-999(PM-S-6) (1953).

[3] SCHLÜTER, A., Z. Naturforsch. 12a (1957) 822.

[4] BERGER, J.M., NEWCOMB, W.A., DAWSON, J.M., FRIEMAN, E.A., KULSRUD, R.M., LENARD, A., Phys. Fluids 1 (1958) 301.

[5] SCHMIDT, H.U., Z. Naturforsch. 14a (1959) 975.

[6] FRANK-KAMENETSKII, D.A., Zh. Eksp. Teor. Fiz. 39 (1960) 669 [Sov. Phys. JETP 12 (1961) 469].

[7] FRANK-KAMENETSKII, D.A., Zh. Tekh. Fiz. 30 (1960) 899 [Sov. Phys. Tech. Phys. 5 (1961) 847].

[8] STEPANOV, K.N., Zh. Eksp. Teor. Fiz. 45 (1963) 1196 [Sov. Phys. JETP 18 (1964) 826].

[9] DOLGOPOLOV, V.V., STEPANOV, K.N., Nucl.Fusion 3 (1963) 205.

[10] CANTIENI, E., SCHNEIDER, H., Helv. Phys. Acta 36 (1963) 993.

[11] DAWSON, J.M., UMAN, M.F., Nucl. Fusion 5 (1965) 242.

[12] DOLGOPOLOV, V.V., SIZONENKO, V.L., Nucl. Fusion 7 (1967) 177.

[13] NEMOV, V.V., STEPANOV, K.N., Nucl. Fusion 8 (1968) 133.

[14] FÄSSLER, K., VACLAVIK, J., SCHNEIDER, H., Helv. Phys. Acta 42 (1969) 23.

[15] CANOBBIO, E., in Controlled Fusion and Plasma Physics (Proc. 4th Europ. Conf. Rome, 1970), (1970) 101.

[16] HOEGGER, B., APPERT, K., FÄSSLER, K., KRLIN, L., SCHNEIDER, H., Helv. Phys. Acta 44 (1971) 321.

[17] VACLAVIK, J., Helv. Phys. Acta 44 (1971) 359.

[18] VACLAVIK, J., J. Plasma Phys. 6 (1971) 607.

[19] SAMAIN, A., KOECHLIN, F., Phys. Rev. Lett. 26 (1971) 490.

[20] SAMAIN, A., KOECHLIN, F., in Plasma Physics and Controlled Nuclear Fusion Research (Proc. 4th Int. Conf. Madison, 1971), Vol. 3, IAEA, Vienna (1971) 505.

[21] CANOBBIO, E., in Plasma Physics and Controlled Nuclear Fusion Reseach (Proc. 4th Int. Conf. Madison, 1971), Vol. 3, IAEA, Vienna (1971) 491.

[22] MESSIAEN, A.M., VANDENPLAS, P.E., Nucl. Fusion 11 (1971) 556.

[23] APPERT, K., HOEGGER, B., SCHNEIDER, H., WEISE, E., Helv. Phys. Acta 45 (1972) 533.

[24] BRAMBILLA, M., GIUFFRE, S., Nucl. Fusion 12 (1972) 199.

[25] CANOBBIO, E., Nucl. Fusion 12 (1972) 561.

[26] SAMAIN, A., KOECHLIN, F., Plasma Phys. 14 (1972) 349.

[27] LASHMORE-DAVIES, C.N., MAY, R.M., Phys. Fluids 15 (1972) 1616.

[28] MESSIAEN, A.M., DUBOIS, D.M., VANDENPLAS, P.E., in Controlled Fusion and Plasma Physics (Proc. 5th Europ. Conf. Grenoble, 1972), Vol. 1 (1972) 115.

[29] DUBOIS, D.M., MESSIAEN, A.M., VANDENPLAS, P.E., in Controlled Fusion and Plasma Physics (Proc. 5th Europ. Conf. Grenoble, 1972), Vol. 1 (1972) 114.

[30] MESSIAEN, A.M., VANDENPLAS, P.E., Plasma Phys. 15 (1973) 505.

[31] MESSIAEN, A.M., KOCH, R., VANDENPLAS, P.E., WEYNANTS, R.R., in Controlled Fusion and Plasma Physics (Proc. 6th Europ. Conf. Moscow, 1973), Vol. 1 (1973) 545.

[32] CATTANEI, G., Nucl. Fusion 13 (1973) 839.

[33] BRAMBILLA, M., Plasma Phys. 16 (1974) 482.

[34] MESSIAEN, A.M., VANDENPLAS, P.E., Phys. Lett. 49A (1974) 475.

[35] MESSIAEN, A.M., VANDENPLAS, P.E., in Plasma Physics and Controlled Nuclear Fusion Reseach (Proc. 5th Int. Conf. Tokyo, 1974), Vol. 3, IAEA, Vienna (1975) 319.

[36] MESSIAEN, A.M., VANDENPLAS, P.E., WEYNANTS, R.R., KOCH R., Nucl. Fusion 15 (1975) 75.

[37] LAPSHIN, V.I., STEPANOV, K.N., Fiz. Plazmy 1 (1975) 970 [Sov. J. Plasma Phys. 1 (1975) 529].

[38] CANOBBIO, E., in Plasma Physics and Controlled Nuclear Fusion Research (Proc. 6th Int. Conf. Berchtesgaden, 1976), Vol. 3, IAEA, Vienna (1977) 19.

[39] CANOBBIO, E., in Controlled Fusion and Plasma Physics (Proc. 8th Europ. Conf. Prague, 1977), Vol. 1 (1977) 160.

[40] CANOBBIO, E., in Controlled Fusion and Plasma Physics (Proc. 8th Europ. Conf. Prague, 1977), Vol. 1 (1977) 161.

[41] SY, W.N.-C., Plasma Phys. 20 (1978) 33.

[42] SY, W.N.-C., Plasma Phys. 20 (1978) 1307.

[43] SAWLEY, M.L., J. Plasma Phys. 22 (1979) 223.

[44] McCARTHY, A.L., I.E.E.E. Trans. Plasma Sci. 7 (1979) 196.

[45] MOSER, F., RÄUCHLE, E., SCHNEIDER, E., SCHÜLLER, P.G., Z. Naturforsch. 34a (1979) 1190.

[46] CANOBBIO, E., in Heating in Toroidal Plasmas (Proc. 1st Joint Varenna - Grenoble Int. Symp. Grenoble, 1978), Vol. 2 (1979) 175.

[47] MESSIAEN, A.M., WEYNANTS, R.R., BHATNAGAR, V.P., BURES, M., VANDENPLAS, P.E., in Heating in Toroidal Plasmas (Proc. 1st Joint Varenna - Grenoble Int. Symp. Grenoble, 1978), Vol. 2 (1979) 229.

[48] PUTVINSKII, S.V., Fiz. Plazmy 5 (1979) 977 [Sov. J. Plasma Phys. 5 (1979) 545].

[49] CAYTON, T.E., LEWIS, H.R., Phys. Fluids 23 (1980) 109.

[50] TURNER, L., Phys. Fluids 23 (1980) 1415.

ALFVEN RESONANCE HEATING

[51] DOLGOPOLOV, V.V., STEPANOV, K.N., Nucl. Fusion 5 (1965) 276.

[52] PNEUMAN, G.W., Phys. Fluids 8 (1965) 507.

[53] DOLGOPOLOV, V.V., STEPANOV, K.N., Zh. Tekh. Fiz. 36 (1966) 1003 [Sov. Phys. Tech. Phys. 11 (1966) 741].

[54] McPHERSON, D.A., PRIDMORE-BROWN, D.C., Phys. Fluids 9 (1966) 2033.

[55] DOLGOPOLOV, V.V., SIZONENKO, V.L., STEPANOV K.N., Nucl. Fusion 8 (1968) 41.

[56] ADAM, J., ALVAREZ DE TOLEDO, F., REBUT, P.H., TOROSSIAN, A., Plasma Phys. 11 (1969) 297.

[57] VACLAVIK, J., Phys. Lett. 36A (1971) 259.

[58] UBEROI, C., Phys. Fluids 15 (1972) 1673.

[59] JANKOVICH, Z., in Controlled Fusion and Plasma Physics (Proc. 6th Europ. Conf. Moscow, 1973), Vol. 1 (1973) 621.

[60] TATARONIS, J.A., GROSSMANN, W., Z. Phys. 261 (1973) 203, 217.

[61] HASEGAWA, A., CHEN, L., Phys. Rev. Lett. 32 (1974) 454.

[62] CHEN, L., HASEGAWA, A., Phys. Fluids 17 (1974) 1399.

[63] VACLAVIK, J., WEISE, E., J. Plasma Phys. 12 (1974) 61.

[64] APPERT, K. GRUBER, R., VACLAVIK, J., Phys. Fluids 17 (1974) 1471.

[65] TATARONIS, J.A., J. Plasma Phys. 13 (1975) 87.

[66] MESSIAEN, A.M., in Controlled Fusion and Plasma Physics (Proc. 7th Europ. Conf. Lausanne, 1975), Vol. 1 (1975) 155.

[67] POCHELON, A., KELLER, R., TROYON, F., GRUBER, R., in Controlled Fusion and Plasma Physics (Proc. 7th Europ. Conf. Lausanne, 1975), Vol. 1 (1975) 157.

[68] KAPPRAFF, J.M., TATARONIS, J.A., GROSSMANN, W., in Controlled Fusion and Plasma Physics (Proc. 7th Europ. Conf. Lausanne, 1975), Vol. 1 (1975) 158.

[69] SWANSON, D.G., Phys. Fluids 18 (1975) 1269.

[70] PAO, Y.P., Nucl. Fusion 15 (1975) 631.

[71] GOEDBLOED, J.P., Phys. Fluids 18 (1975) 1258.

[72] HASEGAWA, A., CHEN, L., Phys. Rev. Lett. 35 (1975) 370.

[73] HASEGAWA, A., CHEN, L., Phys. Fluids 19 (1976) 1924.

[74] HASEGAWA, A., CHEN, L. Phys. Rev. Lett. 36 (1976) 1362.

[75] TATARONIS, J.A., GROSSMANN, W., Nucl. Fusion 16 (1976) 667.

[76] KAPPRAFF, J.M., TATARONIS, J.A., J. Plasma Phys. 18 (1977) 209.

[77] KELLER, R., GRUBER, R., TROYON, F., in Heating in Toroidal Plasmas (Proc. 1st Joint Varenna - Grenoble Int. Symp. Grenoble, 1978), Vol. 2 (1979) 195.

[78] BONNEDAL, M., CANOBBIO, E., in Plasma Physics and Controlled Nuclear Fusion Research (Proc. 7th Int. Conf. Innsbruck, 1978), Vol. 2, IAEA, Vienna (1979) 535.

[79] SHOHET, J.L., TALMADGE, J.N., TATARONIS, J.A., GROSSMANN, W., HASEGAWA, A., CHEN, L., HOLZHAUER, E., JANZEN, G., MOSER, F., MÜLLER, G., RÄUCHLE, E., SCHNEIDER, E., SCHÜLLER, P.G., in Plasma Physics and Controlled Nuclear Fusion Research (Proc. 7th Int. Conf. Innsbruck, 1978), Vol. 2, IAEA, Vienna (1979) 569.

[80] PRITCHETT, P.L., DAWSON, J.M., Phys. Fluids 21 (1978) 516.

[81] OTT, E., WERSINGER, J.-M., BONOLI, P.T., Phys. Fluids 21 (1978) 2306.

[82] KARNEY, C.F.F., PERKINS, F.W., SUN, Y.-C., Phys. Rev. Lett. 42 (1979) 1621.

[83] BALET, B., APPERT, K., GRUBER, R., KELLER, R., TROYON, F., VACLAVIK, J., in Controlled Fusion and Plasma Physics (Proc. 9th Europ. Conf. Oxford, 1979), Vol. 1 (1979) 170.

[84] APPERT, K., BALET, B., GRUBER, R., TROYON F., VACLAVIK, J., in Plasma Physics and Controlled Nuclear Fusion Research (Proc. 8th Int. Conf. Brussels, 1980), Vol. 2, IAEA, Vienna (1981) 43.

[85] PURI, S., in Plasma Physics and Controlled Nuclear Fusion Research (Proc. 8th Int. Conf. Brussels, 1980), Vol. 2, IAEA, Vienna (1981) 51.

[86] STIX, T.H., in Heating in Toroidal Plasmas (Proc. 2nd Joint Varenna - Grenoble Int. Symp. Como, 1980), Vol. 2 (1980) 631.

[87] APPERT, K., BALET, B., GRUBER, R., TROYON, F., TSUNEMATSU, T., VACLAVIK, J., in Heating in Toroidal Plasmas (Proc. 2nd Joint Varenna - Grenoble Int. Symp. Como, 1980), Vol. 2 (1980) 643.

[88] TATARONIS, J.A., SALAT, A., in Heating in Toroidal Plasmas (Proc. 2nd Joint Varenna - Grenoble Int. Symp. Como, 1980), Vol. 2 (1980) 655.

[89] NOZAKI, K., FRIED, B.D., MORALES, G.J., in Heating in Toroidal Plasmas (Proc. 2nd Joint Varenna - Grenoble Int. Symp. Como, 1980), Vol. 2 (1980) 663.

[90] PURI, S., in Heating in Toroidal Plasmas (Proc. 2nd Joint Varenna - Grenoble Int. Symp. Como, 1980), Vol. 2 (1980) 671.

[91] FIORI, C., in Heating in Toroidal Plasmas (Proc. 2nd Joint Varenna - Grenoble Int. Symp. Como, 1980), Vol. 2 (1980) 677.

[92] ELFIMOV, A.G., in Heating in Toroidal Plasmas (Proc. 2nd Joint Varenna - Grenoble Int. Symp. Como, 1980), Vol. 2 (1980) 683.

[93] GREKOV, D.L., KALADZE, T.D., STEPANOV, K.N., Fiz. Plazmy 6 (1980) 319 [Sov. J. Plasma Phys. 6 (1980) 177].

[94] LONGINOV, A.V., TSURIKOV, V.A., Fiz. Plazmy 6 (1980) 745 [Sov. J. Plasma Phys. 6 (1980) 406].

[95] GRISHANOV, N.I., NEKRASOV, F.M., Fiz. Plazmy 6 (1980) 1287 [Sov. J. Plasma Phys. 6 (1980) 704].

[96] GREKOV, D.L., STEPANOV, K.N., TATARONIS, J.A., Fiz. Plazmy 7 (1981) 752 [Sov. J. Plasma Phys. 7 (1981) 411].

[97] MIKHAILENKO, V.S., STEPANOV, K.N., Plasma Phys. 23 (1981) 1165.

[98] CANOBBIO, E., Nucl. Fusion 21 (1981) 759.

[99] PRITCHETT, P.L., CANOBBIO, E., Phys. Fluids 24 (1981) 2374.

[100] PANKRATOV, I.M., Fiz. Plazmy 7 (1981) 1291 [Sov. J. Plasma Phys. 7 (1981) 711].

[101] CHEN, G.L., Kinetic Theory of Alfvén Wave Heating in Tokamaks, Ph.D. dissertation, The University of Texas at Austin (1981)

[102] APPERT, K., BALET, B., GRUBER, R., TROYON, F., VACLAVIK, J., Comput. Phys. Commun. 24 (1981) 329.

[103] APPERT, K., BALET, B., VACLAVIK, J., Phys. Lett. 87A (1982) 233.

[104] BENGTSON, R.D., BENESCH, J.F., CHEN, G.L., EVANS, T.E., LI, J.M., LIN, S.H., MAHAJAN, S.M., MICHIE, R.B., OAKES, M.E., ROSS, D.W., SURKO, C.M., VALANJU, P., in Heating in Toroidal Plasmas (Proc. 3rd Joint Varenna - Grenoble Int. Symp. Grenoble, 1982), Vol. 1 (1982) 151.

[105] KIERAS, C.E., TATARONIS, J.A., in Heating in Toroidal Plasmas (Proc. 3rd Joint Varenna - Grenoble Int. Symp. Grenoble, 1982), Vol. 1 (1982) 179.

[106] APPERT, K., GRUBER, R., TROYON, F., VACLAVIK, J., in Heating in Toroidal Plasmas (Proc. 3rd Joint Varenna - Grenoble Int. Symp. Grenoble, 1982), Vol. 1 (1982) 203.

[107] ROSS, D.W., CHEN, G.L., MAHAJAN, S.M., Phys. Fluids 25 (1982) 652.

[108] KALADZE, T.D., PYATAK, A.I., STEPANOV, K.N., Fiz. Plazmy 8 (1982) 823 [Sov. J. Plasma Phys. 8 (1982) 467].

[109] APPERT, K., BALET, B., GRUBER, R., TROYON, F., TSUNEMATSU, T., VACLAVIK, J., Nucl. Fusion 22 (1982) 903.

[110] KIERAS, C.E., TATARONIS, J.A., Phys. Fluids 25 (1982) 1228.

[111] BALET, B., APPERT, K., VACLAVIK, J., Plasma Phys. 24 (1982) 1005.

[112] ITOH, S.I., ITOH, K., NISHIKAWA, K., Plasma Phys. 24 (1982) 1027.

[113] APPERT, K., GRUBER, R., TROYON, F., VACLAVIK, J., Plasma Phys. 24 (1982) 1147.

[114] WINGLEE, R.M., Plasma Phys. 24 (1982) 1161.

[115] KIERAS, C.E., TATARONIS, J.A., J. Plasma Phys. 28 (1982) 395.

[116] TATARONIS, J.A., TALMADGE, J.N., SHOHET, J.L., Comments Plasma Phys. Controlled Fusion 7 (1982) 29.

[117] BERNSTEIN, I.B., Phys. Fluids 26 (1983) 730.

[118] DONNELLY, I.J., CLANCY, B.E., Aust. J. Phys. 36 (1983) 305.

[119] APPERT, K., VACLAVIK, J., Plasma Phys. 25 (1983) 551.

[120] CRAMER, N.F., DONNELLY, I.J., Plasma Phys. 25 (1983) 703.

[121] ITOH, K., ITOH, S.I., Plasma Phys. 25 (1983) 1037.

[122] MAHAJAN, S.M., ROSS, D.W., CHEN, G.L., Phys. Fluids 26 (1983) 2195.

[123] BURDO, O.S., GORIN, V.V., DMITRENKO, A.G., ELFIMOV, A.G., Fiz. Plazmy 9 (1983) 697 [Sov. J. Plasma Phys. 9 (1983) 403].

[124] ELFIMOV, A.G., Fiz. Plazmy 9 (1983) 845 [Sov. J. Plasma Phys. 9 (1983) 491].

[125] BURES, M., in Controlled Fusion and Plasma Physics (Proc. 11th Europ. Conf. Aachen, 1983), Vol. 7D, Part 1 (1983) 297.

[126] APPERT, K. VACLAVIK, J., VILLARD, L., in Controlled Fusion and Plasma Physics (Proc. 11th Europ. Conf. Aachen, 1983), Vol. 7D, Part 1 (1983) 305.

[127] BERNARDIN, M.P., TATARONIS, J.A., Phys. Fluids 27 (1984) 133.

[128] COLLINS, G.A., CRAMER, N.F., DONNELLY, I.J., Plasma Phys. Control. Fusion 26 (1984) 273.

[129] APPERT, K., VACLAVIK, J., VILLARD, L., Phys. Fluids 27 (1984) 432.

[130] SUCCI, S., APPERT, K., KRITZ, A.H., VACLAVIK, J., Helv. Phys. Acta 57 (1984) 121.

[131] WINGLEE, R.M., Plasma Phys. Control. Fusion 26 (1984) 511.

[132] BENGTSON, R.D., EVANS, T.E., LI, Y.M., MAHAJAN, S.M., OAKES, M.E., ROSS, D.W., SURKO, C.M., VALANJU, P.M., WANG, X.Z., WATKINS, J.G., in Heating in Toroidal Plasmas (Proc. 4th Int. Symp. Roma, 1984), Vol. 1 (1984) 121.

[133] BURES, M., in Heating in Toroidal Plasmas (Proc. 4th Int. Symp. Roma, 1984), Vol. 1 (1984) 165.

[134] KNOX, S.O., SPENCER, R.L., TATARONIS, J.A., CRAY, M., in Heating in Toroidal Plasmas (Proc. 4th Int. Symp. Roma, 1984), Vol. 1 (1984) 187.

[135] ELFIMOV, A.G., Fiz. Plazmy 10 (1984) 700 [Sov. J. Plasma Phys. 10 (1984) 405].

[136] ELFIMOV, A.G., LOZOVSKIJ, S.N., DOROKHOV, Jr., V.V., Nucl. Fusion 24 (1984) 609.

[137] APPERT, K., VACLAVIK, J., VILLARD, L., Lecture Notes: An Introduction to the Theory of Alfvén Wave Heating, Centre de Recherches en Physique des Plasmas, Lausanne, Rep. LRP 238/84 (1984).

[138] DONNELLY, I.J., CRAMER, N.F., Plasma Phys. Control. Fusion 26 (1984) 769.

[139] DONNELLY, I.J., CLANCY, B.E., CRAMER, N.F., in Proc. 6th Int. Conf. on Plasma Physics, Lausanne, Contributed Papers (1984) 228.

[140] KIROV, A.G., LOZOVSKIJ, S.N., RUCHKO, L.F., SUKACHOV, A.V., DOROKHOV, V.V., DOLGANYUK, I.M., GULASARYAN, N.L., MALYKH, L.Ya., in Plasma Physics and Controlled Nuclear Fusion Research

(Proc. 10th Int. Conf. London, 1984), Vol. 1, IAEA, Vienna (1985) 643.

[141] CRAMER, N.F., DONNELLY, I.J., Plasma Phys. Control. Fusion 26 (1984) 1285.

[142] HOFMANN, F., APPERT, K., VILLARD, L., Nucl. Fusion 24 (1984) 1679.

[143] HELLSTEN, T., TENNFORS, E., Physica Scripta 30 (1984) 341.

[144] MAHAJAN, S.M., Phys. Fluids 27 (1984) 2238.

[145] APPERT, K., COLLINS, G.A., HOFMANN, F., KELLER, R., LIETTI, A., LISTER, J.B., POCHELON, A., VILLARD, L., Phys. Rev. Lett. 54 (1985) 1671.

[146] BRUNEL, F., LEBOEUF, J.N., MAHAJAN, S.M., Phys. Rev. Lett. 54 (1985) 1252.

[147] ELFIMOV, A.G., Fiz. Plazmy 11 (1985) 550 [Sov. J. Plasma Phys. 11 (1985) 321].

[148] LOZOVSKIJ, S.N., DOROKHOV, Jr., V.V., Fiz. Plazmy 11 (1985) 539 [Sov. J. Plasma Phys. 11 (1985) 315].

[149] EWAYS, S.E., OAKES, M.E., Phys. Fluids 28 (1985) 444.

[150] CRAMER, N.F., DONNELLY, I.J., Plasma Phys. Control. Fusion 27 (1985) 1323.

[151] SY, W.N.-C., Aust. J. Phys. 38 (1985) 143.

[152] BORG, G.G., BRENNAN, M.H., CROSS, R.C., GIANNONE, L., DONNELLY, I.J., Plasma Phys. Control. Fusion 27 (1985) 1125.

[153] ELFIMOV, A.G., in Controlled Fusion and Plasma Physics (Proc. 12th Europ. Conf. Budapest, 1985), Vol. 9F, Part 2 (1985) 256.

[154] KIROV, A.G., SIDOROV, V.P., LOZOVSKIJ, S.N., ELFIMOV, A.G., RUCHKO, L.F., KOMOSHVILI, K.G., DOROKHOV, V.V., in Controlled Fusion and Plasma Physics (Proc. 12th Europ. Conf. Budapest, 1985), Vol. 9F, Part 2 (1985) 260.

[155] McVEY, B.D., SUND, R.S., SCHARER, J.E., Phys. Rev. Lett. 55 (1985) 507.

[156] VAN RIJ, W.I., VAHALA, G., SIGMAR, D.J., Phys. Fluids 28 (1985) 2484.

[157] DONNELLY, I.J., CLANCY, B.E., CRAMER, N.F., J. Plasma Phys. 34 (1985) 227.

[158] TSUI, K.H., Phys. Fluids 28 (1985) 2617.

[159] APPERT, K., COLLINS, G.A., HELLSTEN, T., VACLAVIK, J., VILLARD, L., Plasma Phys. Control. Fusion 28 (1986) 133.

[160] SHVETS, O.M., DIKIJ, I.A., KALINICHENKO, S.S., LYSOVJAN, A.I., NAZAROV, N.I., RANYUK, T. Yu., GREKOV, D.L., STEPANOV, K.N., TOLOK, V.T., Nucl. Fusion 26 (1986) 23.

[161] DONNELLY, I.J., CLANCY, B.E., CRAMER, N.F., J. Plasma Phys. 35 (1986) 75.

[162] ROSS, D.W., LI, Y.M., MAHAJAN, S.M., MICHIE, R.B., Nucl. Fusion 26 (1986) 139.

[163] TATARONIS, J.A., LEWIS, H.R., Phys. Fluids 29 (1986) 167.

[164] CROSS, R.C., MURPHY, A.B., Plasma Phys. Control. Fusion 28 (1986) 597.

[165] APPERT, K., HELLSTEN, T., VACLAVIK, J., VILLARD, L., Comput. Phys. Commun. 40 (1986) 73.

[166] VILLARD, L., APPERT, K., GRUBER, R., VACLAVIK, J., Comput. Phys. Reports 4 (1986) 95.

[167] FUKUYAMA, A., ITOH, K., ITOH, S.I., Comput. Phys. Reports 4 (1986) 137.

[168] DONNELLY, I.J., CLANCY, B.E., BRENNAN, M.H., in Controlled Fusion and Plasma Heating (Proc. 13th Europ. Conf. Schliersee, 1986), Vol. 10C, Part 1 (1986) 431.

[169] CHENG, C.Z., CHANCE, M.S., Phys. Fluids 29 (1986) 3695.

[170] MOISEENKO, V.E., Fiz. Plazmy 12 (1986) 1376 [Sov. J. Plasma Phys. 12 (1986) 798].

[171] APPERT, K., HELLSTEN, T., SAUTER, O., SUCCI, S., VACLAVIK, J., VILLARD, L., Comput. Phys. Commun. 43 (1986) 125.

[172] PURI, S., Nucl. Fusion 27 (1987) 229.

[173] VACLAVIK, J., APPERT, K., Plasma Phys. Control. Fusion 29 (1987) 257.

[174] MARTIN, Th., VACLAVIK, J., Helv. Phys. Acta 60 (1987) 471.

[175] ELFIMOV, A.G., KOMOSHVILI, K.G., SIDOROV, V.P., in Proc. 7th Int. Conf. on Plasma Physics, Kiev, Contributed Papers, Vol. 1 (1987) 22.

[176] GORDIENKO, I. Ya., DOLGOPOLOV, V.V., ROMANOV, S.S., in Proc. 7th Int. Conf. on Plasma Physics, Kiev, Contributed Papers, Vol. 1 (1987) 30.

[177] APPERT, K., VACLAVIK, J., in Proc. 7th Int. Conf. on Plasma Physics, Kiev, Contributed Papers, Vol. 1 (1987) 130.

[178] APPERT, K., HELLSTEN, T., LÜTJENS, H., SAUTER, O., VACLAVIK, J., VILLARD, L., in Proc. 7th Int. Conf. on Plasma Physics, Kiev, Invited Papers, Vol. 2 (1987) 1230.

[179] APPERT, K., BESSON, G., BORG, G.G., DUVAL, B.P., HOWLING, A.A., JOYE, B., LISTER, J.B., MORET, J.-M., RYTER, F., VACLAVIK, J., WEISEN, H., in Proc. 7th Int. Conf. on Plasma Physics, Kiev, Invited Papers, Vol. 1 (1987) 550.

[180] VILLARD, L., Propagation et absorption d'ondes aux fréquences d' Alfvén et cyclotroniques ioniques dans les plasmas toriques, Ph.D. thesis, Ecole Polytechnique Fédérale de Lausanne, No 673 (1987).

[181] PURI, S., in Controlled Fusion and Plasma Physics (Proc. 14th Europ. Conf. Madrid, 1987), Vol. 11D, Part 3 (1987) 1015.

[182] PURI, S., Nucl. Fusion 27 (1987) 1091.

[183] LI, Y.M., MAHAJAN, S.M., ROSS, D.W., Phys. Fluids 30 (1987) 2101.

[184] KIROV, A.G., SIDOROV, V.P., ELFIMOV, A.G., LOZOVSKIJ, S.N., RUCHKO, L.F., KOMOSHVILI, K.G., ONISHCHENKO, V.V., DOROKHOV, V.V., SUKACHEV, A.V., SAMUSHIA, V.D., MALYKH, L.Ya., GULASARYAN, N.L., VOJTENKO, D.A., in Plasma Physics and Controlled Nuclear Fusion Research (Proc. 11th Int. Conf. Kyoto, 1986), Vol. 1, IAEA, Vienna (1987) 645.

[185] PRIDMORE-BROWN, D.C., Phys. Fluids 9 (1966) 1290.

[186] SCHAPER, U., J. Plasma Phys. 29 (1983) 1.

[187] SY, W.N.-C., Plasma Phys. Contr. Fus. 26 (1984) 915.

[188] RIYOPOULOS, S., MAHAJAN, S.M., Phys. Fluids 29 (1986) 731.

[189] LI, Y.M., MAHAJAN, S.M., ROSS, D.W., Phys. Fluids 30 (1987) 1466.

[190] BATCHELOR, D.B., JAEGGER, E.F., CARRERAS, B.A., LYNCH, V.E., WEITZNER, H., IMRE, K., STEVENS, D.C., FUCHS, V., BERS, A., in Plasma Phys. and Contr. Fusion Research (Proc. 12th Int. Conf. Nice, 1988), Vol. 1, IAEA, Vienna (1989) 611.

[191] DOLGOPOLOV, V.V., KRYUKOV, A.V., ROMANOV, S.S., Phys. Fluids 31 (1988) 1649.

[192] BORG, G.G., KNIGHT, A.J., LISTER, J.B., APPERT, K., VACLAVIK, J., in Contr. Fusion and Plasma Heating (Proc. 15th Europ. Conf. Dubrovnik, 1988), Vol. 12B, Part 3 (1988) 956.

[193] APPERT, K., HELLSTEN, T., VACLAVIK, J., VILLARD, L., Plasma Phys. and Contr. Fusion 30, (1988) 1195.

[194] WEISEN, H., APPERT, K., BORG, G.G., JOYE, B., KNIGHT, A.J., LISTER, J.B., VACLAVIK, J., Phys. Rev. Lett. 63 (1989) 2476.

[195] APPERT, K., BORG, G.G., JOYE, B., KNIGHT, A.J., LISTER, J.B., VACLAVIK, J., WEISEN, H., in Contr. Fusion and Plasma Phys. (Proc. 16th Europ. Conf. Venice 1989), Vol. 13B, Part 3 (1989), 1191.

[196] CATTANEI, G., MURPHY, A.B., Nucl. Fusion 29 (1989) 15.

[197] MOISEENKO, V.E., SHVETS, O.M., in Problems in Atomic Science and Technics, Series Thermonuclear Fusion, No. 2 (1989) 26 (in Russian).

[198] MOISEENKO, V.E., Fiz. Plazmy 15 (1989) 365 [Sov. J. Plasma Phys. 15 (1989) 214].

[199] ROBERTS, D.R., HERSHKOWITZ, N., TATARONIS, J.A., Phys. Fluids B2 (1990) 787.

[200] FU, G.Y., VAN DAM, J.W., Phys. Fluids B1 (1989) 1949.

[201] LI, W.-Q., ROSS, D.W., MAHAJAN, S.M., Phys. Fluids B1 (1989) 2353.

[202] LI, W.-Q., ROSS, D.W., MAHAJAN, S.M., Phys. Fluids B1 (1989) 2364.

[203] BORG, G.G., APPERT, K., KNIGHT, A.J., LISTER, J.B., VACLAVIK, J., Nucl. Fusion 30 (1990) 1433.

[204] JAUN, A., VACLAVIK, J., APPERT, K., Plasma Phys. Contr. Fusion 33 (1991) 521.

GENERAL REFERENCES

[205] LIGHTHILL, M.J., Phil. Trans. R. Soc. London, Ser. A252 (1960) 397.

[206] BERNSTEIN, I.B., TREHAN, S.K., Nucl. Fusion 1 (1960) 3.

[207] GINZBURG, V.L., Propagation of Electromagnetic Waves in Plasma, Gordon and Breach, New York (1961).

[208] STIX, T.H., The Theory of Plasma Waves, McGraw-Hill, New York (1962).

[209] ALLIS, W.P., BUCHSBAUM, S.J., BERS, A., Waves in Anisotropic Plasmas, The M.I.T. Press, Cambridge, Massachusetts (1963).

[210] SIVUKHIN, D.V., in Reviews of Plasma Physics, Vol. 1, ed. by M.A. Leontovich, Consultants Bureau, New York (1965) 1.

[211] BRAGINSKII, S.I., in Reviews of Plasma Physics, Vol. 1, ed. by M.A. Leontovich, Consultants Bureau, New York (1965) 205.

[212] SHAFRANOV, V.D., in Reviews of Plasma Physics, Vol. 3, ed. by M.A. Leontovich, Consultants Bureau, New York (1967) 1.

[213] KADOMTSEV, B.B., in Reviews of Plasma Physics, Vol. 2, ed. by M.A. Leontovich, Consultants Bureau, New York (1967) 153.

[214] AKHIEZER, A.I., AKHIEZER, I.A., POLOVIN, R.V., SITENKO, A.G., STEPANOV, K.N., Collective Oscillations in a Plasma, The M.I.T. Press, Cambridge, Massachusets (1967).

[215] BALDWIN, D.E., BERNSTEIN, I.B., WEENINK, M.P.H., in Advances in Plasma Physics, Vol. 3, ed. by A. Simon and W.B. Thompson, Interscience Publishers, New York (1969) 1.

[216] AKHIEZER, A.I., AKHIEZER, I.A., POLOVIN, R.V., SITENKO, A.G., STEPANOV, K.N., Plasma Electrodynamics, Pergamon Press, Oxford (1975).

[217] HASEGAWA, A., UBEROI, C., The Alfvén Wave, Technical Information Center, U.S. Department of Energy (1982).

[218] CROSS, R., An Introduction to Alfvén Waves, Adam Higher, Bristol (1988).

[219] SWANSON, D.G., Plasma Waves, Academic Press, Boston (1989).

Figure Captions

Fig. 1 Plasma-antenna-wall configuration in the cylindrical geometry.

Fig. 2 Slab configuration.

Fig. 3 Toroidal configuration.

Fig. 4 The frequency spectrum of a plasma cylinder as a function of the axial wavenumber k_z. For the two azimuthal wavenumbers $m = \pm 1$, the lowest radial modes of the fast magnetoacoustic wave are designated as F_1 and F_2, those of the Alfvén wave as A_1. The broken line A_∞ represents the accumulation point of the eigenfrequencies of the Alfvén wave. The symbol S stands for "surface eigenmode".

Fig. 5 The wave field of the surface eigenmode in a plasma cylinder as a function of radius. The three figures for different axial wavenumber k_z illustrate the metamorphosis of the global mode F_1, $m = -1$ (at $k_z r_p = 0.4$) into a surface-confined mode S (at $k_z r_p = 1.5$).

Fig. 6 The radial wavenumber squared and the frequency of the surface mode as a function of the axial wavenumber k_z for different wall positions r_w. The accumulation point of the eigenfrequencies of the Alfvén wave, A_∞, is shown with a broken line.

Fig. 7 The frequency spectrum, $x = \omega/\omega_{ci}$, of a currentless plasma cylinder with parabolic density profile as a function of the axial wavenumber k_z. The upper and lower bounds of the Alfvén continuum are shown

with broken lines, $x_A(r = r_p)$ and x_A $(r = 0)$ respectively. Only the most important modes, F_1, S and A_1 are shown.

Fig. 8 The frequency spectrum, $x = \omega/\omega_{ci}$, of a current-carrying plasma cylinder with a parabolic density profile as a function of the axial wavenumber k_z. The Alfvén continuum is characterized by the values of x_A in the center $r = 0$ and at the plasma edge, $r = r_p$. In the region $-0.8 < k_z r_p < 0.3$, $x_A(r)$ is not monotonous in r and has a minimum which is also shown. The stable global eigenmodes of the Alfvén wave are connected with the unstable kink (A_1) and the internal kink (A_2, A_3) modes. The surface mode (S) is only slightly affected by the current.

Fig. 9 Absorbed power (solid lines) and quality factor (dashed lines) versus k_z for different positions of the resonance surface. The parameters used are: $\bar{j}_0 = 0.6$ and $\alpha = 2$.

Fig. 10 Maximal absorbed power, $M(r_s)$, versus the position of resonance surface for different equilibrium currents of the same profile ($\alpha = 2$).

Fig. 11 Maximal absorbed power, $M(r_s)$, versus the position of resonance surface for different profiles of the same equilibrium current.

Fig. 12 Flux-surface-averaged ψ-component of the Poynting vector versus radial coordinate, s, in large-aspect-ratio tori ($\rho_p/R_0 = 0.0055$) of different ellipticity, ε. All the components for $\varepsilon \geq 0.5$ exhibit steep gradients near the plasma edge. For the sake of clarity, the

components for ε = 0.5, 1.0 and 1.25 have not been plotted in the vicinity of the plasma edge.

Fig. 13 Absorbed power versus the position of resonance surface for different values of ω/ω_{ci}. The parameters used are: $\bar{j}_o = 0.6$, $\alpha = 2$, $m = -1$ and $k_z r_p = -2.5$.

Fig. 14 Absorbed power (a), resonance width (b) and the position of resonance surface (c) versus k_z for the case $\bar{j}_o = 0.6$, $\alpha = 2$, $m = 1$ and $\omega/\omega_{ci} = 0$.

Fig. 15 Absorbed power (a), resonance width (b) and the position of resonance surface (c) versus k_z for the second radial eigenmode. The parameters used are the same as in Fig. 14 except that $\omega/\omega_{ci} = 0.3$.

Fig. 16 Total absorbed power versus central density for TCA.

Fig. 17 Imaginary parts of the radial component of the wave electric field (a) and the power deposition profiles (b) versus radius for different regimes defined in Fig. 16.

Fig. 18 Real parts of the wave electric components (a) and, the power deposition profile and the total energy flux (b) versus radius for PLT.

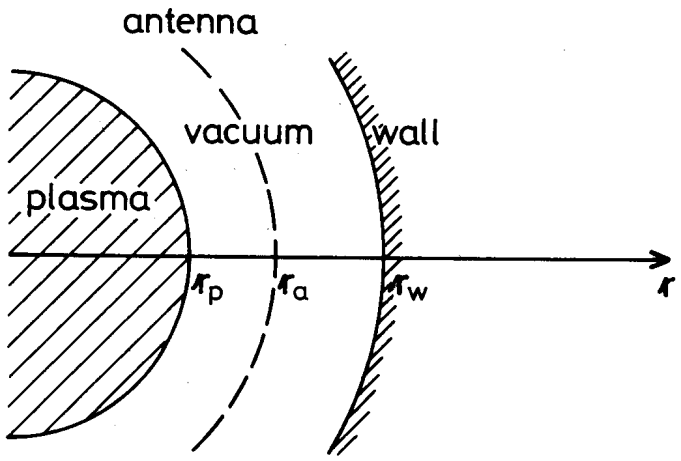

Fig. 1

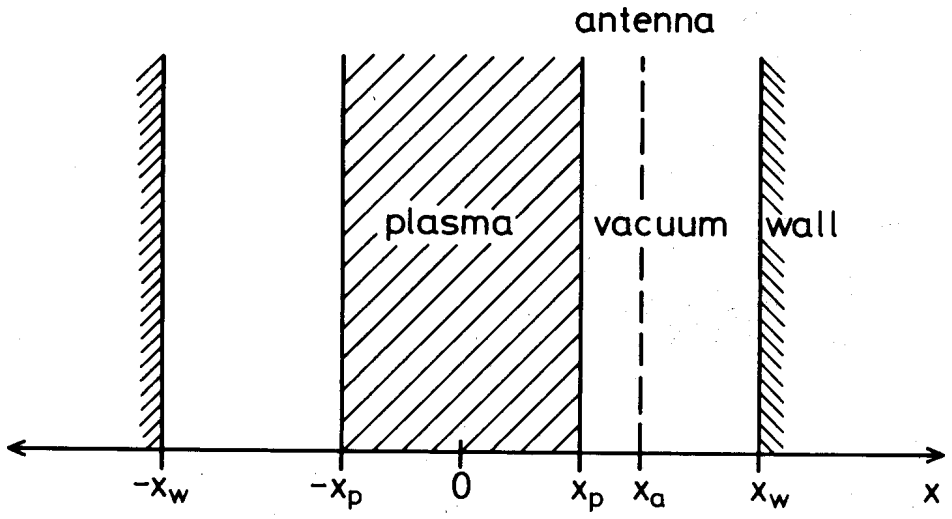

Fig. 2

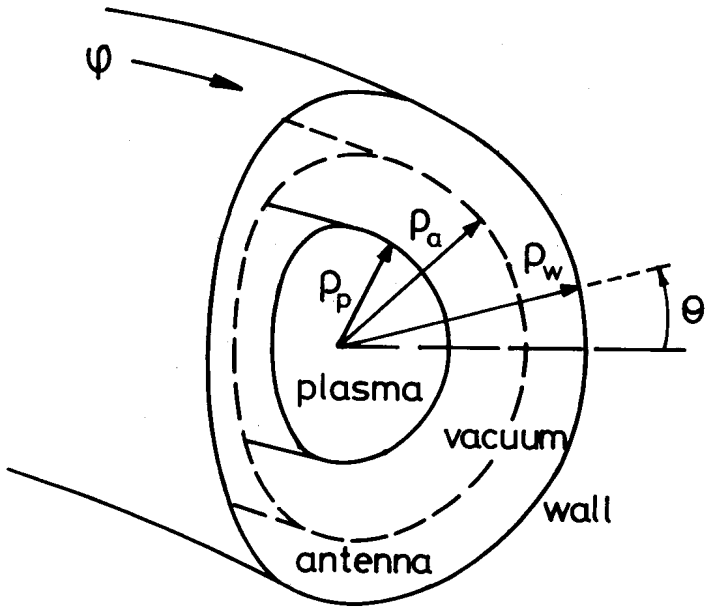

Fig. 3

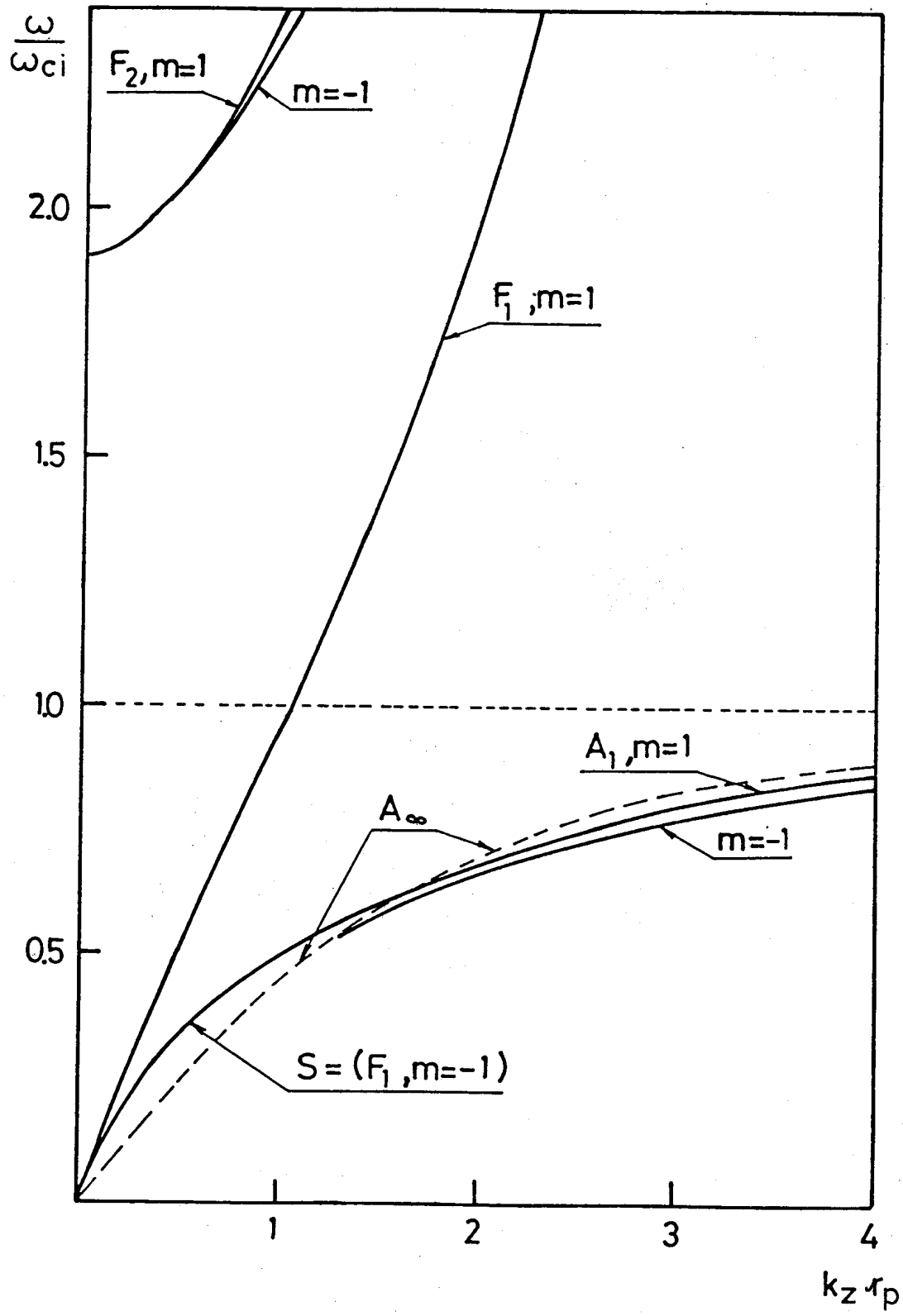

Fig. 4

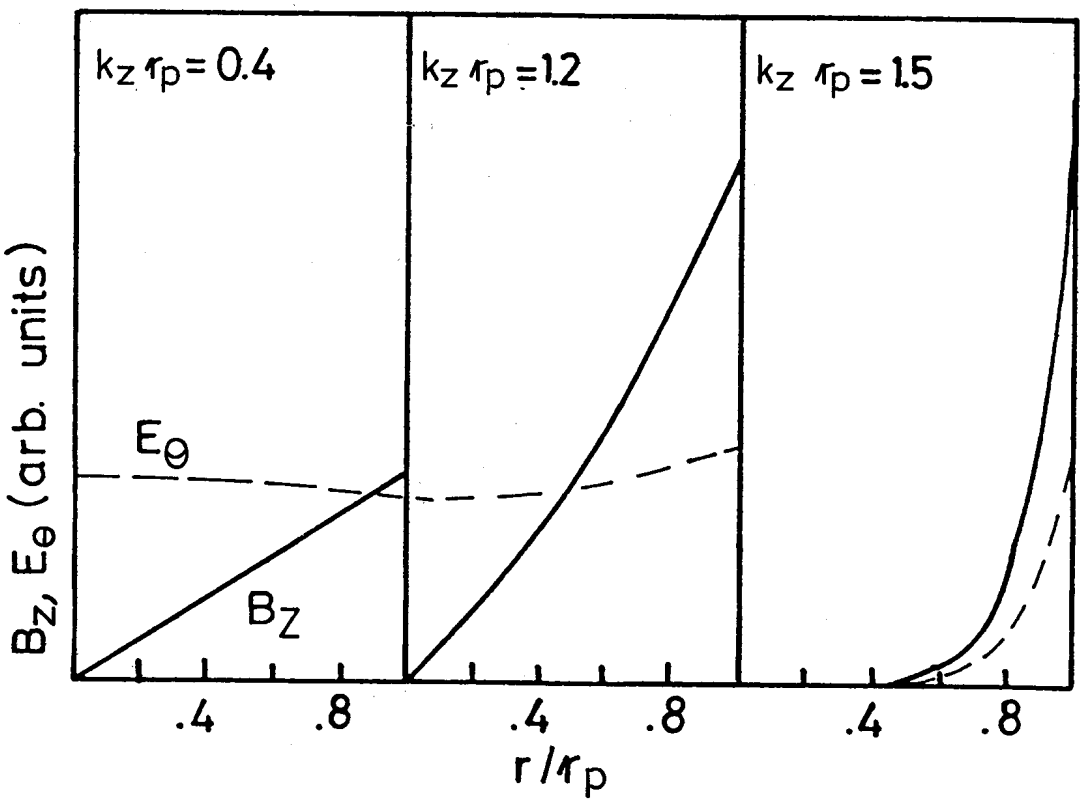
$k_z r_p = 0.4$
$k_z r_p = 1.2$
$k_z r_p = 1.5$
E_θ
B_z
B_z, E_θ (arb. units)
.4
.8
.4
.8
.4
.8
r/r_p

Fig. 5

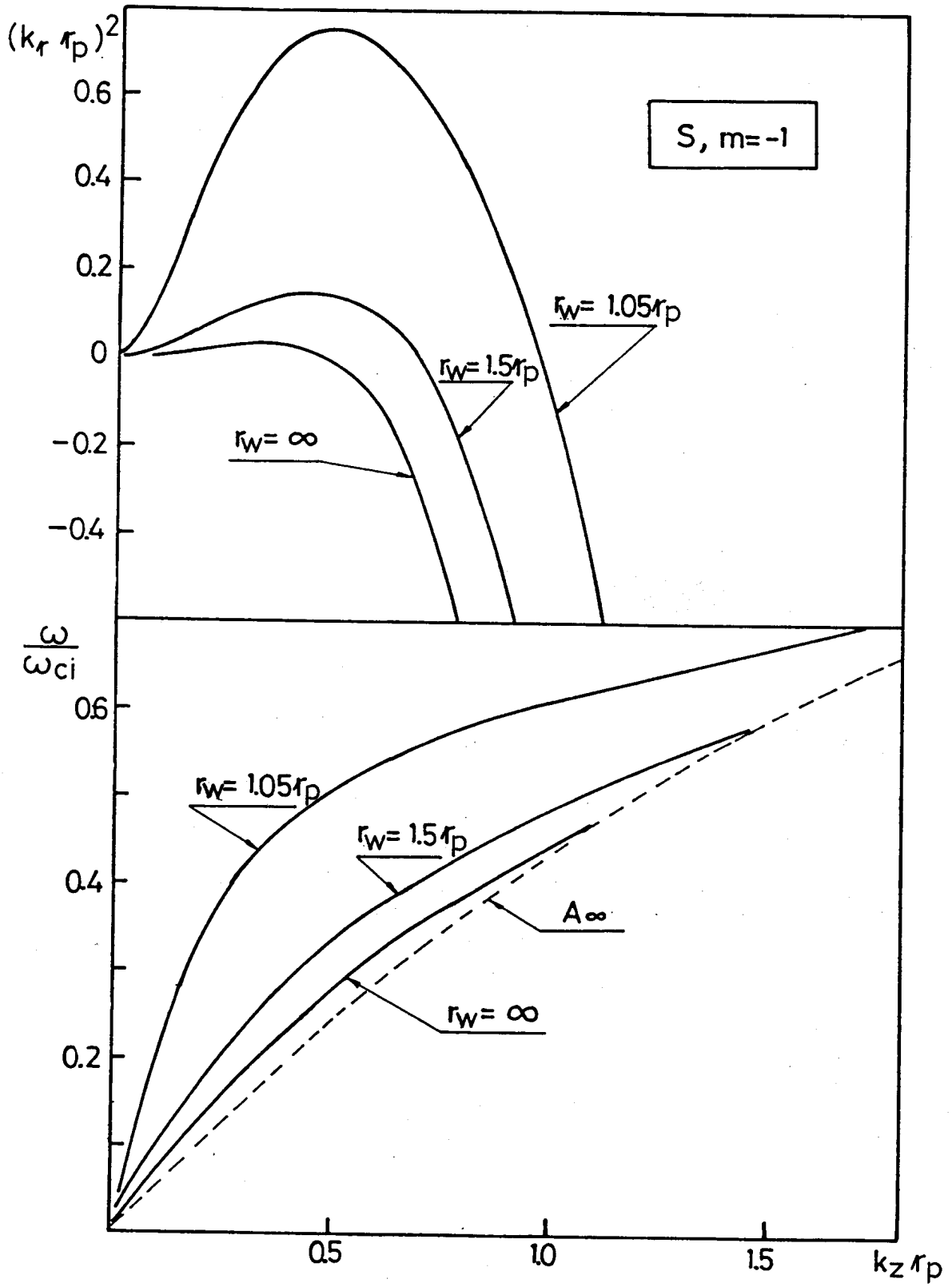
$(k_r r_p)^2$
0.6
0.4
0.2
0
−0.2
−0.4
S, m=-1
$r_w = 1.05 r_p$
$r_w = 1.5 r_p$
$r_w = \infty$
$\frac{\omega}{\omega_{ci}}$
0.6
0.4
0.2
$r_w = 1.05 r_p$
$r_w = 1.5 r_p$
A_∞
$r_w = \infty$
0.5
1.0
1.5
$k_z r_p$

Fig. 6

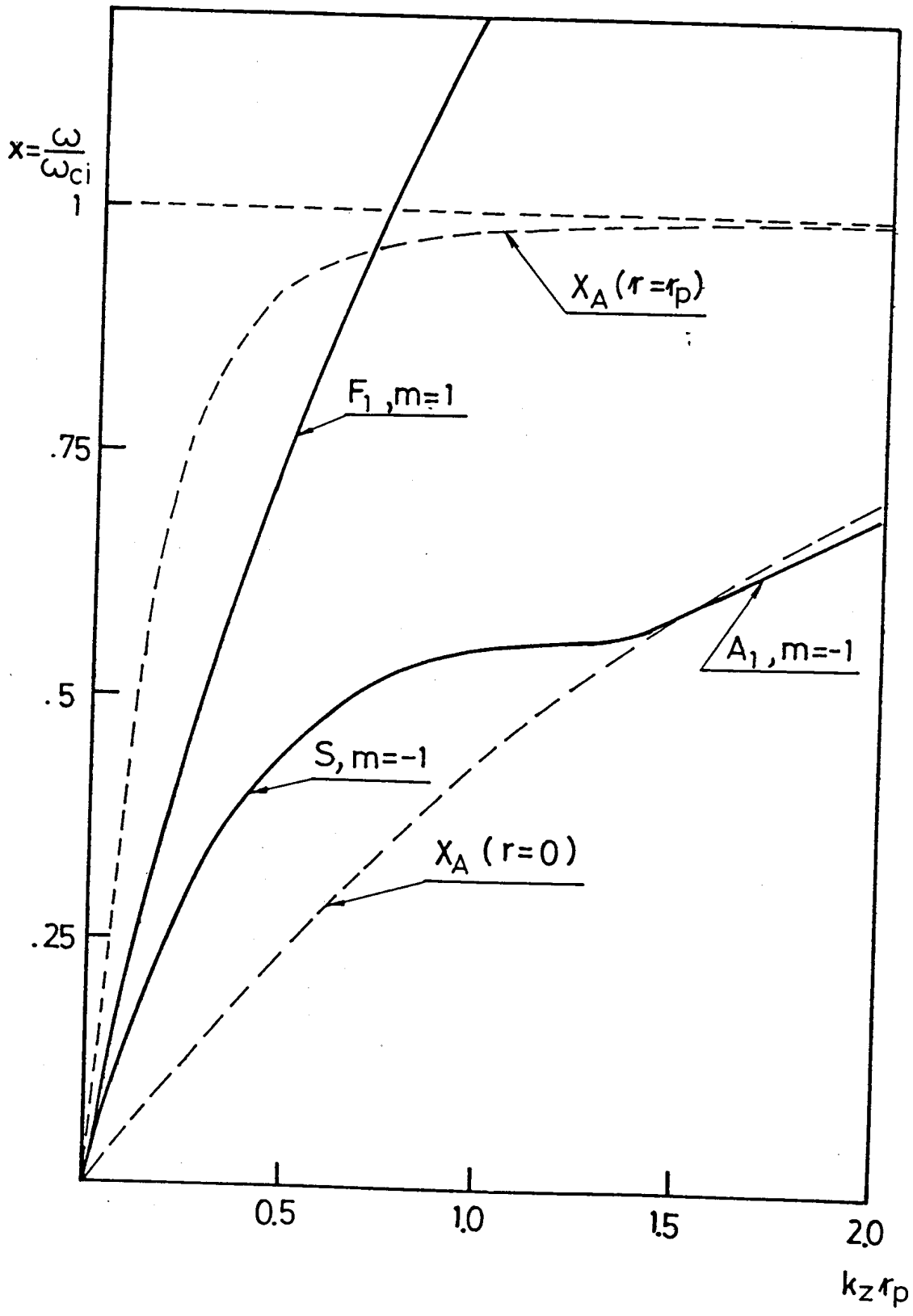

Fig. 7

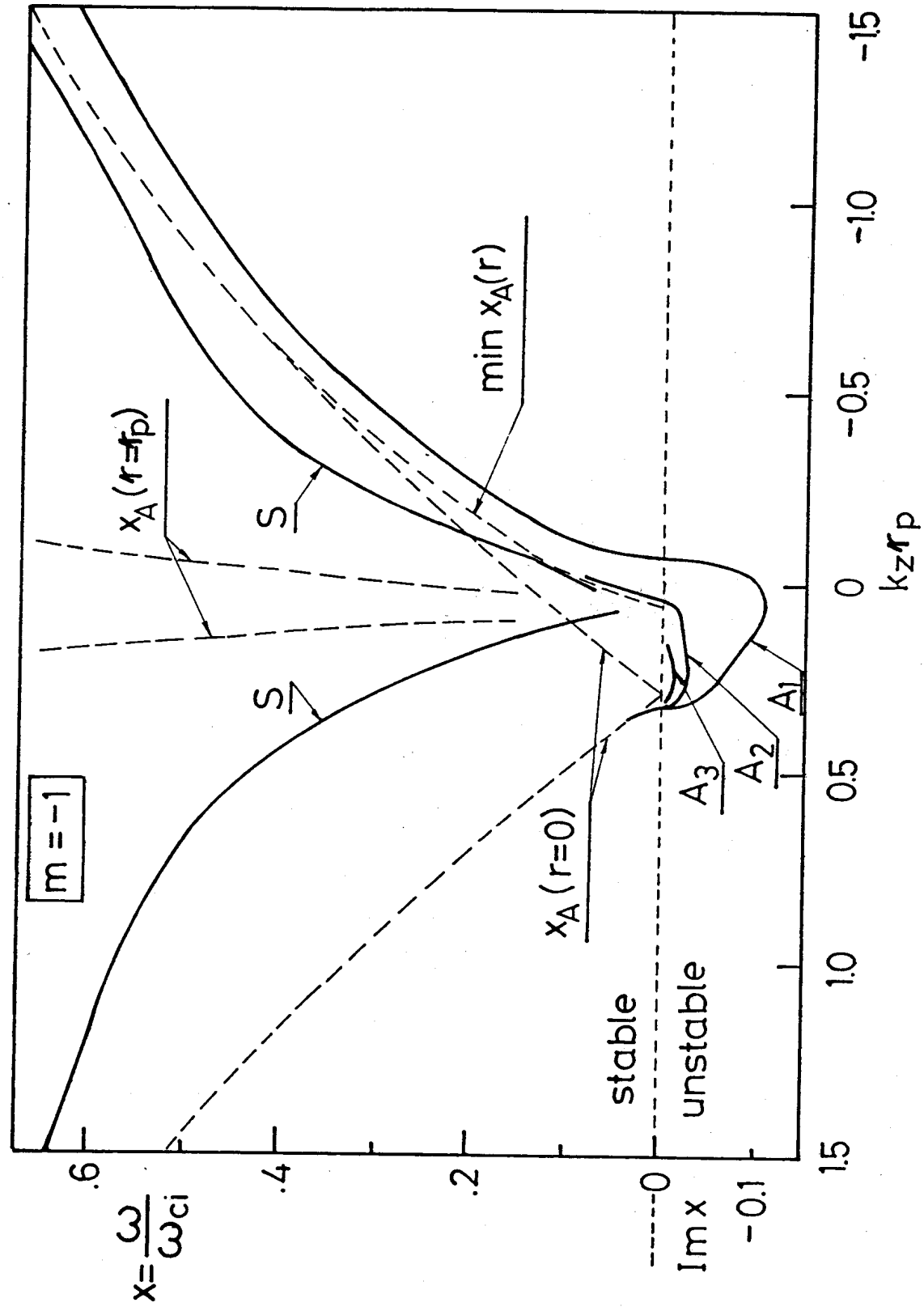
m = -1
$x_A(r=r_p)$
S
min $x_A(r)$
S
$x_A(r=0)$
A_3
A_2
A_1
stable
unstable
$x = \frac{\omega}{\omega_{ci}}$
Im x
$k_z r_p$
.6
.4
.2
0
-0.1
1.5
1.0
0.5
0
-0.5
-1.0
-1.5

Fig. 8

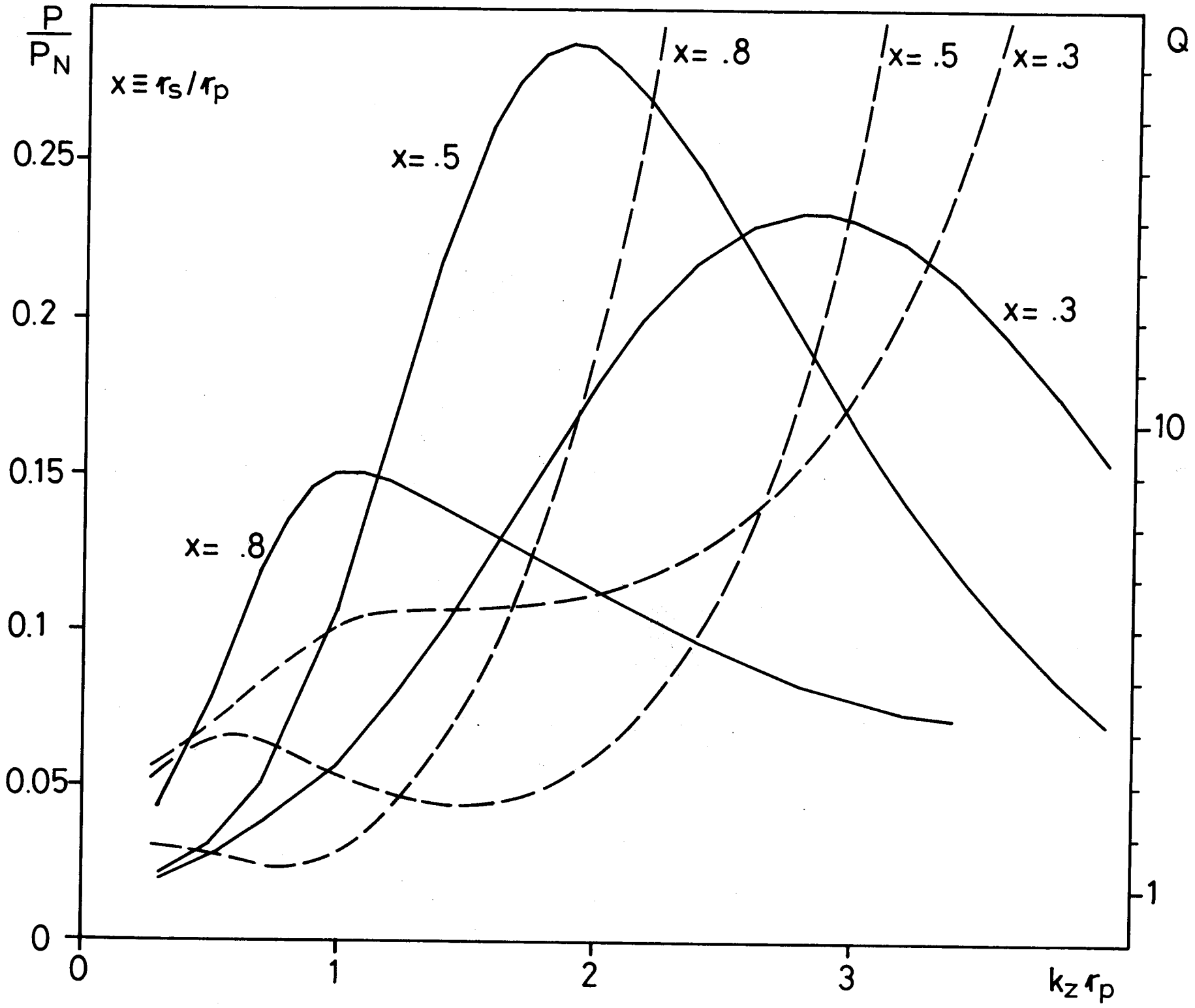

Fig. 9

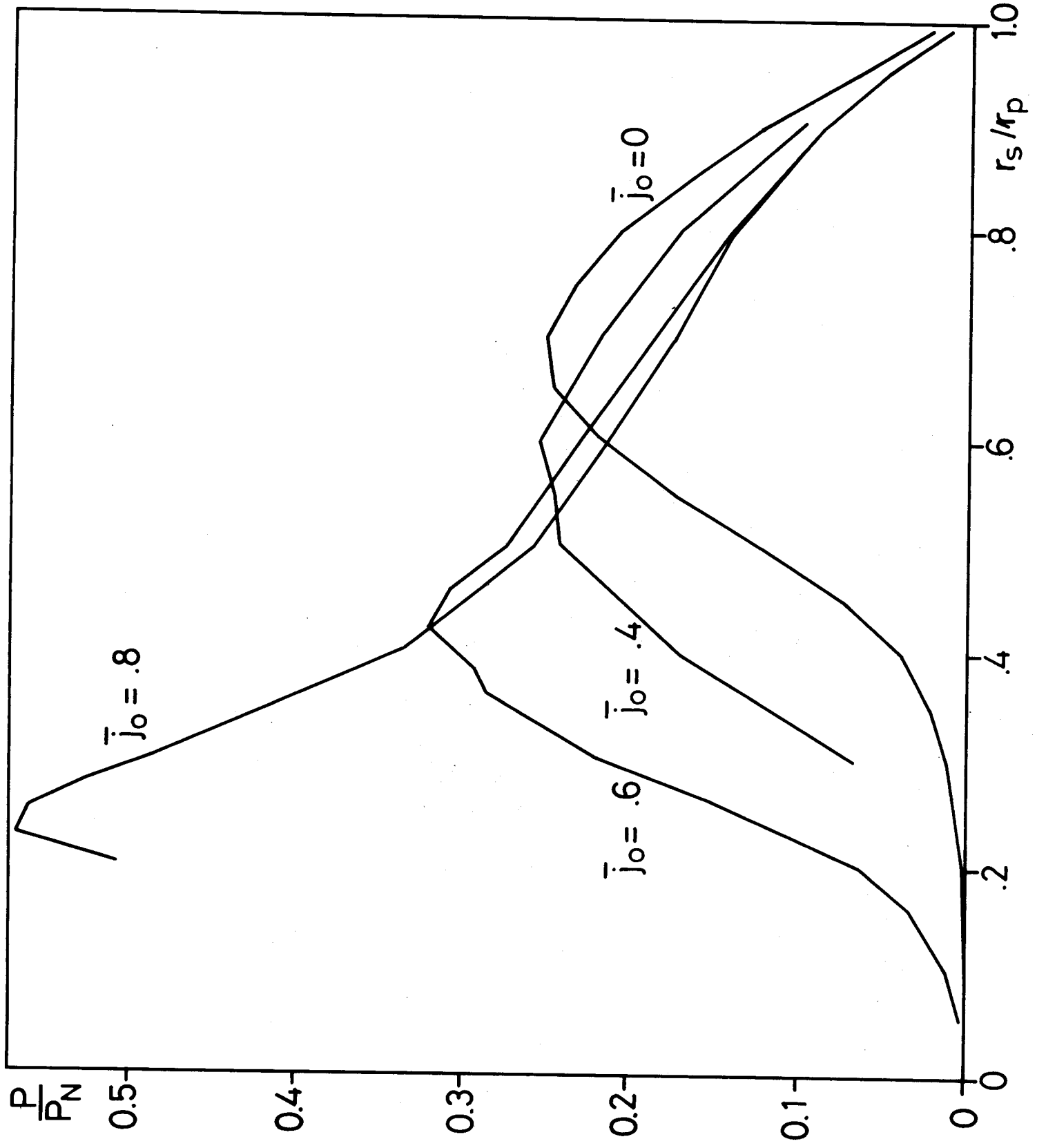

Fig. 10

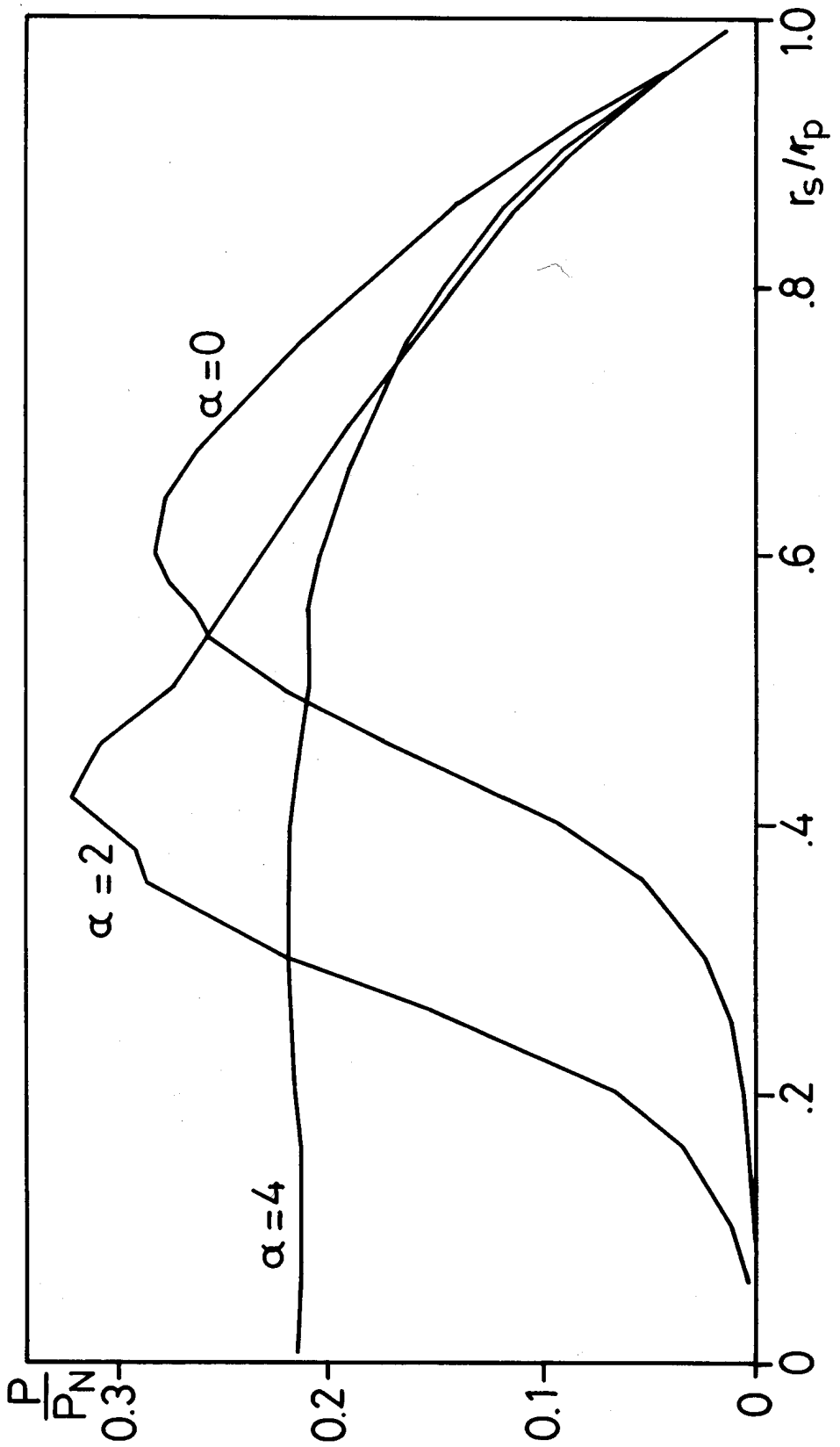

Fig. 11

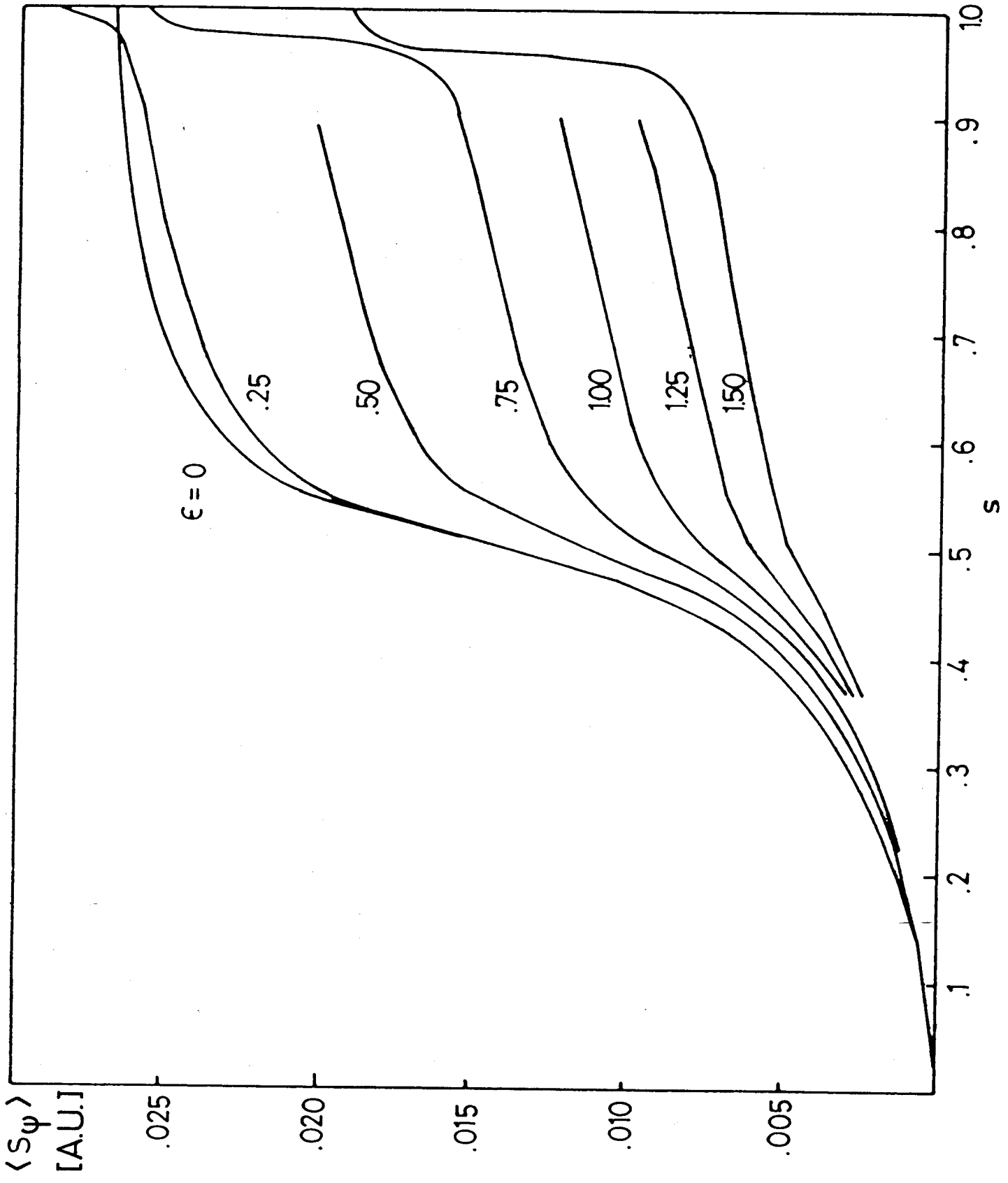

Fig. 12

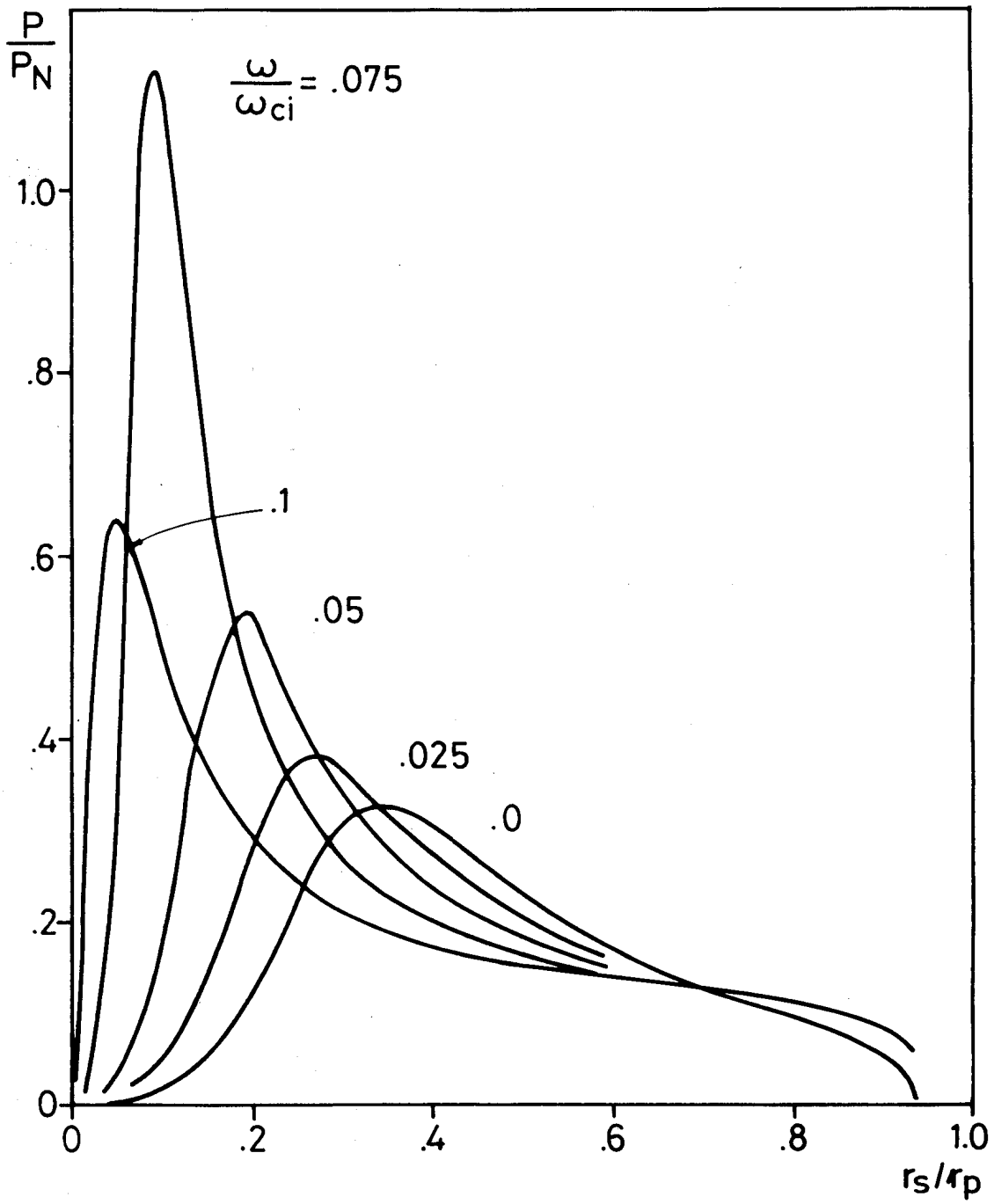

Fig. 13

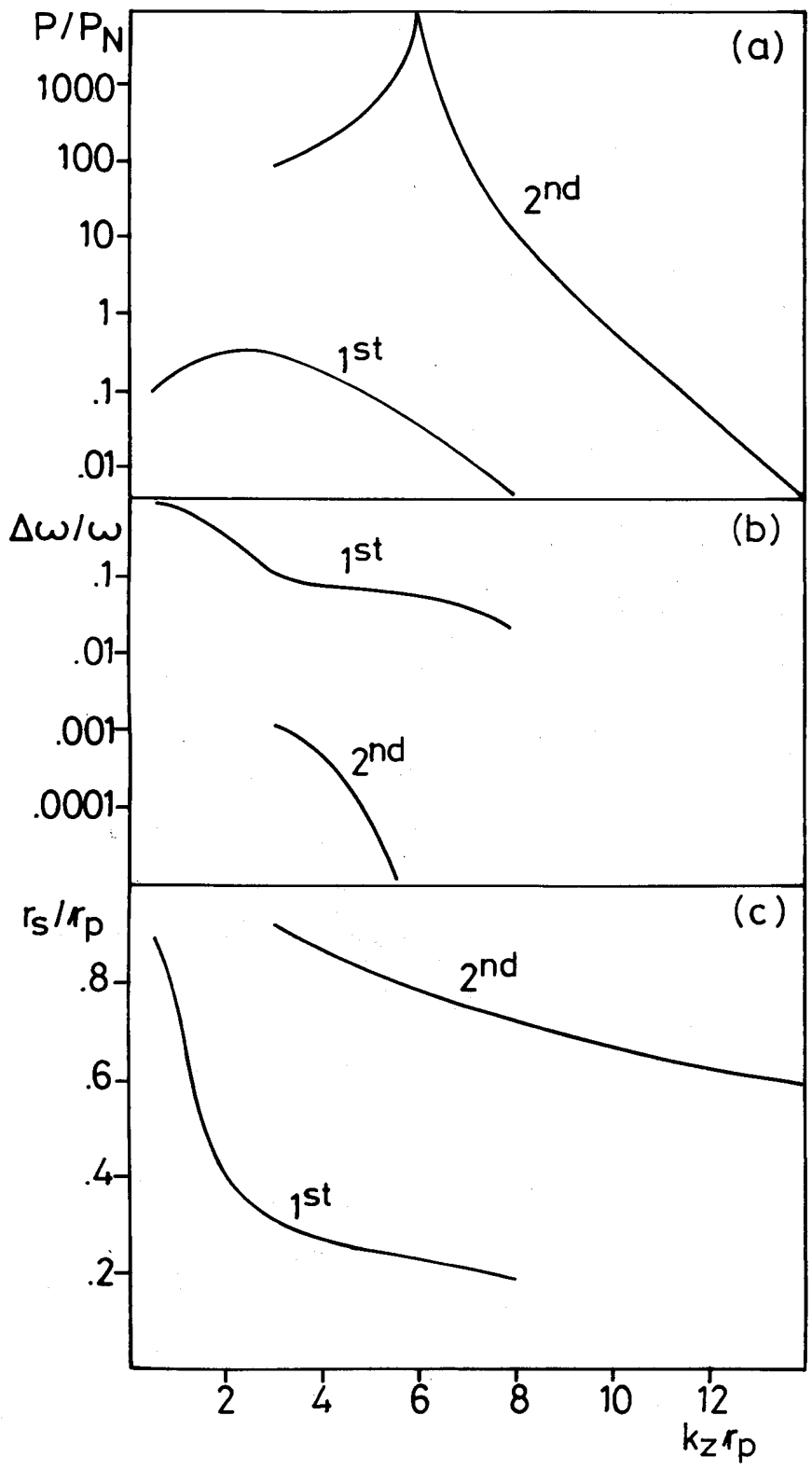
P/P_N
1000
100
10
1
.1
.01
(a)
2nd
1st
Δω/ω
.1
.01
.001
.0001
(b)
1st
2nd
r_s/r_p
.8
.6
.4
.2
(c)
2nd
1st
2
4
6
8
10
12
k_z r_p

Fig. 14

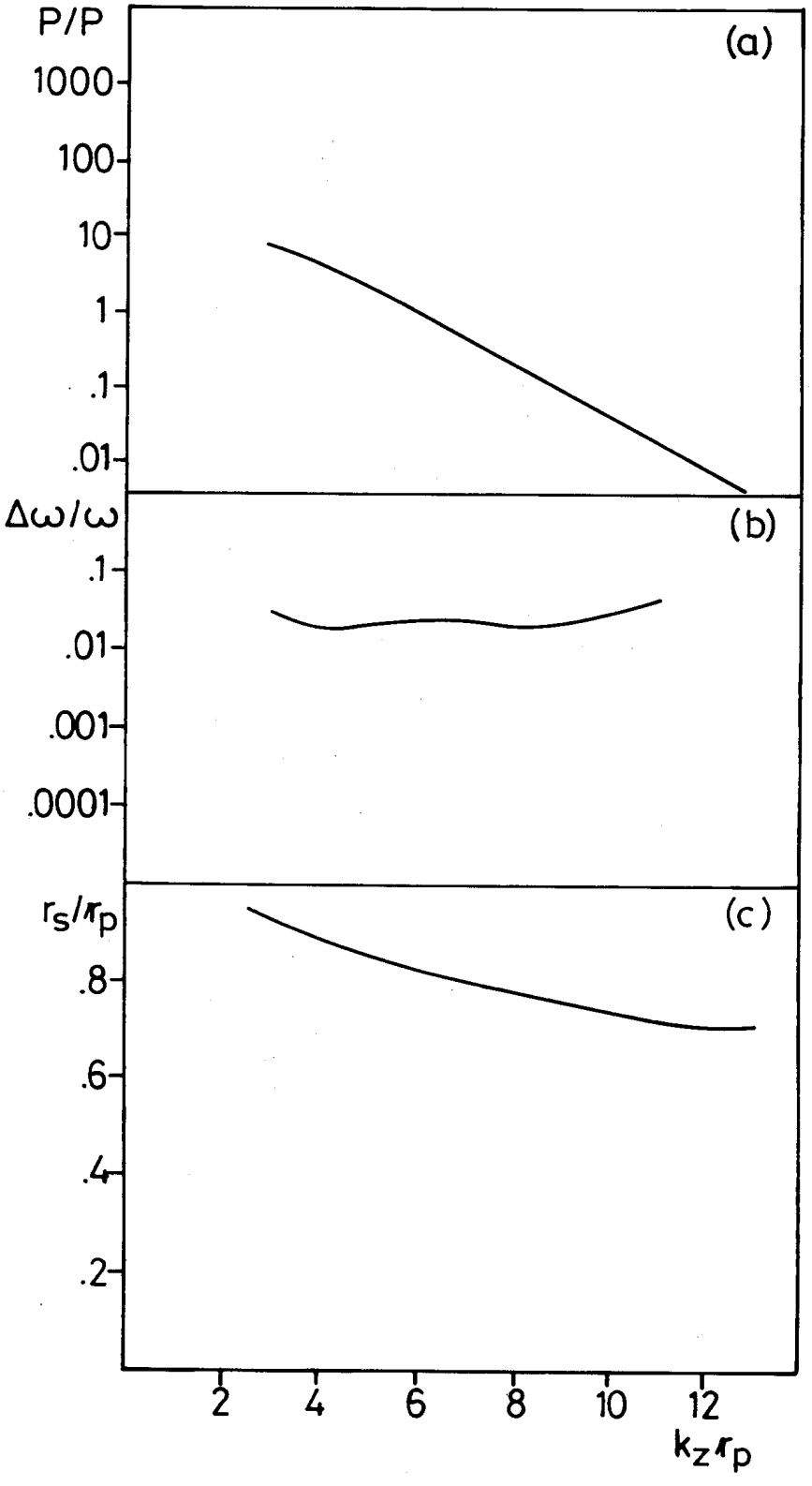
P/P
1000
100
10
1
.1
.01
(a)
Δω/ω
.1
.01
.001
.0001
(b)
r_s/r_p
.8
.6
.4
.2
(c)
2
4
6
8
10
12
$k_z r_p$

Fig. 15

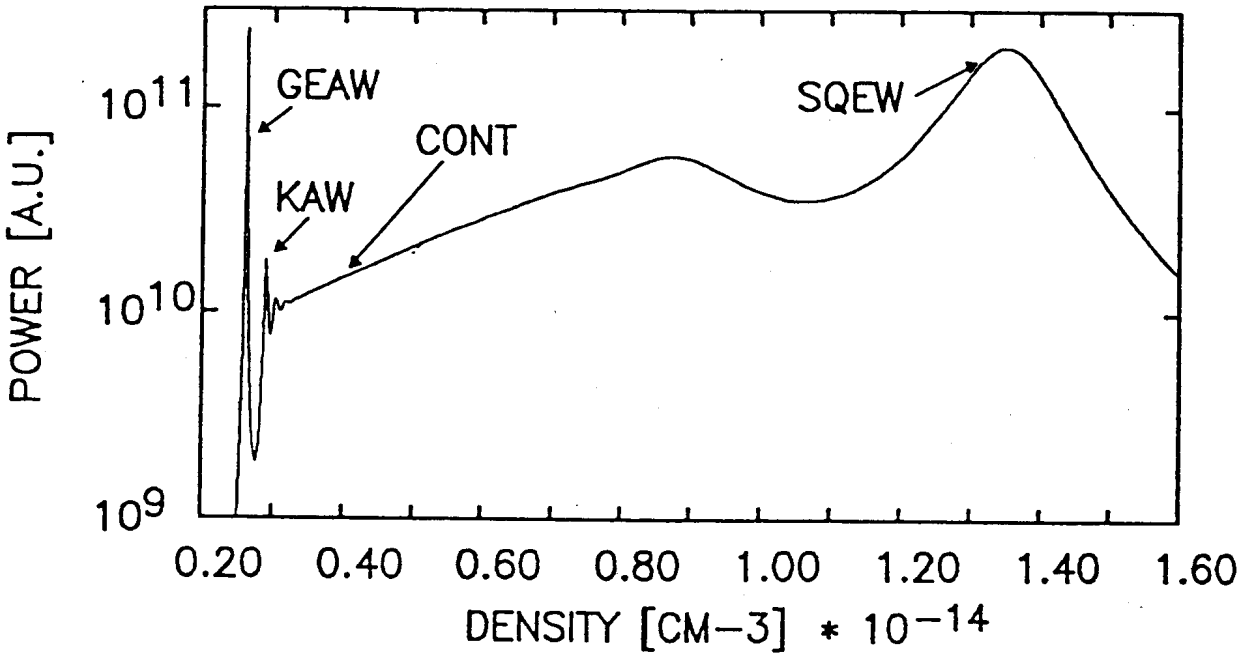
POWER [A.U.]
10^{11}
10^{10}
10^{9}
GEAW
CONT
KAW
SQEW
0.20
0.40
0.60
0.80
1.00
1.20
1.40
1.60
DENSITY [CM−3] * 10^{-14}

Fig. 16

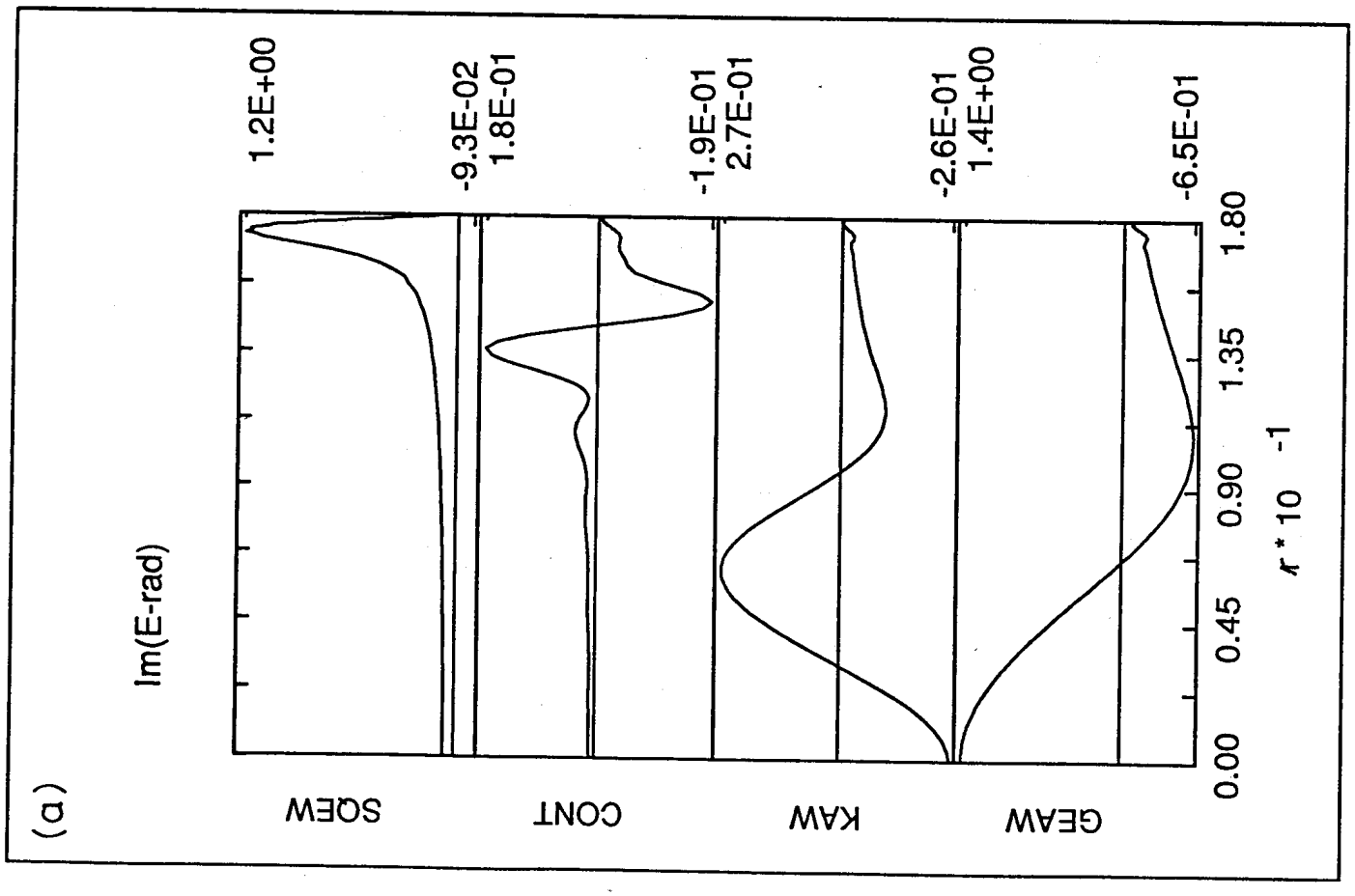
(a)
Im(E-rad)
1.2E+00
-9.3E-02
1.8E-01
-1.9E-01
2.7E-01
-2.6E-01
1.4E+00
-6.5E-01
SQEW
CONT
KAW
GEAW
0.00
0.45
0.90
1.35
1.80
r * 10 -1

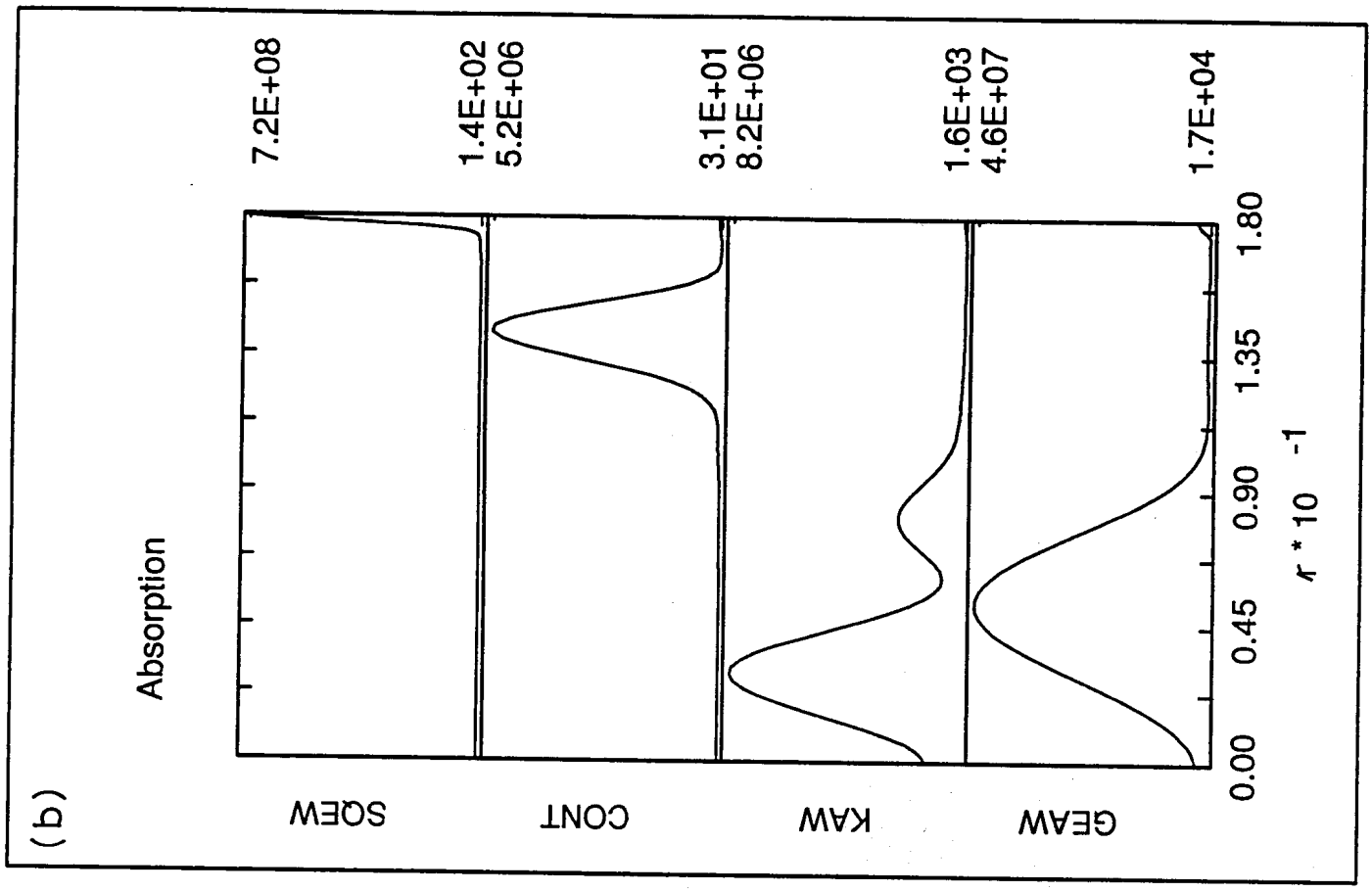
(b)
Absorption
7.2E+08
1.4E+02
5.2E+06
3.1E+01
8.2E+06
1.6E+03
4.6E+07
1.7E+04
SQEW
CONT
KAW
GEAW
0.00
0.45
0.90
1.35
1.80
r * 10 -1

Fig. 17

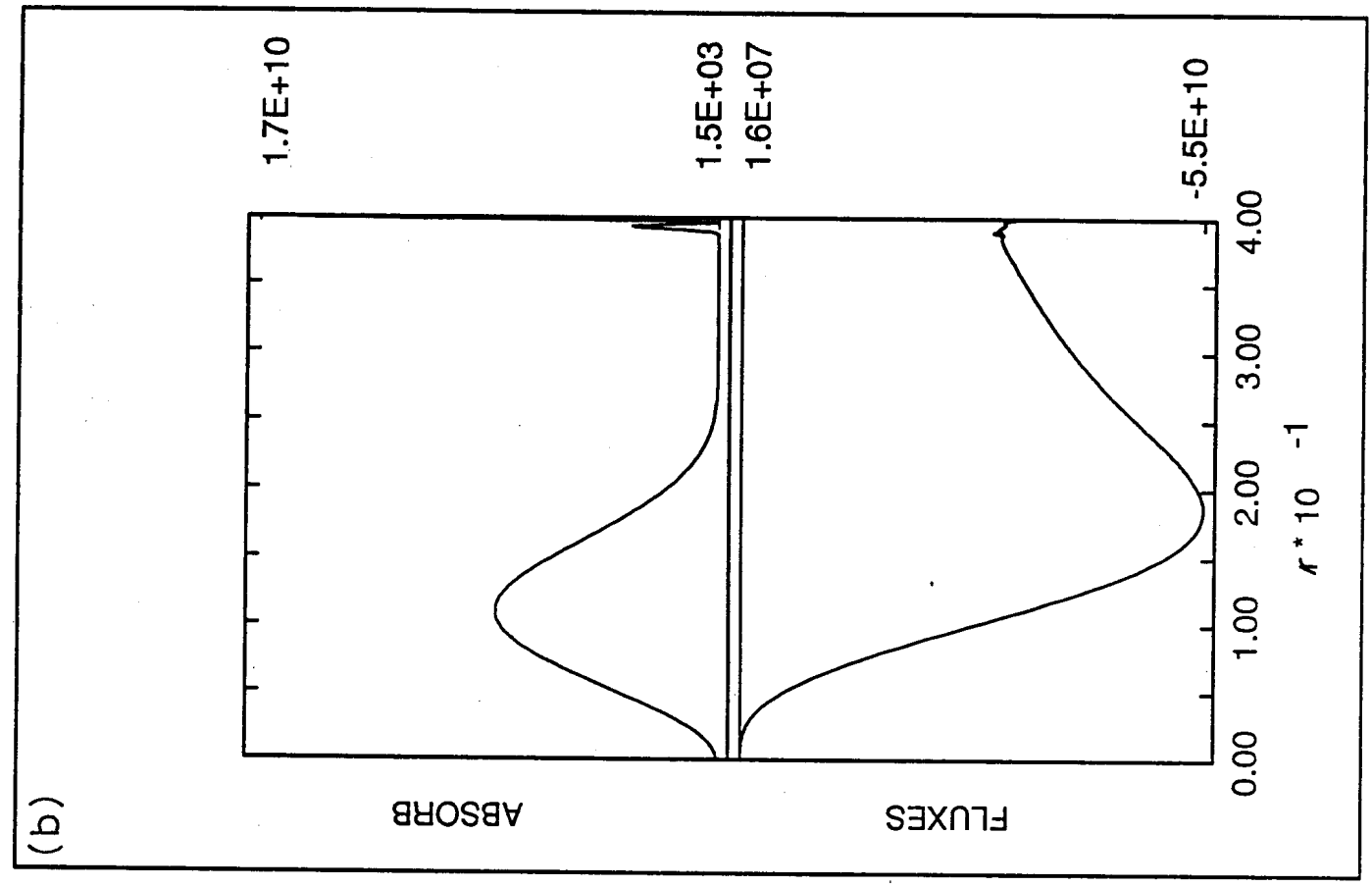
(b)
ABSORB
FLUXES
1.7E+10
1.5E+03
1.6E+07
-5.5E+10
0.00
1.00
2.00
3.00
4.00
r * 10 -1

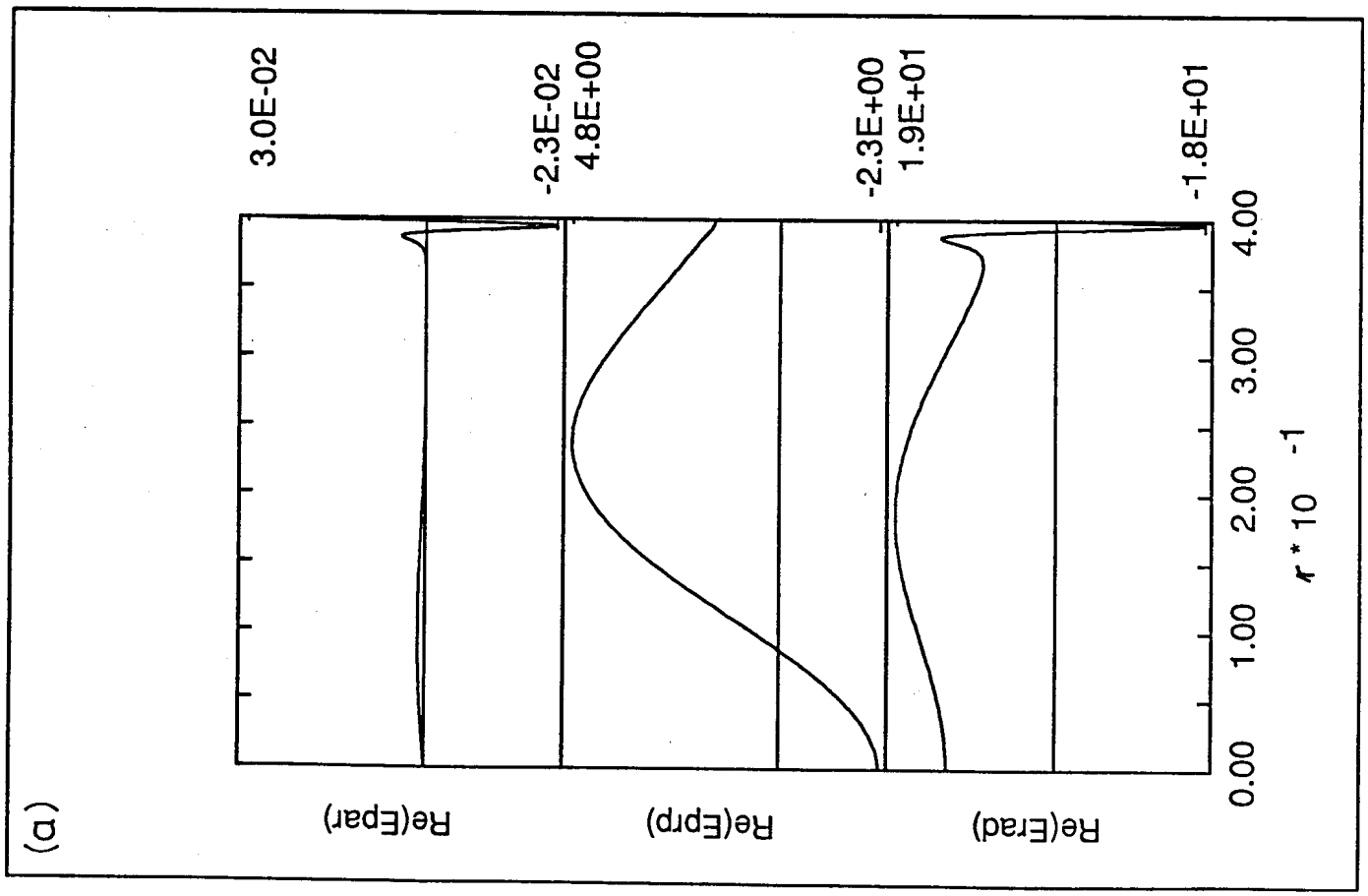
(a)
Re(Epar)
Re(Eprp)
Re(Erad)
3.0E-02
-2.3E-02
4.8E+00
-2.3E+00
1.9E+01
-1.8E+01
0.00
1.00
2.00
3.00
4.00
r * 10 -1

Fig. 18